

**A RHEOLOGICAL INVESTIGATION OF FLY-ASH WATER SLURRY  
USING CATIONIC, ANIONIC AND NON-IONIC ADDITIVES**

*Submitted in partial fulfilment of the requirements for the award of degree of*

**Master of Engineering**

**In**

**Thermal Engineering**

*Submitted by*

**KUNAL SINGH**

**Roll No: 801083012**

**Under the guidance of**

**Mr. Kundan Lal**

**Assistant Professor**

**Mechanical Engineering Department**

**Thapar University, Patiala**



**MECHANICAL ENGINEERING DEPARTMENT  
THAPAR UNIVERSITY**

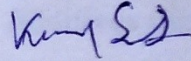
**PATIALA - 147004**

## AUTHOR'S DECLARATION

I, "**Kunal Singh**", hereby declare that the work which is being presented in this thesis entitled "**A Rheological Investigation of Fly Ash Water Slurry using Cationic, Anionic and Non-Ionic Additives**" by me in partial fulfilment of the requirements for the award of degree of Master of Engineering in Thermal Engineering from Thapar University, Patiala, is an authentic record of my work carried out under the supervision of **Mr. Kundan Lal**, Assistant Professor, MED, Thapar University, Patiala.

The matter embodied in this thesis has not been submitted in any other University/Institute for the award of any other degree

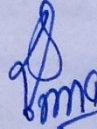
Date: 27-6-2012

  
(KUNAL SINGH)

Reg. No. 801083012

This is to certify that the above statement made by the student concerned is correct to the best of my knowledge and belief.

Date: 16-07-12



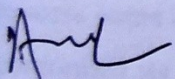
(Mr. KUNDAN LAL)

Assistant Professor

Mechanical Engineering Department

Thapar University, Patiala

Countersigned by:




(Dr. AJAY BATISH)

Professor and Head

Mechanical Engineering Department

Patiala - 147004

  
(Dr. S.K. MOHAPATRA)

Dean of Academic Affairs

Thapar University

Patiala - 147004

## Abstract

The problems faced by Thermal power plants during the hydraulic transportation of residual fly ash is well known, commonly a lean mixture of 20 to 25% by weight of fly ash is mixed with water to form a slurry and is pumped through pipelines to ash ponds. Rheological properties of fly ash water slurry play a crucial role in estimating the power requirements for such process, fluid properties of such complex fluids such as viscosity and shear stress are strongly related to the pumping power. Clearly low values of such properties demand less power requirement. The idea of using a surfactant to reduce drag properties of such slurries have been established long since. In this work the effect of 3 different drag reducing additives is studied through experimentation. The cost, availability and effectiveness of additives are important parameters to be considered before using them in power plants. Additives used are Cetylpyridinium chloride (referred to as CPC) which is cationic in nature, non-ionic Triton x-100 (referred to as triton), and anionic Sodium Dodecyl sulfate (referred to as SDS). These 3 additives bear hydrophobic tail, which increase the hydrophobic activity of fly ash by reacting on surface. The action of these additives on flow behaviour of slurry is studied at different dosages using a rheometer. The effect of cmc (critical micelle formation) plays an important role in determining viscosity at higher shear rates. It is found that effect of cmc can be used to determine the optimal amount of dosage of additive required for drag reduction. Also in general, composition or particle size of fly ash is not fixed, in this work the particles of different size range are extracted through mechanical sieving and flow behaviour of slurries made from these particles is studied. Large particle size adversely affects good flow behaviour. Another way to study good flow behaviour is by matching actual data with the modelled values. Rheological models are excellent mathematical tools available, which help to analyse good flow behaviour. In this work, extensive amount of data has been analysed with 'Oswald de Waele' model, which is basically a power law model. During this process some advantages and shortcomings of this model are discovered, which ultimately conformed its range of reliability and area of application. In this work settling characteristics of fly ash slurry is studied by the use of gravitational settling technique. The effect of additives on settling rate is studied, it is observed that action of these large molecular size additives increase the mass and inertial properties of fly ash particles, thus leading to increase in settling rate. An entirely new approach is adopted to compare the effect of different dosages of additives on settling behaviour of slurry. The process involves the analyses of data points through regression and comparing the slopes of these regression lines. The

coefficient of co-relation 'r' (a parameter which indicates strength of regression) is adopted as a tool to measure the consistency and reliability of the process of regression.

## ACKNOWLEDGEMENT

I express my sincere gratitude to my supervisor **Mr. Kundan Lal, Assistant Professor, Mechanical Engineering Department, Thapar University, Patiala**, for his continuous support and guidance during last two years, without him this work could not be completed. I am thankful for his patience and cooperation. I also appreciate his efforts in thoroughly revising the thesis, and thankful to him for sharing his valuable experience and suggestions.

I am sincerely thankful to Mr. Chander Singh (Chemical Dept.) for helping me in my work with his lab facilities. I would also like to thank Prof. Satnam Singh for permitting me to use his lab instruments. I would also like to thank Mr. Naveen saini (JRF mechanical dept.) for helping me with my experiments on rheometer and Mr. Ayush kumar for sharing his valuable knowledge with me. I am thankful to Mr. Bhupender Singh, Assistant Professor, Physics Dept. for guiding me through my work. I express my gratitude to Dr. Ajay Batish (HOD Mechanical dept.) for his fast and sincere response to my applications each and every time.

Lastly, I am thankful to my parents for their patience and understanding and also for the continuous encouragement they gave me in my rough times.

**(KUNAL SINGH)**

# INDEX

<b>CONTENTS</b>	<b>Page No.</b>
<hr/>	
LIST OF FIGURES	viii
LIST OF TABLES	x
<b>Chapter 1: INTRODUCTION</b>	<b>1</b>
1.1 Background for the Study	1
1.2 Brief Overview on Fly Ash Slurry	2
1.2.1 Fly ash composition	2
1.2.2 Fly ash slurry	3
1.3 Brief Overview on Additives	4
1.3.1 Additives	4
1.3.2 Types of additives	5
1.3.3 Action of additives	5
1.3.4 Difference between charged and non-ionic polymer surfactant	8
1.4 Rheological Modelling	9
1.4.1 Modelling	9
1.4.2 Oswald de Waele rheological model	10
1.5 Research Objectives	12
<b>Chapter 2 LITERATURE REVIEW</b>	<b>13</b>
<b>Chapter 3 EXPERIMENTAL WORK</b>	<b>20</b>
3.1 Surfactants Used	20
3.1.1 Cetylpyridinium Chloride (CPC)	20
3.1.2 Sodium Dodecyl Sulphate (SDS)	21
3.1.3 Triton x-100	22
3.2 Fly Ash Used	23
3.2.1 Chemical composition (EDS) and SEM analysis of fly ash	23
3.2.2 Particle size distribution (PSD) of fly ash	24
3.3 Instrument Used	26
3.3.1 Rheolab QC (Make: Anton paar)	26
3.3.2 Technical features	27
3.3.3 Detailed specifications	27
3.4 Experimental Procedure	28

3.4.1 Preparation of slurry for rheometer	28
3.4.1.1 Slurry without additive	28
3.4.1.2 Slurry with additive	28
3.4.1.3 Slurry of specific particle size range	29
3.4.2 Gravitational settling experiment	29
3.4.2.1 Preparation of slurry	29
3.4.2.2 Method of measurement	29
<b>Chapter 4 RESULTS AND DISCUSSIONS</b>	<b>30</b>
4.1 Study of Flow Behaviour of Slurry with Variable Fly Ash Concentration	30
4.1.1 Effect on viscosity of slurry with increase in concentration	30
4.1.2 Calculation of co-relations	31
4.1.3 Modelling using Oswald de Waele rheological model	32
4.2 Effect of Additives on Drag Reduction of 40% Fly Ash Slurry	35
4.2.1 Effect of CPC on drag reduction	35
4.2.2 Modelling of slurries containing CPC	36
4.2.3 Effect of SDS on drag reduction	38
4.2.4 Modelling of slurries containing SDS	39
4.2.5 Effect of Triton x-100 on drag reduction	40
4.2.6 Modelling of slurries containing triton	41
4.3 Comparison between the Effectiveness of CPC, SDS and Triton	43
4.4 Effect of Particle Size (PS) on Drag Properties of Slurry	44
4.4.1 Flow behaviour at 50% concentration	44
4.4.2 Effect of 0.5% of CPC on different particle size slurries	46
4.5 Effect of Additives on Settling Characteristics of 30% Fly Ash Slurry	48
4.5.1 Effect of CPC on settling rate	48
4.5.2 Effect of SDS on settling rate	51
4.5.3 Effect of Triton x-100 on settling rate	54
4.5.4 Comparison	56
4.6 Effect of Different Concentration of Additives on pH of Slurry	56
<b>Chapter 5 CONCLUSIONS AND RECOMMENDATIONS</b>	<b>58</b>
5.1 Conclusions	58
5.2 Recommendations for Future Work	60
<b>REFERENCES</b>	<b>61</b>
<b>Annexure A FLOW BEHAVIOUR OF SLURRY</b>	<b>64</b>

<b>Annexure B ADDITIVES WITH 40% FLY ASH SLURRY</b>	72
<b>Annexure C 50% SLURRY WITH DIFFERENT PARTICLE SIZE</b>	83
<b>Annexure D SETTLING OF 30% SLURRY WITH ADDITIVES</b>	92
<b>Annexure E PARTICLE SIZE DISTRIBUTION</b>	95
<b>Annexure F pH OF 40% SLURRY WITH ADDITIVES</b>	97

## LIST OF FIGURES

FIGURE NO.	FIGURE DESCRIPTION	PAGE NO.
1.2.1b	Variation in colour of fly ash depending on chemical constituents	3
1.2.2a	Flow behaviour of complex fluids	3
1.3.1a	Action of surfactants on surface tension reduction	5
1.3.1b	Action of surfactants during micelle formation (cmc)	5
1.3.3a	Hydration forces without additive, causing repulsion	7
1.3.3b	Hydration forces with additive causing hydrated bilayers	7
1.3.3c	Hydrophobic particles without additive	7
1.3.3b	Hydrophobic nature achieved using additives	7
1.3.3e	Creation of zero osmotic pressure between 2 particles	8
1.3.3f	Attraction of 2 particles due to outside osmotic pressure	8
1.3.3g	Building of osmotic pressure due to clusters of polymer bonds	8
1.3.3h	Repulsion proceeds due to this pressure	8
3.1.1a	Molecular structure of CPC monohydrate	20
3.1.2a	Structure of SDS with hydrophobic and hydrophilic regions	21
3.1.3a	Structure of Triton x-100 with benzyl head and hydrophobic tail	22
3.2.1a	SEM results for fly ash sample at 2000 magnification	23
3.2.1b	SEM results for fly ash sample at 5000 magnification	23
3.2.1c	Selected section of fly ash during EDS analysis	24
3.2.1e	Visual view of elements present in fly ash sample	24
3.2.2a	Fly ash sample used during sieve analysis	25
3.2.2b	Sieve system arranged for mechanical sieving process	25
3.2.2c	Mechanical sieving machine	25
3.2.2d	Particle size distribution histogram, with cumulative curve	25
3.2.2e	Visuals of particles greater than 100 $\mu$ m size	26
3.2.2f	Visuals of particles less than 100 $\mu$ m size	26
3.3.1a	Visual of Rheolab QC rheometer used for research	27
3.3.1b	Geometry used for measurements of higher concentration slurry	27
3.4.2.2a	Cylinder with measuring tape attached	29
4.1.1(a,b,c)	Shear stress graph at 10%,20% and 30% fly ash	30
4.1.1(d,e,f)	Shear stress graph at 40%,50% and 60% fly ash	30
4.1.2a	Comparison of shear stress at different fly ash concentration	31
4.1.2b	Comparison of actual apparent viscosities with variable fly ash	31
4.1.2c	Actual increase in average shear stress	32
4.1.2d	Actual increase in average viscosity	32
4.1.2e	Calculated average shear stress using co-relation	32
4.1.2f	Calculated average viscosity using co-relation	32
4.1.3a	Comparison of shear stress vs shear strain on logarithmic scale	33
4.1.3b	Regression lines plotted	33
4.1.3(d,e,f,g,h,i)	Modelling results compared with actual viscosities	34
4.2.1a	Viscosity reduction with addition of CPC	36
4.2.1b	Shear stress plot of slurry with and without CPC	36

4.2.2a	Data points on log-log plot	37
4.2.2b	Regression lines of points with equations on display	37
4.2.2(e,f,g,h)	Modelling results obtained for different dosages of CPC	37-38
4.2.3a	Effect of SDS on viscosity	38
4.2.3b	Reduction in shear stress using SDS	38
4.2.4a	Shear stress on logarithmic plot for SDS	39
4.2.4b	Regression lines with equations on display	39
4.2.4(e,f,g,h)	Modelling results obtained for different dosages of SDS	40
4.2.5a	Viscosity change with Triton x-100	41
4.2.5b	Change in shear stresses using Triton x-100	41
4.2.6a	Log-log plot of shear stresses for Triton x-100	42
4.2.6b	Regression lines of logarithmic plot	42
4.2.6(e,f,g,h)	Modelling results obtained for different dosages of Triton x-100	42-43
4.3a	Effect of 0.5% additives on viscosity of 40% slurry	44
4.3b	Effect of 0.5% additives on shear stress of 40% slurry	44
4.4.1(a,b,c)	Shear stress for 50% slurry with particles more than 100 $\mu$ m	44
4.4.1(d,e)	Shear stress for 50% slurry with particles less than 100 $\mu$ m	45
4.4.1(f,g,h)	Modelling results for particles less than 100 $\mu$ m size	45
4.4.2(a,b,c,d)	Effect of 0.5% CPC on flow behaviour different particle size slurries	46
4.4.2(f,g,h)	Modelling results obtained for 0.5% CPC with particles less than 100 $\mu$ m size	47
4.4.2i	Effect of 0.5% CPC on particle size range of 150 to 106 $\mu$ m	47
4.5a	Height vs Time graph for 30% slurry without additive	48
4.5b	Settling rate vs time graph for 30% slurry without additive	48
4.5.1(a,b,c,d)	Effect of different dosages of CPC on settling rate of 30% slurry	49
4.5.1e	Regression lines drawn up to one standard deviation for CPC	49
4.5.1h	Effect of CPC dosages on average settling rate	50
4.5.1i	Increase in acceleration of settling using CPC	50
4.5.1j	Comparison of slopes of regression lines on % scale for CPC	51
4.5.2(a,b,c,d)	Effect of SDS on settling rate of 30% fly ash slurry	51-52
4.5.2e	Regression lines drawn up to one standard deviation for SDS	52
4.5.2h	Effect of SDS on average settling rate	53
4.5.2i	Comparison of slopes of regression lines for SDS	53
4.5.2j	Increase in acceleration of settling using SDS	53
4.5.3(a,b,c,d)	Effect on settling rate using triton x-100	54
4.5.3f	Regression lines drawn for triton x-100	55
4.5.3h	Increase in average settling rate using triton x-100	55
4.5.3i	Increase in acceleration of settling process using triton x-100	55
4.5.3j	Increase in acceleration expressed as % for triton x-100	56
4.6a	Effect on pH of slurry with addition of CPC, Triton x-100 and SDS	57

## LIST OF TABLES

TABLE NO.	TABLE DESCRIPTION	PAGE NO.
1.2.1a	General layout of chemical compounds (% weight) present in fly ash generated from different types of coal	2
3.1.1b	Physical and chemical properties of CPC including cost	21
3.1.2b	Physical and chemical properties of SDS including cost	22
3.1.3b	Physical and chemical properties of Triton x-100 including cost	22
3.2.1d	Chemical composition of fly ash determined through EDS	24
3.3.3d	Specifications of Rheolab QC rheometer	28
4.1.3c	Modelling parameters calculated using experimental data	33
4.2.2c	Coefficient of correlation 'r' of regression lines for CPC	37
4.2.2d	Modelling parameters of slurries containing CPC	37
4.2.4c	Coefficient of correlation 'r' of regression lines for SDS	39
4.2.4d	Modelling parameters of slurries containing SDS	39
4.2.6c	Coefficient of regression 'r' of data points for Triton x-100	42
4.2.6d	Modelling parameters for slurries containing Triton x-100	42
4.4.1i	Modelling parameters of slurries with different particle sizes	45
4.4.2e	Flow parameters of slurries with different particles sizes, with and without CPC	47
4.5.1f	Coefficient of co-relation of settling rate lines with CPC	50
4.5.1g	Acceleration of settling process using CPC	50
4.5.2f	Coefficient of co-relation of settling rate lines with SDS	52
4.5.2g	Acceleration of settling process using SDS	52
4.5.3e	Coefficient of co-relation of settling rate lines with triton	54
4.5.3g	Coefficient of co-relation of settling rate lines with triton	55
4.5.4	Comparison between slurries containing CPC, SDS and Triton	56
A.1,A.2,A.3	Rheometer data for 10%,20% and 30% fly ash slurries	64-65
A.4,A.5.A.6	Rheometer data for 40%,50% and 60% fly ash slurries	65-66
A.7	Calculations for exponential co-relations for average stress	67
A.8	Calculations for exponential co-relations for average viscosity	68
A.9	Regression data for 10%,20%,30%,40%,50%,60% slurry	68
A.10	Modelling data for 10% and 20% fly ash slurry	69
A.11	Modelling data for 30% and 40% fly ash slurry	70
A.12	Modelling data for 50% and 60% fly ash slurry	71
B.1	Rheometer data for 40% fly ash slurry without additive	72
B.2, B.3, B.4	Rheometer data for 40% slurry with 0.5%, 1% and 1.5% SDS	72-73
B.5, B.6, B.7	Rheometer data for 40% slurry with 0.5%, 1% and 1.5% triton	74-75
B.8, B.9, B.10	Rheometer data for 40% slurry with 0.5%, 1% and 1.5% triton	75-76
B.11	Modelling data for 40% slurry with 0% and 0.5% CPC	77
B.12	Modelling data for 40% slurry with 1% and 1.5% CPC	78
B.13	Regression data calculated for 40% slurry with CPC	79
B.14	Regression data calculated for 40% slurry with SDS	79
B.15	Regression data calculated for 40% slurry with triton	79

B.16	Modelling data for 40% slurry with 0.5% and 1% SDS	80
B.17	Modelling data for 40% slurry with 1.5% SDS and 0.5% triton	81
B.18	Modelling data for 40% slurry with 1% and 1.5% triton	82
C.1, C.2, C.3	Rheometer data of 50% fly ash of particle size range of 255-150 $\mu$ m, 150-106 $\mu$ m and 106-75 $\mu$ m	83-84
C.4, C.5	Rheometer data of 50% fly ash of particle size range of 75-53 $\mu$ m and 53-0 $\mu$ m	84-85
C.6, C.7, C.8	Rheometer data for 50% fly ash with size range of 255-150 $\mu$ m, 150-106 $\mu$ m and 106 to 75 $\mu$ m with 0.5% CPC	85-86
C.9, C.10	Rheometer data for 50% fly ash with size range of 75-53 $\mu$ m and 53 to 0 $\mu$ m with 0.5% CPC	87
C.11	Modelling data of 50% slurry with PS range of 106-75 and 0.5% CPC	88
C.12	Modelling data of 50% slurry with PS range of 75-53 and 0.5% CPC	89
C.13	Modelling data of 50% slurry with PS range of 53 to 0 and 0.5% CPC	90
C.14	Regression data of 50% slurry with different PS range and 0.5% CPC	91
D.1	Regression data of 30% slurry used in settling process with different dosages of SDS	92
D.2	Regression data of 30% slurry used in settling process with different dosages of CPC	92
D.3	Regression data of 30% slurry used in settling process with different dosages of Triton x-100	92
D.4	Height of fly ash settled in slurry at 30% fly ash concentration with and without additives	93
D.5	Settling rate of fly ash slurry at 30% fly ash concentration with and without additives	94
E.1	Data obtained during calculation of particle size distribution (PSD) of fly ash	95
E.2	Conversion table showing relation between size in microns, British standard sieve no. system and ASTM standard.	96
E.3	pH data for 40% fly ash slurry with different dosages of SDS, Triton and CPC	97

## CHAPTER 1

### INTRODUCTION

#### 1.1 Background for the Study ‘A Rheological Investigation of Fly Ash Water Slurry using Additives’

Disposal of residual fly ash is one of the major problems faces by thermal power plants in India today; the work presented here is an attempt to solve some problems faced during transportation of this fly ash. Generation of fly ash is increasing yearly. In 2004-05 it was 112 million tonnes and in 2011-12 it is expected to be 170 million tonnes [21, 26]. This fly ash is usually transported in a form of slurry with a lean mixture of 20-25% concentration of fly ash mixed with water. The method is clean, but it requires large amount of water. Heavy metal compounds such as  $\text{SiO}_2$ ,  $\text{CaO}$  and many others [21], which are present in fly ash, degrade the quality of water to such extent that it becomes unfit for any domestic use. It is beneficial to use more concentration of fly ash in slurry. High concentration of fly ash in slurry gives rise to high viscosity and shear stresses, which in turn requires large pumping power to transport it to ash ponds [16].

Recently, numerous studies have been done on 30% to 40% [22, 25] of fly ash and the effect of additives on drag properties of slurry has been studied. It is a well known that small percentage of drag reducing additives (cationic, non-ionic or anionic in nature) can help reduce viscosity, surface tension and other properties when added to water [4, 29, 30]. Recent studies have indicated that additives play a crucial role in reducing drag properties of complex fluids (non-newtonian fluids) such as slurries and emulsions [22, 25]. In these studies the action of additives on surface of fly ash particles is analysed, and explanation is given in terms of surface charge of fly ash particle, charge of additive and chemical properties of additives [22]. Although the action of additives on surface of fly ash is quite complex in nature, it is easier to do experiments and study the effect of additive and then make a conclusion about this effect. Any study without a mathematical analysis is incomplete, so is the case with slurries. Many studies indicate that non-newtonian behaviour of fly ash slurry can be approximated with a mathematical rheological model [16, 32]. There are many rheological models available, some give very accurate predictions but at the cost of simplicity. In recent years, there has been a growing interest in settling behaviour of fly ash in ash ponds [2], it has been noticed that additives can help in increasing the settling rate of fly ash and increase the water extraction process from ash ponds, a little work has been done in this area and it requires further research.

## 1.2 Brief Overview on Fly Ash Slurry

### 1.2.1 Fly ash composition

In India combustion of high ash bituminous coal in pulverized fuel fired system is major which results in low-lime (CaO) fly ash (similar to Class F of ASTM C618 standard) generation in major quantity [21, 22, 26]. The CaO content is typically less than 10% in this case and the colour is observed to be light to mid grey similar to cement powder. Pulverized lignite fired boilers and pressurized fluidized bed combustion systems are limited which results in generation of smaller volumes of high lime (CaO) fly ash (Class C of ASTM C618 standard). The CaO content is usually found to be more than 20% for this class of fly ash.

In general colour of fly ash can be tan (light brown) to dark grey depending on the chemical and mineral constituents. The specific surface areas of fly ashes collected using multi field electrostatic separators varies from 250 m<sup>2</sup>/kg to 850 m<sup>2</sup>/kg [26]. Fly ash mainly constitutes oxides of silicon (SiO<sub>2</sub>), aluminium (Al<sub>2</sub>O<sub>3</sub>), iron (Fe<sub>2</sub>O<sub>3</sub>), and calcium (CaO). Fly ash consists of traces of toxic elements, glass content and many minerals. The composition of fly ash is not specific and different coal sources produce fly ash of different colour, density and composition. The quality of coal also plays a crucial role in fly ash composition.

Metal compound	Bituminous coal	Sub bituminous coal	Lignite coal
SiO <sub>2</sub>	20-60%	40-60%	15-45%
Al <sub>2</sub> O <sub>3</sub>	5-35%	20-30%	10-25%
Fe <sub>2</sub> O <sub>3</sub>	10-40%	4-10%	4-15%
CaO	1-12%	5-30%	15-40%
MgO	0-5%	1-6%	3-10%
SO <sub>3</sub>	0-4%	0-2%	0-10%
Na <sub>2</sub> O	0-4%	0-2%	0-6%
K <sub>2</sub> O	0-3%	0-4%	0-4%
LOI	0-15%	0-3%	0-5%

**Table 1.2.1a General layout of chemical compounds (% by weight) present in fly ash generated from different types of coal.**



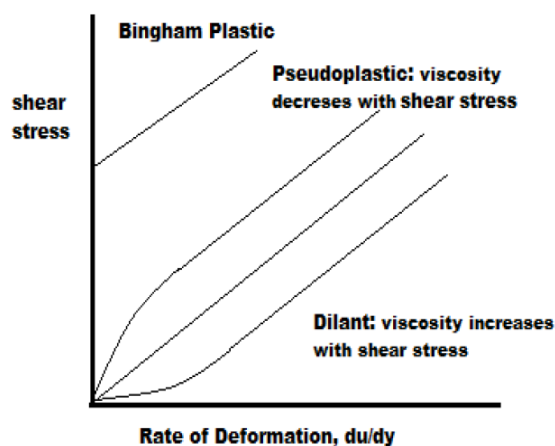
**Figure 1.2.1b Variation in colour of fly ash depending on chemical and mineral constituents [40]**

It has been observed through SEM [20] microphotographs of fly ash that most of the particles are spherical in shape with size ranging from  $1\mu\text{m}$  to at most  $150\mu\text{m}$  [20, 26]. Size distribution of fly ash can be estimated using mechanical sieve analysis or by using an instrument called particle size analyser [20, 22]. This instrument is more accurate and uses laser diffraction technique to calculate particle size; it has been observed that this distribution is almost normal in nature.

### 1.2.2 Fly ash slurry

Fly ash slurry is a complex fluid (non-Newtonian fluid) composed of a fixed percentage of fly ash (by weight or by volume) and water, the leaner the mixture the more it follows Newtonian behaviour of flow, at higher concentrations of fly ash the behaviour of slurry is usually dilatant (Shear thickening) in nature [22]. Also viscosity is a strong function of concentration of fly ash which increases drastically with increase in concentration of fly ash in slurry.

In Newtonian flow, the viscosity is given by the slope of the line drawn between shear



rate (independent variable) and shear stress (dependent variable), however in case of complex fluids such as fly ash slurry, viscosity is changing at every point on dilatant curve, this viscosity can be calculated experimentally on devices such as 'rheometer' (a device which measures viscosity of complex fluids), the viscosity in this case is called apparent viscosity. Instrument like

**Figure 1.2.2a Flow behaviour of complex fluids**

rheometer can calculate apparent viscosity of slurry at number of discrete points, and basic trend of flow (pseudo plastic, Newtonian, dilatant) can be observed using this data.

In thermal power plants a lean mixture of slurry is used because it approximates Newtonian flow with constant viscosity throughout the pumping process. In actual practice as we increase concentration of fly ash, the behaviour of slurry will be different at higher and lower shear rates. There are many rheological models available which can predict this behaviour; the applicability of a rheological model can only be estimated through prior experimentation on sample of slurry and by understanding the data obtained.

### **1.3 Brief Overview on Additives**

#### **1.3.1 Additives**

Additives are chemical compounds (metallic, polymer based, organic) which affects the fluid properties of a solution when added to it in small quantities, they can change the properties like viscosity, surface tension, pH value of solution. Detergent additives can change the viscosity and other properties of fly ash slurry when added to it in small quantities. Detergent additives are also termed as surfactants which are amphiphilic in nature, meaning they contain either lyophobic or hydrophobic (when solvent is water) groups (tails) and lyophilic or hydrophilic groups (heads). Surfactants have the tendency to absorb at surfaces and interface. Hydrophobic group is a water insoluble compound, while hydrophilic group (head) is water soluble. Head of additive can interact with particles dispersed in water or any other solvent depending on the nature of forces involved between the head of additive and surface of particle. The action is to lower the free surface energy of particle, and the process is in compliance with 2<sup>nd</sup> law of thermodynamics. Overall entropy is increased in this process.

It has been observed through studies and experimentation that small amount of surfactant can decrease the surface tension of a solution. However after a limit, any further addition of surfactant does not affect the surface tension. The phenomena can be explained through the process of micelle formation. A micelle is a cluster of surfactant molecules. When small amount of surfactant is added to a solution, the surfactant molecules tries to move toward the surface of solution with hydrophilic heads attached towards the surface of water and tails away from water and shown in figure (1.3.1a). This process is responsible for decrease in surface tension. As the concentration of additive increases and there is no room for surfactant molecules at surface they cluster together inside the liquid with their heads together facing the liquid and tails hidden inside as shown in figure (1.3.1b). The concentration at which micelles start to form is called cmc (critical micelle concentration).

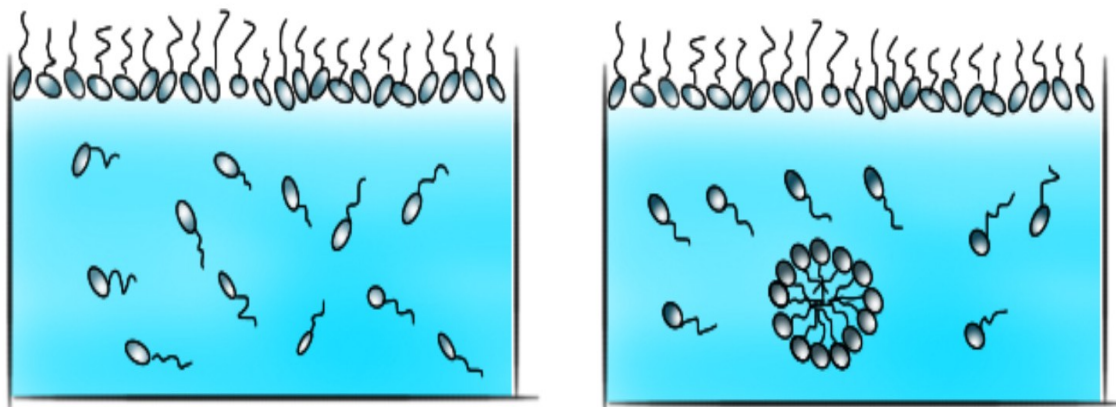


**Figure 1.3.1 Exaggerated view of action of surfactant in water solution (a) Maximum surface tension reduction achieved (b) Micelle formation at cmc**

### 1.3.2 Types of additives

Additive can be cationic, anionic and non-ionic depending on the charge on head, the tail of additives consist of long chain of hydrocarbons, the difference in reactivity is created by the charge on the head. Studies indicate that in case of fly ash slurry, charged additives such as cationic and anionic are proven to be good in reduction of viscosity [4, 22, 20]. Cationic surfactants work well with an organic counter ion [22]. Non ionic polymer based surfactants can even increase the viscosity at buffer (boundary wall) layer of slurry [35, 28, 37], this increase in viscosity is due to twisting and bending of polymer chain and this effect results in appreciable decrease in wall friction. Ironically, we can say that even after increase in viscosity of slurry after addition polymer additive, the flow will be smooth due to reduction in wall friction.

### 1.3.3 Action of additives

To understand the phenomena of drag reduction, we have to first understand the forces involved between particles, Molecules of all matter at temperature more than absolute zero possesses internal energy which causes motion (rotation, vibration and translation) of molecules if there is enough space for this [23, 24]. This random motion called Brownian motion is expressed as thermal energy in terms of  $k_B T$ , where  $k_B$  is the Boltzmann constant [ $1.381 \times 10^{-23} \text{JK}^{-1}$ ] and  $T$  is absolute temperature in [K]. If internal energy is the only source of energy the molecules possess, then aggregation will likely occur if bonds formed between 2 particles during collision process possess energy greater than internal energy. Example at  $25^\circ \text{C}$  attractive forces between 2 particles will be effective if potential energy possessed by the bonds between them is greater than their internal energies [ $1.31 \times 10^{-23} * 298 = 4.12 \times 10^{-21}$ ].

<sup>21</sup>J], the bonds with energies less than that will break at 25<sup>0</sup>C. The smaller the size of particles, the greater will be the effect of internal energy on stability of particles and less effect will be accounted due to gravity and magnetic forces. In case of unrefined fly ash the particle size has a normal distribution with particle size ranging from as small as 1 μm to 150 μm at most [21], there are other impurities in very minute quantities such as coal chips, dust etc with size of at most 500 μm, due to small quantities of these impurities their effect on smooth flow behaviour of slurry can be neglected. In fly ash slurry, the stability is affected by both gravitational forces (due to large particle present) and internal energy (presence of small particles). Previously, it was thought that primary force behind attraction and repulsion between particles in a solution is electrostatic in nature. Ever since 1970's, scientists have been trying to establish the cause of repulsion force occurring between different electrostatically charged particles, but the theory of electrostatic repulsion is not quite predictable. The process of aggregation and stability of particles is quite complex and not yet truly uncovered. Studies [24] indicate that there are 2 forces whose existence is proven by experimental measurements. These forces are based on the idea that it is rather convenient to consider the forces between water and particles dispersed in water rather than considering only the forces between dispersed particles and neglecting dispersion medium (water). The origin of these forces is not clearly understood but these are thought to be entropic in nature, entropic forces arise when a system progresses to a state in which entropy is maximized. It can result in effective forces between hard spheres like small fly ash particles. These forces are repulsive hydration forces and attractive hydrophobic forces.

Theory of hydration says that two hydrated bilayers experience strong repulsion as they approach each other. If the surface of particle is hydrophilic in nature then it forms bonds with water molecule, these network of bonds extends a long distance away from the particle surface due to hydrogen bonds between water molecules (Vander Waals forces between H and O atoms in a molecule), if such 2 particles come close to each other, then a strong repulsion occurs due to films of water present between them. It has been known through studies that surface of fly ash particles are charged similarly [26, 22]. We can see that according to this theory an additive with head of opposite charge than those of fly ash particle and with hydrophilic tail can increase the hydration effect in slurry. In layman words, the longer the hydrophilic tail the more layers of water will be present on surface of water and stronger will be the repulsion.

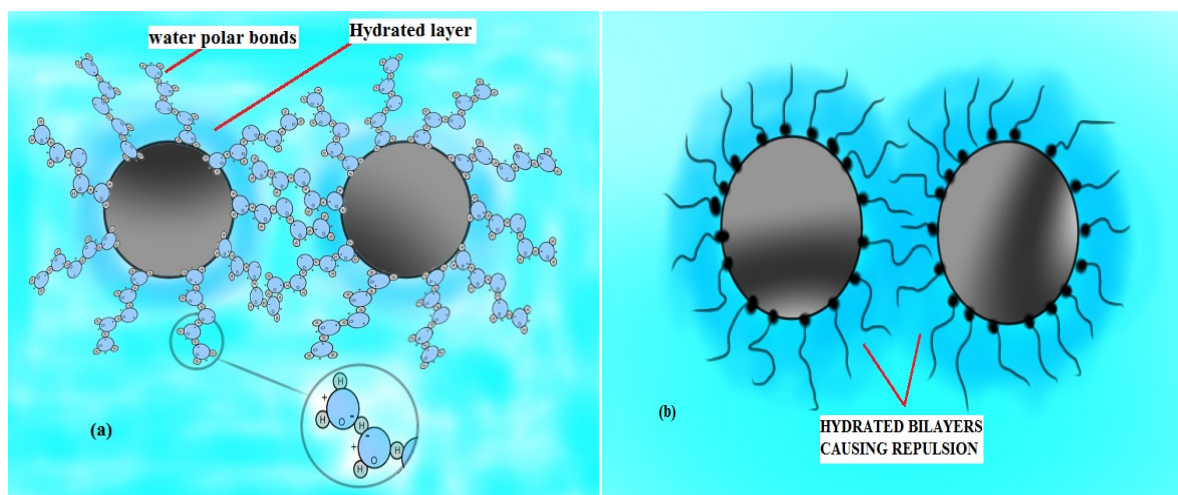


**Figure 1.3.3 (a) Hydration forces without additive, with water covalent bonds causing repulsion. (b) Hydration forces with additive, and hydrated bilayers formed around particles.**

Hydrophobic forces on the other hand, arise when surface of the particles have no attraction to water molecules, in such as case these particles have no barrier of water layers present between them, so they attract each other with a range and magnitude greater than the van der Waals forces. The hydrophobic nature of surface can be achieved or totally reverted using appropriate surfactant with hydrophobic or hydrophilic tail.

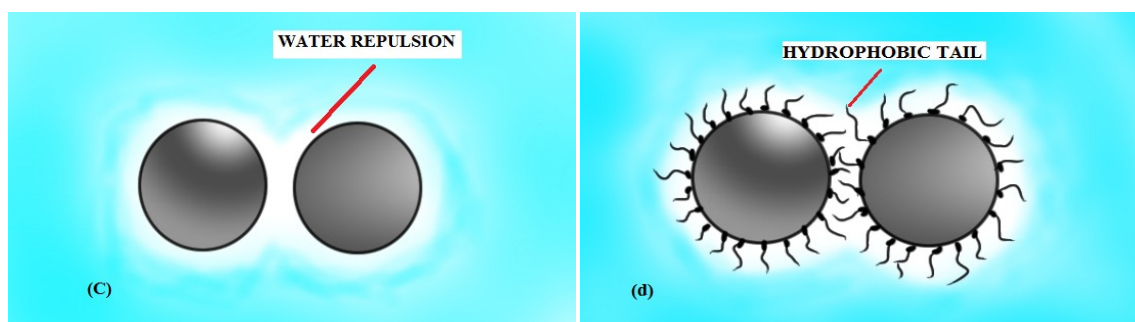


**Figure 1.3.3 (c) Hydrophobic particles without additive (d) Hydrophobic nature achieved on surface of particles using additives with hydrophobic tails**

Polymer additives with short range hydrocarbon groups can also cause forces of entropic origin; these are repulsive *steric forces* and attractive *depletion forces*.

Depletion forces or attractive forces are the result of presence of non-adsorbing (non-adhesive to surface of particle) polymer in a solution. Depending on the ratio of polymer to particle concentration, this polymer increases the osmotic pressure around the particles. In such a case when 2 particles comes really close to each other and the gap between them is so small that polymer particles cant enter in between, the bulk osmotic pressure forces the 2 particles to attract each other as shown in figure(1.3.3f) below.

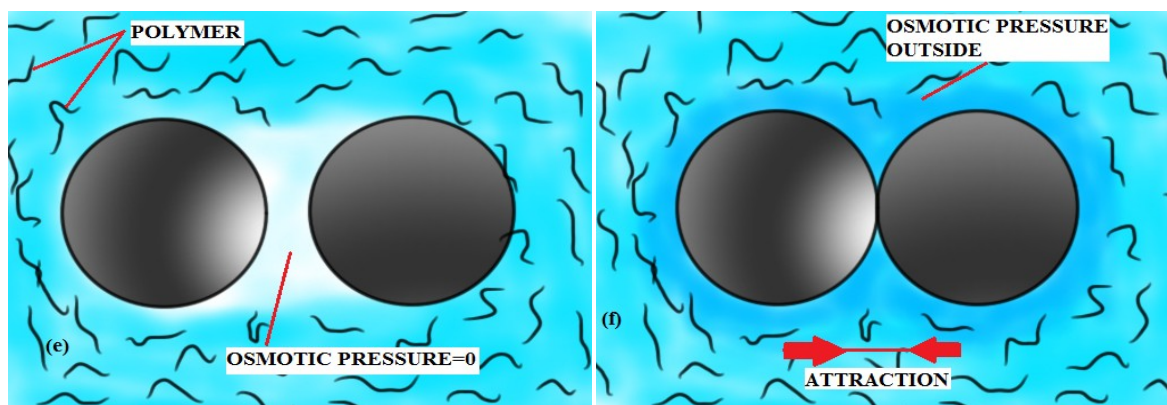


**Figure 1.3.3 (e) Creation of zero osmotic pressure in between 2 particles (f) Attraction of 2 particles due to outside osmotic pressure.**

Steric forces or repulsive forces arise due to polymer with adsorbing characteristics. Such polymers form bonds on the surface of particles with their tails winding around as shown in figure. When 2 such particles come closer to each other, the increased concentration in between them due to clusters of tails causes osmotic pressure to increase between them and hence repulsion proceeds as show below.

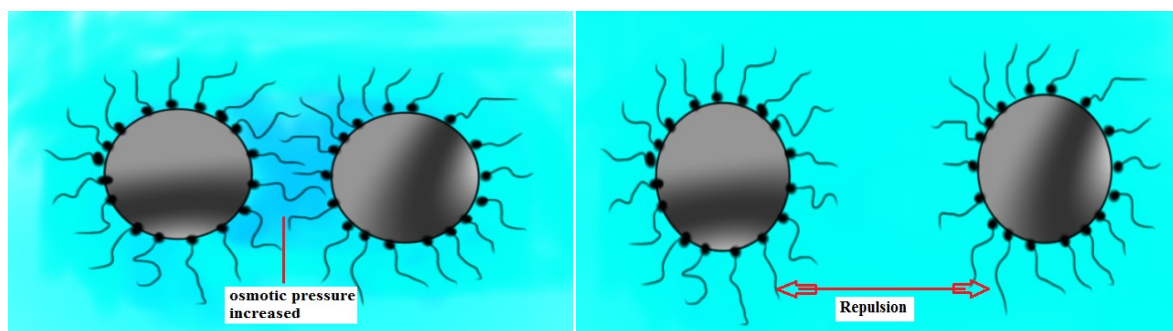


**Figure 1.3.3 (g) First, osmotic pressure builds up due clusters of polymer bonds (h) Second, repulsion proceeds due to this pressure.**

#### 1.3.4 Difference between Charged and non-ionic Polymer surfactant

- Polymer surfactant shows drag reduction at very low concentration in ppm [35]. While for charged surfactants high dosage is required to see some appreciable reduction in drag properties.
- Effect of polymer surfactant is not dependent on temperature and reduction in drag is virtually stable at wide range of temperatures, on the other hand charged surfactants are effective only for a range of temperature, and there cmc (critical micelle formation) change with temperature.
- Polymer additives have long shelf life, they are very stable and can remain intact for years, and most of them are biodegradable and environment friendly. But, charged

surfactants are mostly toxic, their stability is uncertain and depends on variety of parameter and operating conditions.

- When a solution containing polymer additive is subjected to high shear rates, the bonds are broken down due to mechanical effects which results in permanent loss of drag reduction properties of additive. On the other hand bonds formed by charged additives are strong, at high shear rates a temporary disruption occurs, and strength is regained afterwards.

## 1.4 Rheological Modelling

### 1.4.1 Modelling

Any research without a mathematical analysis is incomplete, so is the case with slurries, modelling is a process of finding a relation between different variables, using inherent knowledge of mathematics and observation of experimental data. In case of slurries it is useful to find a relation between shear stress and shear strain. If the relation is successful then apparent viscosity can be calculated at different shear rates without doing experiments again. However, in real world there is no relation which can give actual true values of viscosity no matter how complex is the mathematics involved. Sometimes it is useful to use a simple model which gives approximate results rather than a time consuming complex model.

There are many rheological models available for slurries [24]. These models can be applied for a wide variety situations and processes involved. No matter how complex the model is the reliability of a model can only be checked by observing experimental data, calculating errors and thinking about the accuracy required. In this work, a special version of power law model called ‘Oswald De Waele’ rheological model is used to analyse data and find apparent viscosity. This model is based on the assumption of time independence, it means it is characterised by viscosity relations that are a function of shear rate, but not a function of time of application of shear. The basic governing equation of a solution of fluids containing solid particle in suspended state is given by the relation between shear stress ( $\tau$ ) and shear rate ( $\dot{\gamma}$ ).

$$\tau = f(\dot{\gamma})$$

This form of equation is used for simple, unidirectional shear flows of Newtonian and non-Newtonian fluids. However, under the action of Interparticle attractions as in case of slurries, and in the presence of complex molecular structure, this relation cannot withhold all the stresses associated with the deformation. Manipulation of this relation with the use of tensors in 3dimensional space is helpful in generalizing the flow behaviour for complex fluids. Considering that total stress tensor  $T$  depends only on the rate of deformation tensor  $\dot{\gamma}$ .

$$T = f(\gamma)$$

All the possible stresses can be visualized by expanding the above relation

$$T = f_0 \gamma^0 + f_1 \gamma^1 + f_2 \gamma^2 + \dots$$

For an incompressible fluid, the shear rate tensor raised to the zero power is identity tensor with its invariant equal to the negative of the pressure. With the use of Cayley-Hamilton theorem the above equation can be written in terms of the scalar functions  $\eta_1$  and  $\eta_2$  of the invariants of  $\gamma$

$$T = -pI + \eta_1 (I_{2,\gamma}, I_{3,\gamma}) \gamma + \eta_2 (I_{2,\gamma}, I_{3,\gamma}) \gamma^2$$

This equation is known as ‘Reiner-Rivlin’ equation. Here  $\eta_1$  term is the viscosity function that determines the shear behaviour of the system. The  $\eta_2$  term gives rise to normal stresses in steady shear flow. As the normal stresses in steady shear flow cannot be related to any function of the rate of deformation tensor in this group of fluids,  $\eta_2$  term is set equal to zero.

The equation then reduces to

$$T = -pI + \eta_1 (I_{2,\gamma}, I_{3,\gamma}) \gamma$$

In simple shear flows, like flow through pipes  $I_{3,\gamma} = 0$ , reducing the general equation to

$$T = pI + \eta_1 (I_{2,\gamma}) \gamma$$

Or, in terms of a shear stress and shear rate

$$\tau = \eta_1 (I_{2,\gamma}) \gamma$$

#### 1.4.2 Oswald de Waele rheological model (Power law model)

This model is used for slurries where shear thinning behaviour is observed at low concentrations for particles and shear thickening at higher concentrations. As per the experiments performed in this work, the same behaviour is observed for low and high concentrations fly ash slurries. Based on the observations this model is selected for analysis. This model is also called power law model because shear stress is proportional to a certain power of shear strain. According to this model viscosity function  $\eta_1(I_{2,\gamma})$  is given by

$$\eta_1(I_{2,\gamma}) = K |I_{2,\gamma}|^{(n-1)/2}$$

$$\tau = K |I_{2,\gamma}|^{(n-1)/2} \gamma$$

In steady unidirectional shear flows  $|I_{2,\gamma}| = \gamma^2$ , and equation reduces to

$$\tau_{ij} = (K \gamma_{ij}^{n-1}) \gamma_{ij} = K \gamma_{ij}^n \quad \text{-----(1)}$$

Taking log on both sides

$$\ln(\tau_{ij}) = \ln(K) + n \ln(\gamma_{ij}) \quad \text{-----(2)}$$

This is the power law equation on logarithmic scale, it can be used as one of the method to observe data and estimate whether the relation between shear stress and shear strain obeys

power law. We can see that above log equation is linear in nature, so we can say that if we plot the values of shear stress ( $\tau$ ) and shear strain ( $\gamma$ ) on logarithmic scale and we get a straight line, then it is obeying power law relation.

Although there are many functions which can give a straight line on log-log plot, and can give a deceptive sense of being power law in nature, the applicability of power law can always be estimated by comparing actual data with calculated values. Also many previous studies [16, 22] indicate that this model is applicable for fly ash slurries and give quite accurate results. Another feature of this model is its simplicity and ease of understanding. Although the model is not so accurate for very low shear rates, because first 2 or 3 values on log-log plot are wider and linear regression is not so accurate for these points, it approximates viscosity values very well at higher shear rate which is usually the case with pumping process in thermal power plants. From equation (1) we can calculate apparent viscosity.

$$\eta = K \gamma^{n-1}$$

$\eta$  is the apparent viscosity

$K$  = consistency coefficient and higher values of it gives more viscous flow.

$n$  = viscosity index

Here,  $n < 1$  for shear thinning fluids (pseudoplastic)

$n = 1$  for Newtonian fluids

$n > 1$  for shear thickening fluids (dilatant)

From previous studies on suspensions and dilute polymer solutions it is observed that in this model apparent viscosity approaches a constant value at low shear rates, and Newtonian behaviour at high shear rates.

## 1.5 Research Objectives

Following are the objectives of the work presented here

1. To study and compare the effect of different kind of additives (cationic, anionic and non-ionic polymer) on drag reduction of fly ash slurry at 40% concentration. To analyse the experimental data and study the effective range of shear rates for each additive in which maximum drag reduction is obtained.
2. To study the effect of different dosages (0.5%, 1%, and 1.5%) of additives on drag properties of fly ash slurry and find the optimal dosage in each case. To give justifications for the change in behaviour of slurry with different additive dosage in terms of cmc formation, hydration forces, hydrophobic forces and polymer bending at high shear rates.
3. To study the effect on viscosity with change in concentration of fly ash in slurry, and to find a co-relation to predict this change in behaviour. For example, it was found that average viscosity increases exponentially with increase of 10% of concentration of fly ash, so an exponential co-relation was calculated and results are compared with actual data.
4. To study the behaviour of slurry using a rheological model and analyse the applicability of the model by comparing it with real data. There are many rheological models available; the crucial part is the selection of model. For example, considering the dilatant behaviour of slurry and high shear rate environment, a rheological model named 'Oswald de Waele' was selected to analyse the flow behaviour of slurry.
5. To study the effect of particle size of fly ash on drag properties of slurry with and without additive, fly ash has a normal particle size distribution. Although large particles are present in minute quantities, they increase viscosity and adversely affect smooth flow behaviour. Proper analyses can reveal the effectiveness of additives on such size range.
6. To study the settling characteristics of fly ash slurry with and without additives, the effect of cationic, anionic and non-ionic additives at 4 different concentrations is studied. Study of settling characteristics is helpful in designing ash ponds; it is observed that settling increases with increase in dosage of additive, a proper justification for change in settling rate with change in concentration is given in terms of cmc formation and particle size increase.

## CHAPTER 2

### LITERATURE REVIEW

A detailed literature review has been done in order to study the rheological behaviour of fly ash

**Roh N.S *et al.* [1]:** Effects of properties of coal, volume fraction of solids and the mean size and size distribution of the coal particles on coal water mixture (CWM) are investigated. Seven bituminous coals were used. An anionic surfactant, CWM 1002 (formaldehyde condensate of sodium naphthalene sulfonate) was selected as the dispersing agent to concentrate CWM. The apparent viscosity was measured with a Brookfield viscometer, and the non-Newtonian properties based on the power law model were investigated using Haake rotational viscometer. Slurry exhibited shear thinning and it become more viscous as the mean particle size decreased, but less viscous with decreasing equilibrium moisture content.

**Turian R.M *et al.* [2]:** The properties, the settling rates and the rheological behaviour of concentrated aqueous slurries of titanium dioxide, laterite, and gypsum & silica flour were investigated. Their pH & zeta potentials were measured. The rates of settling of slurry as a function of concentration were determined. The settling rate concentration data for the suspensions were analyzed within the context of available hindered settling correlations; correlations of the dependence between model parameters & solid concentration were developed. Yield stress of the suspension is measured by vane geometry. Titanium dioxide suspensions were obtained from DU pont as a 74 wt % slurry, laterite mud form AMAX (30% slurry), Silica flour form Ottawa Industrial Sand & gypsum donated by US Gypsum. PSD were determined using 3 instruments: the Micromerities Sedigraph 5000E, the Particle Data Computerized Elzone & the Leeds and Northrup Microtrac. Interparticle interactions were quite strong for all test suspensions. The 3 parameter sisko model, which combines low & intermediate shear power law with high shear Newtonian limiting behaviour, was found to provide the best overall description of the flow curves for all slurries.

**Aomari N *et al.* [3]:** Rheological study of simplified sea water in crude oil emulsions in done. Viscosity dependence on shear rate, creep experiments and oscillatory shear measurements are done. All emulsions were prepared from Crude Arabian Light (CAL) oil which has been previously heated at 110<sup>0</sup>C. Rheological studies were carried out by means of a stress-controlled rheometer (CarriMed CSL 100) with the cone plate geometry. All experiments were carried out at 20<sup>0</sup>C and for various water volume fractions in the range 0.457 – 0.826. Results showed the existence of a critical water volume fraction  $\Phi_c$  in addition

to the maximum packing fraction  $\Phi_m$ . the determined thickness of the hydrodynamic layer due to surfactant molecules is shown to decrease as the water volume fraction increases.

**Aktas Zeki *et al.* [4]:** The Rheological properties of a coal water mixture (CWM) of up to 60% prepared from Bickershaw coal samples with low ash content (4.0% & 6.86%) was studied in the presence of a non-ionic surfactant Triton X405. Viscometer used was a Brookfield Synchroelectric viscometer LVT model, which has 4 interchangeable spindles for different viscosity ranges. The viscosities of the slurries with low ash content were significantly reduced by the surfactant addition; it resulted in a behaviour change of slurries from non-Newtonian towards Newtonian fluids. But, sample containing very fine particles with a high ash content (24.5%) showed non-Newtonian behaviour even in the presence of reagent

**Turian R.M *et al.* [5]:** Rheological behaviour of fine particulate CWM made up of different coals was studied. Aim was to study the effective properties, the stability, the rheology and the flow behaviour in straight pipe and through pipeline transitions of highly loaded CWM, and to establish their relationship to suspension microstructure. Yield stress measurement was done using the vane method and shear-stress/shear-rate measurements using capillary rheometer. Highly loaded CWM exhibit strong non-Newtonian behaviour. Concentrated suspended particles with a narrow particle-size distribution are found to be Newtonian. Viscosities of the suspensions are increased as the concentration is increased.

**Atesok G *et al.* [6]:** effect of coal properties on CWSs have been investigated using two Turkish coals of different ranks and a Siberian bituminous coal. Physical, chemical and surface properties of coal samples were determined. Adsorption tests were performed. Coal samples were ground with a laboratory size ball mill. PSS (sodium polystyrene sulphonate), a product of Japanese COM and Lion Corporation, was used as the dispersant agent. A Zeta Meter 3.0 type device was used to perform zeta potential measurements. Viscosity measurements were performed using rotating type viscosimeter (Make: Brookfield) (Model: RVD2). The adsorption density of PSS decreases in the order of decreasing coal rank. Low rank Turkish coals used in this investigation permit less solids loading capacity compared to the Siberian coal for the same slurry viscosity.

**K. Umesh *et al.* [7]:** The particle size effect on pressure drop has been analyzed through the measured solid distribution pattern in the pipeline. An integral flow model has been used for prediction of the pressure drop & solids distribution under varying conditions. Pilot plant test loop of 150 mm diameter was used for the flow. The parametric study has revealed that the

optimum particle size distribution for transport of fly ash – bottom ash mix is the one which corresponds to a solid phase having FA: BA in the range of 4:1 to 3:2. Coarse particulate slurries require high operating velocities for transportation resulting in higher energy consumption per unit solid throughput.

**K.T Kaushal *et al.* [8]:** The effect of the two newly developed anionic additives in the formulation of CWS (coal-water slurry) has been studied. The Ledo coal of Makum field in Assam and Sirka coal of North Karanpura Field, Jharkhand, were used. Ball mill was used to obtain products of different PSD. Rheological properties of CWS were measured by a Rotoviscometer (Make: Haake) (Model: RV-12) using MVIP profiled sensor system and M500 measuring head. PSD characteristics were determined using Fritsch Particle Size Analysette 22. Slurries with high coal concentration (65-70%) having acceptable viscosities (<1000mPa s) can be formulated using the additive concentration of 0.8 and 0.9 wt. % on coal charge

**Lu Ping *et al.* [9]:** The slip phenomenon of coal – water paste (CWP) flowing in pipes is investigated by tube flow test in different tubes and real rheological models of CWP by correcting the influence of slip flow phenomenon is put forward. Test set up used for conducting the experiments consists of 2 parts: the CWP preparation loop to prepare the CWP and the test loop to characterize the CWP. Test coal was taken from Jiawang in china. Standard mesh sieves (0-6mm) were used to measure PSD (particle size distribution). At a certain particle size distribution the apparent viscosity of CWP increases with the increase of solid concentration. Fluidity of coal-water paste increases with increasing desulphurization additives under same concentration and particle size distribution. The optimum ratio of coarse coal powders to the fines in CWP is obtained in the experimental range, i.e. (PB=60:40).

**Xu Renfu *et al.* [10]:** 2 kinds of inorganic nanoparticles were used as stabilizers of coal water mixtures (CWMs). The properties, zeta potential, rheology and the stationary stability of coal water mixtures made up nano-stabilizers and different coal samples were investigated. Panjiang coal, Xinglong coal and Datong coal samples taken from different areas of China were used. All samples were initially crushed in hammer mill then pulverized in dry mill. PSD was determined by LS-CWM (Make: Omec Science and Tech. Ltd., Zhuhai). Viscosity was measured using NXS-11A (Make: Chengdu of china). Spherical nanoparticles can increase the zeta potential and static repulsion, and fibrous nanoparticles can enhance the steric hindrance by forming cross linking network structures

**Gurses .A *et al.* [11]:** Effects of parameters such as coal loading (wt. %), the initial pH of mixture, the addition of various electrolytes, surfactants and temperature on the viscosity and rheologic parameters of CWM have been investigated. RV8-Brookfield rotating type viscosimeter was used. It was found that the most effective additives, in terms of the viscosity reduction, were CTAB (Cetyltrimethyl Ammonium Bromide) and  $K_2HPO_4$  and that the CWM which had coal concentration up to 50% could be prepared by using each additive. Viscosities of CWM with increasing temperature were found to increase at low speed, and decrease at high speeds.

**Chandra .S *et al.* [12]:** Rheological properties of coal-oil-water suspensions containing coal particles of different sizes have been investigated. Newtonian, shear thinning and shear thickening behaviour of suspension has been observed depending on component content and operating conditions. Different coal stocks provided by TATA Colliery Jamshedpur, India with varying average sizes have been used. Cup and bob type, coaxial, cylindrical viscometer was used. Investigation reveals that the rheological behaviour of COW suspension can be shear thickening, shear, thinning or Newtonian depending on the percentage of component content as well as the operating conditions.

**C. Sunil *et al.* [13]:** An attempt to establish the relationship between the settled solid profile in ash pond and the physical/ rheological properties of coal ash slurry at high concentration was made to evaluate some characteristics of slurry which favour (HCSD) high concentration slurry disposal system. A hopper shaped mixing tank made from 3 mm thick GI sheet was placed on a flat base of FI tray, plug type valve (Make: AUDCO) was used for the flow of slurry from top. Experiment on FA: BA (4:1) slurry at higher concentration 60%, 65% & 70% (by weight) was done to determine angle of repose of the settled solids. The cone angle was measured for both impervious & pervious beds. For making pervious bed, dry fly ash was used & it was spread evenly over the whole tray to height of 4 cm. Higher values of yield stress & Bingham viscosity of the slurry result in higher cone angle of the deposited slurry. Cone angle increases with increase in solid concentration for FA slurry as well as mixture of FA & BA slurry but its values are lower.

**Liu Meng *et al.* [14]:** Characteristics of coal-water slurry (CWS) flowing through three types of piping components, namely gradual contraction, sudden contractions and  $90^\circ$  horizontal bends, were investigated at a transportation test facility. A pilot scale slurry transport system with computerized data acquisition system was designed. The test slurries were made by mixing coal powder with tap water and additives (provided by Nanjing Nanda Surface and

Interface Chemical Engineering & Technological Research Centre Co. Ltd) in slurry tank. SHEN-HUA (S-H) coal powder and YAN-ZHOU (Y-Z) coal powder were used. when CWS flow through sudden contraction the local pressure loss increases, while for  $90^\circ$  bend, local pressure loss is the least at optimal value of bend diameter ratio ( $R_c/D$ ).

**C. Sunil *et al.* [15]:** Fly ash and Bottom ash slurry (4:1) at high concentration (above  $C_w$  50% by weight) is considered and pressure drop have been measured at various flow velocities using a pilot plant test loop at various concentrations ranging from 50-70% by weight. Analytical measurement of pressure drop was compared with experimental data for a straight pipeline of 42 mm diameter. The slurry is drawn from the mixing tank into the pipe loop by a “Rotaflow” (Make: Roto pumps limited) pump. They have concluded that Relative pressure drop increases in with increase in solid concentration. The prediction model prepared by Darby & Melson is suitable for the Bingham plastic fluid flow such as mixture of FA & BA (4:1) slurry at concentration above 50% (by weight). Specific energy consumption decreases up to a concentration of 65% by weight & steeply increases beyond this value.

**Senapati P.K *et al.* [16]:** A model incorporating maximum solids fraction ( $\Phi_m$ ), power law index ( $n$ ), median particle size ( $d_{50}$ ), co-efficient of uniformity ( $C_u$ ), shear rate ( $\dot{\gamma}$ ) has been developed to predict the viscosity of slurry which is highly pseudo-plastic & whose behaviour can be described by a non-Newtonian power law model in the range of solids concentration. Prediction of  $\Phi_m$  has been determined directly from rheological data measured experimentally in a realistic system which is 0.62 in value. 5 fly-ash samples were obtained from the captive power plant of NALCO located at Angul Orissa. The particle size distribution was determined using Malvern make laser particle size analyzer, Morphological studies of 2 ash samples were undertaken using a Joel Super Probe (JXA -8100). The elemental analyzer of the bulk ash samples was carried out by Philips PW2440X-ray spectrometer. Shear thinning behaviour for all the samples at higher solids volume fractions in the range 0.32-0.49. Proposed model helped to access the motion of solid particles in a non-Newtonian flow regime.

**Masalova I *et al.* [17]:** Effect of surfactants on the rheology of water-in-oil highly concentrated emulsions (HCE) is studied. The surfactants used are oligomers of the PIBSA-type with different headgroups and low-molecular-weight sorbitan monooleate (SMO). The emulsifiers were dissolved in the oil phase prior to emulsification. The oil phase was Mosspar-H, a paraffin compounds that is produced and supplied by Lake International Technologies, Republic of South Africa. The emulsification process was conducted in 2.5 kg

batches by Hobart N50 mixer (manufactured and supplied by the Hobart Corporation). Role of surfactant nature in HCE is substantial and becomes more pronounced for smaller droplet size. The elasticity and the yield stress have dissimilar trends to interfacial tension and dilatational elasticity for HCE stabilized with different emulsifiers.

**He Qihui *et al.* [18]:** The effect of particle size distribution of petroleum coke on the properties of petroleum coke-oil slurry (PCOS) was investigated. The size and morphology of petroleum coke particle with different grinding time and the corresponding stabilizing mechanisms were analyzed by SEM and zeta potential measurements. Petroleum coke samples taken from four different petro-refining plants in china were used. Zeta potential was measured on Zetasize 3000 HS (Malvern, UK). The apparent viscosity was measured using NXS-11A rotary viscometer. PCOS with 4 different kinds of petroleum coke samples have similar apparent viscosity and stability. The prepared PCOS system exhibits shear-thinning or pseudo-plastic behaviour and displays excellent stability and fluidity.

**Chen R *et al.* [19]:** Objective was to produce homogeneous fuel slurry of char/coal-water with sufficiently high solid concentration and low apparent viscosity using selected additives as wetting agents and dispersants. The study involves Oil Mallee biomass char (derived from native Australian Mallee eucalyptus plants) and a lignite char, and several sub-bituminous coals. Malvern Mastersizer was employed to measure the particle size distribution of the prepared char slurries. The yield stress of the slurries was measured with a range of Brookfield DV II + Pro vane viscometers. The copolymeric charged additives D101 and D102 are most effective in increasing the solid loading of the slurry. For low ash content lignite char slurries, these additives introduced strong Interparticle repulsive forces as indicated by the high negative zeta potential and caused the slurries to display Newtonian and mild dilatants behaviour at high solids loading.

**Naik H.K *et al.* [22]:** The characteristics of fly ash slurry at 40% solid concentration with and without an additive were studied. Influence of cationic tenside on drag reduction of fly ash slurry was studied. Six number of fly ash slurry samples were prepared from the fly ash obtained from a power station in south India. Slurry constitutes fly ash, water, cationic surfactant namely Cetyltrimethyl ammonium bromide (CTAB) and a counter ion namely Sodium Salicylate (NaSal). They have used cylindrical co-axial rotational rheometer (Make: Antor paar) (Model: 101 Physica) at shear rates varying from 100 to 1000<sup>-1</sup>. All the treated slurries exhibited shear-thinning and Newtonian properties. Slurries developed in above

manner have a potential to be transported through pipelines with minimal energy consumption.

## CHAPTER 3

### EXPERIMENTAL WORK

#### 3.1 Surfactants Used

Three different additives of different nature (cationic, anionic and non-ionic) are used to study their effect on drag reduction, after careful study of cost, availability, toxic behaviour and stability criteria of different additives, following 3 additives are selected for the study and experimental work.

- ✓ Cationic surfactant – Cetylpyridinium chloride (referred to as CPC)
- ✓ Anionic surfactant – Sodium Dodecyl sulphate (referred to as SDS)
- ✓ Non-ionic surfactant - Triton X-100 (referred to as triton)

A brief description of each of these surfactants is given below

##### 3.1.1 Cetylpyridinium Chloride (CPC)



CPC is a cationic quaternary ammonium compound [38] with molecular formula  $C_{21}H_{38}ClN \cdot H_2O$ . It is solid pale yellow at room temperature. It is used in some types of mouthwashes, toothpastes [30], throat sprays etc. It is an antiseptic that kills bacterial and other microorganisms. It is also used as an ingredient in certain pesticides.

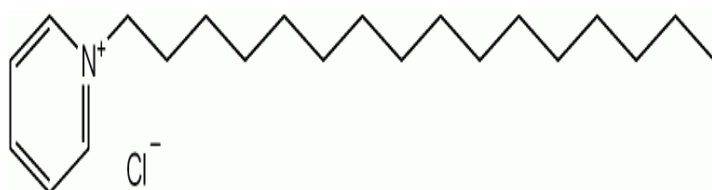


**Figure 3.1.1a** Molecular structure of CPC monohydrate

S NO.	Parameters	Value
1	CAS number	6004-24-6 (monohydrate)
2	Molecular Weight (M.W.)	$358.01 \text{ g mol}^{-1}$
3	Minimum Assay activity	99.0%
4	Melting Point	$80-84^\circ\text{C}$
5	pH (1% aqueous solution)	4.7-5.7
6	Sulphated ash	Max. 0.2%
7	Water content	4.5 – 5.5%
8	Heavy metals	Max. 0.002%

9	Pyridine, Acidity	Passes test
10	Cost per 100 gm	500 Rs
11	Manufactured by	Loba Chemie Pvt. Ltd (Mumbai) – 400 005

**Table 3.1.1b Physical and chemical properties of CPC including cost**

CPC has a long chain of hydrocarbon which is hydrophobic in nature; it has a bulky benzyl group as a head. Studies indicate [39] that CPC molecules form worm shaped micelles in a water solution after crossing their critical micelle concentration (cmc) value. It has also been found that as shear rate increases viscosity of water solution containing CPC increases drastically after a certain threshold value. This behaviour is considered to be associated with aggregation of micelles induced by high shear flow.

### 3.1.2 Sodium Dodecyl Sulphate (SDS)



SDS is an organic anionic surfactant derived from coconut [34] and palm oils. It comes in a very fine powder form. It has molecular formula  $C_{12}H_{25}OSO_3Na$ . It is used in many cleaning products, and it is an organosulfate consisting of a 12-carbon tail attached to a sulfate group, giving it the amphiphilic (compound containing long unbranched hydrocarbon chain) properties required of a drag reducing additive. It is quite inexpensive and commonly used in domestic cleaning purposes such as laundry, floor cleaners and car wash soaps, toothpastes, shampoos and shaving foams etc.

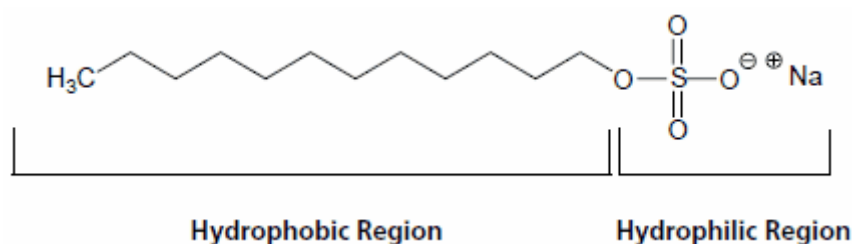


**Figure 3.1.2a Structure of SDS with hydrophobic and hydrophilic regions**

S NO.	Parameters	Value
1	CAS number	151-21-3
2	Molecular Weight (M.W.)	238.38 g mol <sup>-1</sup>
3	Minimum Assay activity	90%
4	Density	1.01 g/cm <sup>3</sup>
5	Maximum free acid	0.5 ml N/1%
6	Maximum free alkali	0.5 ml N/1%

7	Maximum Chloride (Cl)	0.01%
8	Cost per 250 gm	250 Rs
9	Manufactured by	Nice chemical Pvt. Ltd., Cochin – 682 024

**Table 3.1.2b Physical and chemical properties of SDS including cost**

At concentration more than cmc (critical micelle concentration) in aqueous solution, SDS molecules form micelles spherical in shape with hydrophobic long chain pointing towards center and hydrophilic region in contact with water molecules. However actual micelle structure can change depending on solution and concentration of SDS.

### 3.1.3 Triton x-100

Triton x-100 or Iso-octyl phenoxy polyethoxy ethanol is a non-ionic surfactant very viscous at room temperature, it has a hydrophilic (head) polyethylene oxide group (on average it has 9.5 ethylene oxide units) and a hydrocarbon hydrophobic (tail) group. The part of head formed from ethylene oxide is more hydrophilic than the part from propylene oxide. It is commonly used in laboratories for cleaning purposes, and has longer shelf life.

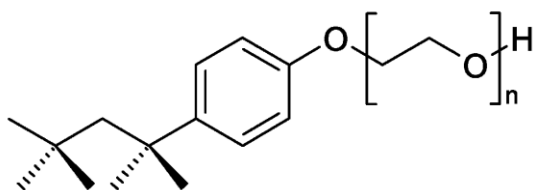


**Figure 3.1.3a Structure of Triton x-100 with heavy benzyl head and hydrophobic tail**

S NO.	Parameters	Value
1	CAS number	9002-93-1
2	Moles of Ethylene oxide	10 moles
3	pH (5% aqueous solution)	6-8
4	Weight per ml at 20 <sup>0</sup> C	1.06 gm
5	Activity	100%
8	Cost per 500 ml	1000 Rs
9	Manufactured by	Loba Chemie Pvt. Ltd (Mumbai) – 400 005

**Table 3.1.3b Physical and chemical properties of Triton x-100 including cost**

Studies indicate [37] that at high shear rate these additives undergo permanent degradation in their drag reduction properties; the bonds formed by the polyethylene group are not so strong at higher shear rates. But, the action of Triton x-100 is quite stable and environmental friendly than most of the charged surfactants. The effect of Triton on drag reduction is stable in a wide range of temperature.

## 3.2 Fly Ash Used

### 3.2.1 Chemical composition (EDS) and SEM analysis of fly ash

SEM (scanning electron microscope) analysis of raw fly ash sample is done without grinding or refining it, to see and study the actual microstructure of fly ash particles. Results showed that shape of the particles is spherical as shown in figure 3.2.1b at 5000 magnification, also due to moisture content present in fly ash, some particles are clustered together to form rock like images as shown in figure 3.2.1a at 2000 magnification, it is noticeable that grinding the raw fly ash can greatly improve the flow behaviour of the slurry by increasing surface contact area for the action of additives, but in this work effect of additives on raw fly ash is studied.

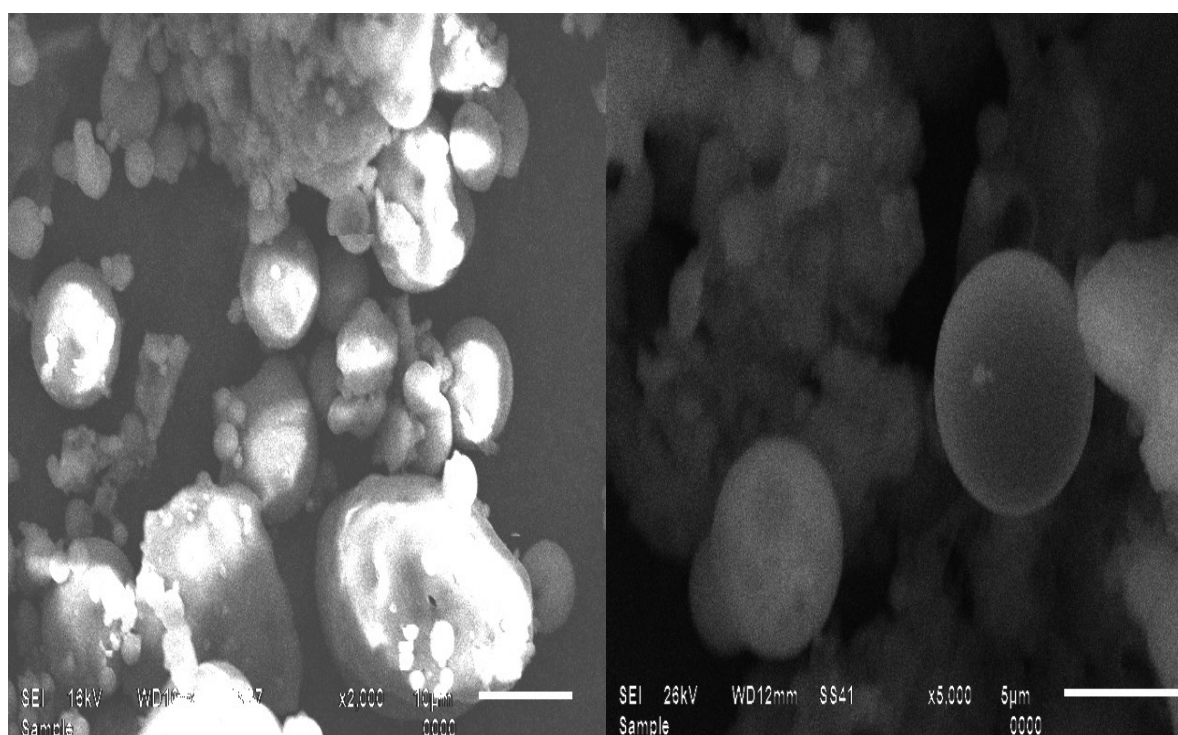
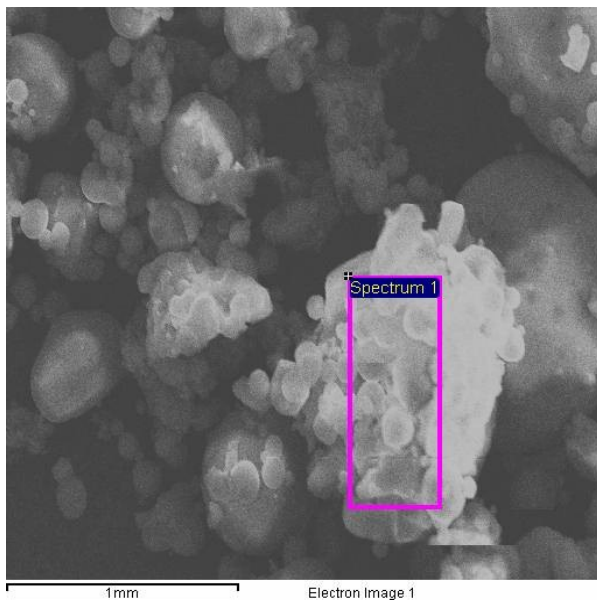


**Figure 3.2.1 (a) SEM results for fly ash sample at 2000 and (b) 5000 magnification**

Chemical composition of fly ash sample is determined through EDS analysis, a small section of fly ash sample is selected as shown in figure 3.2.1c and the composition of this section is determined as shown in figure 3.2.1d., we can observe that lime (CaO) content is very less which is generally known as a property of low calcium class F fly ash according to ASTM standards. This type of fly ash is pozzolanic in nature and requires a cementing agent such as Portland cement and calcium hydroxide with water to produce some cementing properties.



Element	Weight %	Compd %	Formula
C	6.74	24.69	CO <sub>2</sub>
Al	15.96	30.15	Al <sub>2</sub> O <sub>3</sub>
Si	17.09	36.57	SiO <sub>2</sub>
K	0.90	1.09	K <sub>2</sub> O
Ca	0.35	0.49	CaO
Ti	1.39	2.32	TiO <sub>2</sub>
Fe	1.27	1.64	FeO
Cu	1.36	1.70	CuO
Zn	1.10	1.37	ZnO
O	53.84	-	-
<b>Total</b>	100.00	100.00	

**Figure 3.2.1c Selected section of fly ash**

**Table 3.2.1d Composition determined**

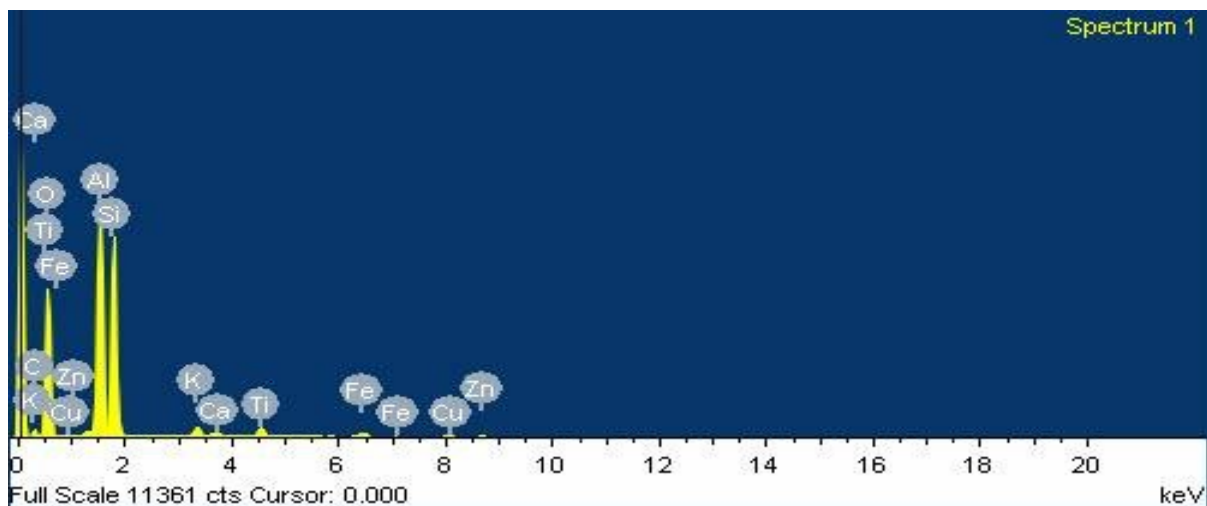


**Figure 3.2.1e Spectrum of elements present in fly ash sample**

### 3.2.2 Particle size distribution (PSD) of fly ash

PSD of fly ash is estimated using the process of mechanical sieving. In this process sieves are arranged from top to bottom, with topmost sieve having mesh width of maximum size. Sizes in sieves are measured in micro meter ( $\mu\text{m}$ ). There are basically 2 standards to designate a sieve; these are British and American standards. In both these standards a given sieve is designated with a number called mesh number. A conversion table between British and American standard is given in Annexure E. The sieves used for this experiment are designated with British standard.



**Figure 3.2.2 (a) Fly ash sample (b) Sieve system arrangement (c) Mechanical sieving machine.**

#### Procedure

- 100 grams of fly ash sample is dried in an oven at 200°C for 60 minutes to remove any moisture content.
- After drying the next step is putting this sample on top most sieve of the sieve system and closing this sieve tightly with metal bin. In this sieve system, sieves are arranged from largest size sieve at top to smallest sieve at bottom. At the bottom a pan is placed to collect remaining fly ash after sieving is done.
- This arranged sieve system is then placed on a mechanical shaker, and timer is set for 20 minutes of sieving time.
- After sieving the particles collected in each sieve are measured and particle size distribution is calculated.

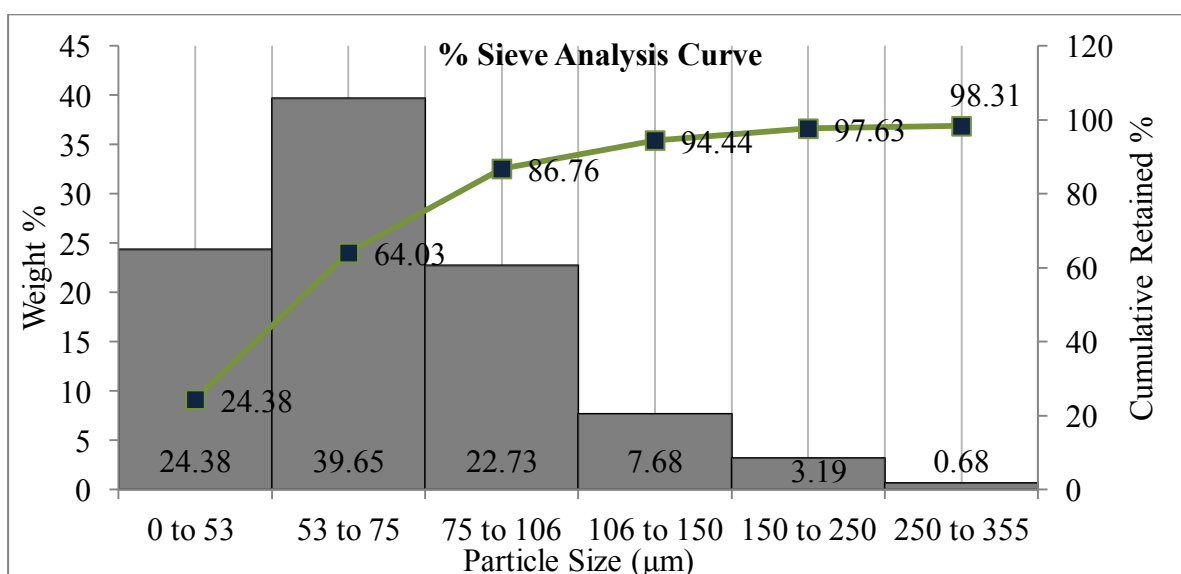


**Figure 3.2.2d Particle size distribution of fly ash with curve for cumulative weight retained**

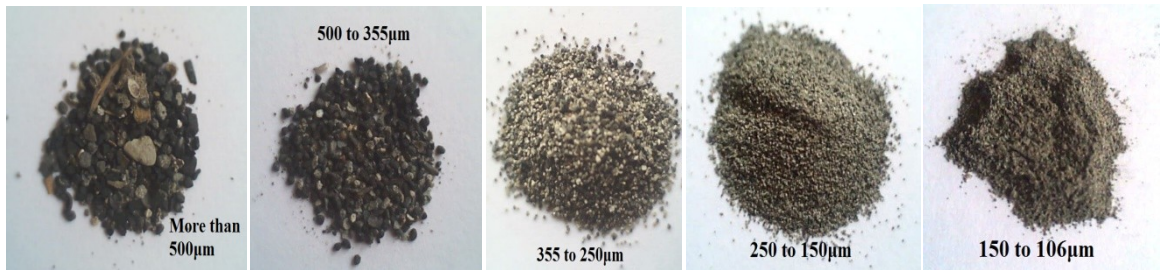


**Figure 3.2.2e Visuals of particles greater than 100 µm size**



**Figure 3.3.2f Visuals of particles less than 100 µm size**

It can be observed that majority of fly ash particles (about 40%) lie in the range of 53 to 75 µm, 24% lie from 0 to 53 µm range and about 23% lie in 75 to 106 µm range. From cumulative retained graph we can observe that these 3 particle ranges cover about 87% of the total weight. It will be analysed in the upcoming results that the overall viscosity of fly ash slurry depends mainly on these 3 particle ranges. It will also be observed that presence of large particles (size more than 100 µm) affects the flow properties adversely by increasing viscosity. But due to their smaller percentage smooth flow is maintained. Calculations involved for the process are given in Annexure E

### **3.3 Instrument Used**

#### **3.3.1 Rheolab QC (Make: Anton paar)**

The Rheolab QC rheometers are based on a concept at the cutting edge of technology. The EC motor technique, the low friction bearing and the patented normal force sensor have been optimized over years to satisfy the highest demands of rheologists. Any type or combination of rheological tests, both in rotational and oscillatory mode, is possible with the Rheolab QC rheometers. The modularity of the system allows the integration of a wide range of temperature accessories and special modules. The innovative and patented features Toolmaster™ and TruGap™ are breakthroughs in terms of user-friendliness.



**Figure 3.3.1 (a) Rheolab QC rheometer (b) Geometry used for measurements of higher concentration slurry.**

### 3.3.2 Technical features [20]

Some highlights are as follows

- Powerful, synchronous EC motor drive
- High-precision air bearing, including patented sensor for normal force measurement
- TruGap™: Innovative and patented system for measuring the gap
- Real-time position control oscillation (DSO): Fast and accurate strain control
- Nano rheology for nonmaterial science
- Different MCR models with outstanding specifications for various applications.

Other Features

- Toolmaster™: Patented system for automatic recognition of measuring system and accessories.
- Quickfit coupling: Easy, one-hand measuring system connection.
- Wide range of measuring systems for all kinds of applications.
- Ethernet connection for remote control of the instrument through the company network.
- RheoPlus: User-friendly application software with 21 CFR Part 11 compatibility and LIMS/SAP interface.

### 3.3.3 Detailed specifications [20]

Property	Range
R.P.M	$0.01\text{min}^{-1}$ to $1200\text{min}^{-1}$
Torque	0.25 m-Nm to 75m-Nm
Shear stress	$0.5$ to $3 \times 10^4$ Pa
Shear rate	$10^{-2}$ to $4000\text{ s}^{-1}$
Viscosity range	1 to $10^9$ mPas

(depending on geometry used)	
Temperature range	-20 <sup>0</sup> C to 180 <sup>0</sup> C
Angular resolution	2 μrad
Physical variable (measurement and evaluation)	<ul style="list-style-type: none"> <li>▪ Dynamic viscosity</li> <li>▪ Shear stress</li> <li>▪ Shear rate</li> <li>▪ Speed</li> <li>▪ Torque</li> <li>▪ Temperature</li> <li>▪ Time</li> <li>▪ Kinematic viscosity</li> <li>▪ Yield Stress</li> <li>▪ Deformation</li> <li>▪ Compliance</li> </ul>

**Table 3.3.3d Specifications of Rheolab QC rheometer**

### 3.4 Experimental Procedure

#### 3.4.1 Preparation of slurry for rheometer

##### 3.4.1.1 Preparation of slurry without additive

All the samples of fly ash slurry are prepared by weight ( $C_w$ ). The required concentration of fly ash is weighted on a weighting scale with accuracy of 0.001gram, water as a solvent is measured in millilitres (ml), and its concentration is calculated by subtracting the % conc. of fly ash from 100. Required solution is mixed thoroughly for 20 minutes for homogeneous mixing. All the samples are freshly prepared just before any experiment. After thorough mixing the slurry is poured immediately to the geometry used. The geometry is then connected to magnetic coupling of rheometer for experiment.

##### 3.4.1.2 Preparation of slurry with additive

All the additives in this study are used as purchased and no further refinement was done. All the Samples are prepared by weight ( $C_w$ ). The required concentration of fly ash is weighted, and concentration of water is calculated same as before, the weight of additive is measured on weight scale with accuracy of 0.001 gram. The weight is calculated based on the percentage concentration of total solution. Example: if total solution (fly ash + water) weigh 66.666 gm then 0.5% by weight of additive would be 0.33 gram (i.e.  $66.666\text{gm} * 0.5\%$ ). These concentrations of fly ash and additive are mixed thoroughly with water for 20 minutes for proper mixing. The slurry obtained is immediately poured into the geometry and then connected with rheometer for measurement.

### 3.4.1.3 Preparation of slurry of a specific particle size range

Mechanical sieving of fly ash is done; the process of sieving is same as adopted for the determination of particle size distribution, samples of different particles sizes are collected from sieves and sealed in air tight plastic bags. For preparation of slurry, fly ash of specific size range is weighted on a weighing scale, and then the process goes same as for the preparation of slurry with or without additive.

## 3.4.2 Gravitational settling experiment

### 3.4.2.1 Preparation of slurry

All the samples are prepared by weight; a vertical 1 litre cylinder, with markings in ml is used to measure water content required. The calculation involved for finding percentage weight of fly ash and water is same as used in preparation of slurry for rheometer. Weighted fly ash sample is mixed with water; a minute amount of potassium permanganate is added to the solution for clear demarcation. The solution is stirred in the cylinder for 20 minutes with a glass rod and shaken well before keeping it on a horizontal still surface for the process of measurements. In case of addition of additive, weighted percentage dosage of additive is added with fly ash and mixed with water.

### 3.4.2.2 Method of measurement



A measuring tape with a scale in centimetres is pasted to the surface of cylinder in vertical direction starting from bottom to top as shown in figure (3.4.2.2a). After shaking the slurry solution in cylinder, it is kept on a still horizontal surface; a stopwatch is used for measuring time. Time of measurement is started when a slurry start settling down and a dark line of potassium permanganate in water became visible. Values of settled height are measured in centimetre from the scale pasted on it. Due to very clear demarcation all the readings were taken up to 2 decimal places of a centimetre.

**Figure 3.4.2.2a Cylinder with measuring tape attached**

## CHAPTER 4

## RESULTS AND DISCUSSIONS

## 4.1 Study of Flow Behaviour of Slurry with variable Fly Ash Concentration

## 4.1.1 Effect on viscosity of slurry with increase in concentration

In this experiment, concentration of fly ash is varied from 10% to 60% by weight and the effect on viscosity of slurry with each concentration is studied for a range (0 to 500s<sup>-1</sup>) of shear rate. The shear stresses vs shear rate graphs are shown in figures (4.1.a to 4.1.f). It can be observed that at low concentrations (i.e. 10%, 20% and 30%) the graph is almost a straight line and so viscosity is approximately constant at all the shear rates, this is one of the reasons that a leaner slurry is preferred for transportation in power plants, it can be observed from figures (4.1.1d to 4.1.1f) that at higher concentrations the slurry shows dilatant or shear thickening behaviour.

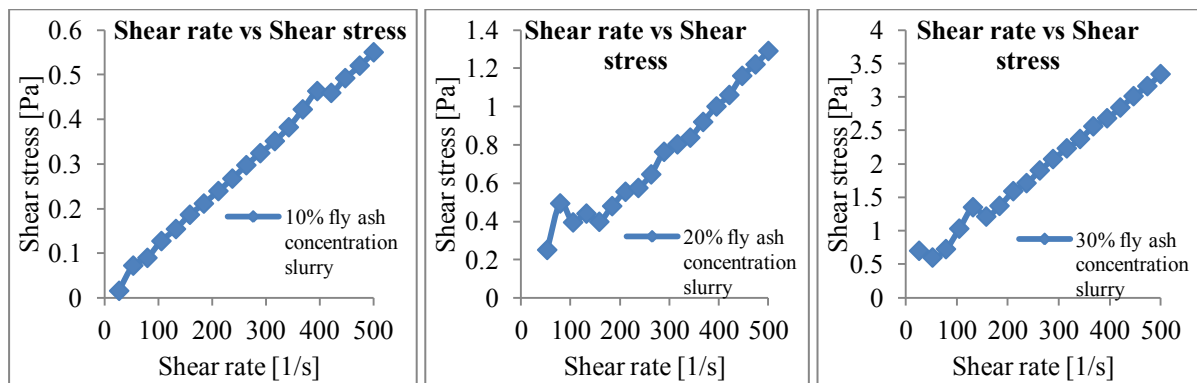


Figure 4.1.1 (a) System generated shear stress graph at 10% fly ash (b) at 20% fly ash (c) at 30% fly ash

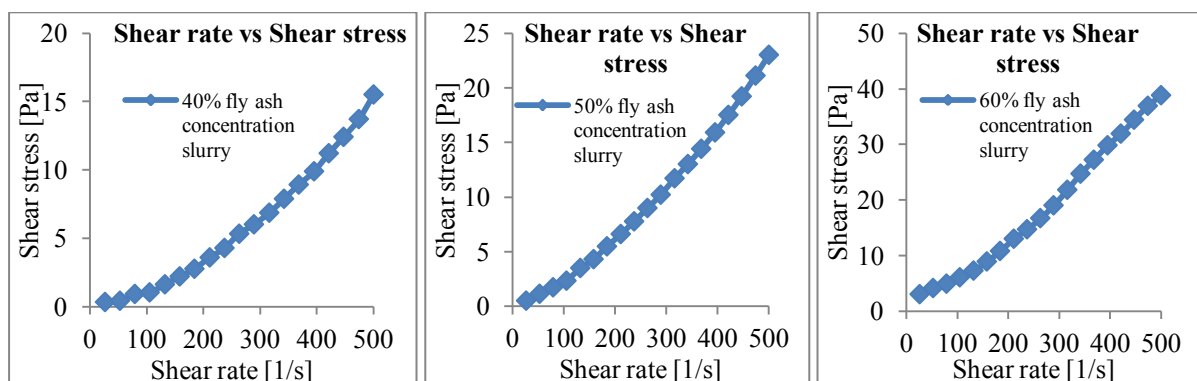
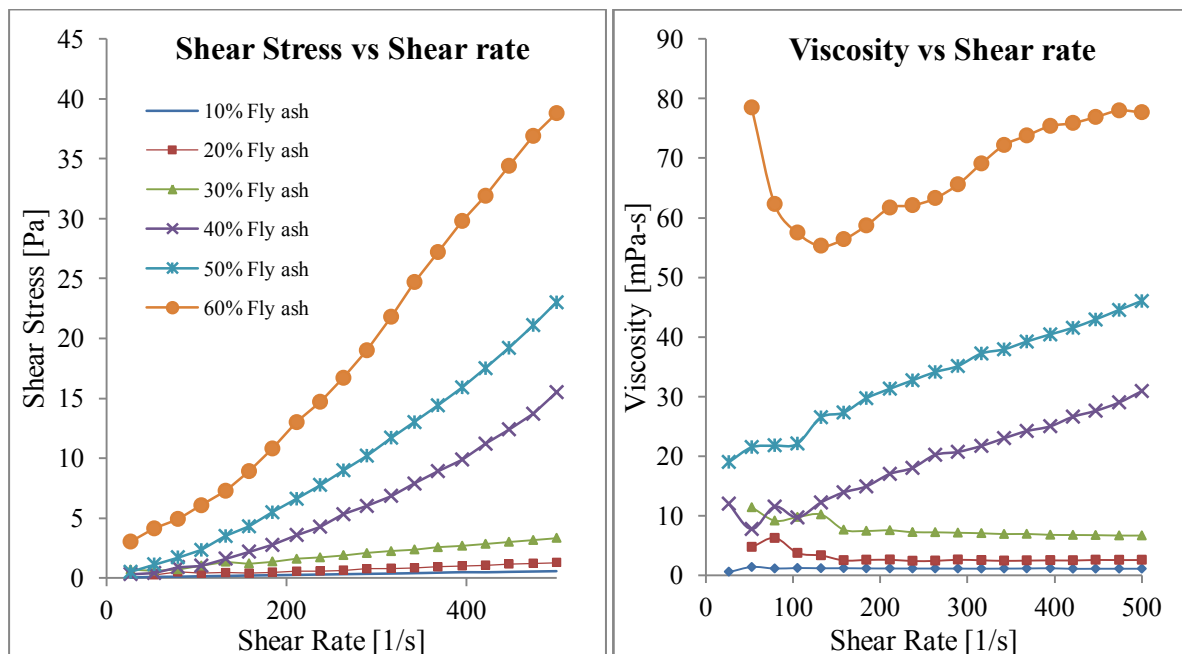


Figure 4.1.1 (d) System generated graph at 40% fly ash (e) at 50% fly ash (f) at 60% fly ash

Measurement data is listed in Annexure A

#### 4.1.2 Calculation of co-relation relating average viscosities and shear stresses of different concentration slurries

Figure 4.1.2a and figure 4.1.2b compare the shear stresses and viscosities of slurries at different concentrations. It can be observed that shear stresses increased drastically with increase in fly ash concentration. To analyse the data, average viscosities and shear stresses of different slurries are calculated, and by observing them it is estimated that the relation between change in average viscosity and shear stress with increase in concentration of fly ash is exponential in nature. Based on the analysis it is observed that due to this exponential rise, large concentration of fly ash in slurry give sudden fluctuation in viscosity, which adversely affect the flow behaviour. Also dilatant behaviour is increased giving unpredictable results at high shear rates.



**Figure 4.1.2 (a) Comparison of shear stresses of different concentration slurries (b) Comparison of actual apparent viscosities.**

It is observed through figure 4.1.2b that after 30% concentration there is a rise in slope, indicating increase in viscosity with increase in shear rate. Figures 4.1.2c and 4.1.2d depicts the actual increase in average viscosity and shear stress with increase in concentration. Figures 4.1.2e and 4.1.2f shows the exponential increase in average viscosity and shear stress calculated from the co-relations. The co-relations are listed at the bottom of figures 4.1.2e and 4.1.2f. Calculations involved in the analysis are listed in Annexure A

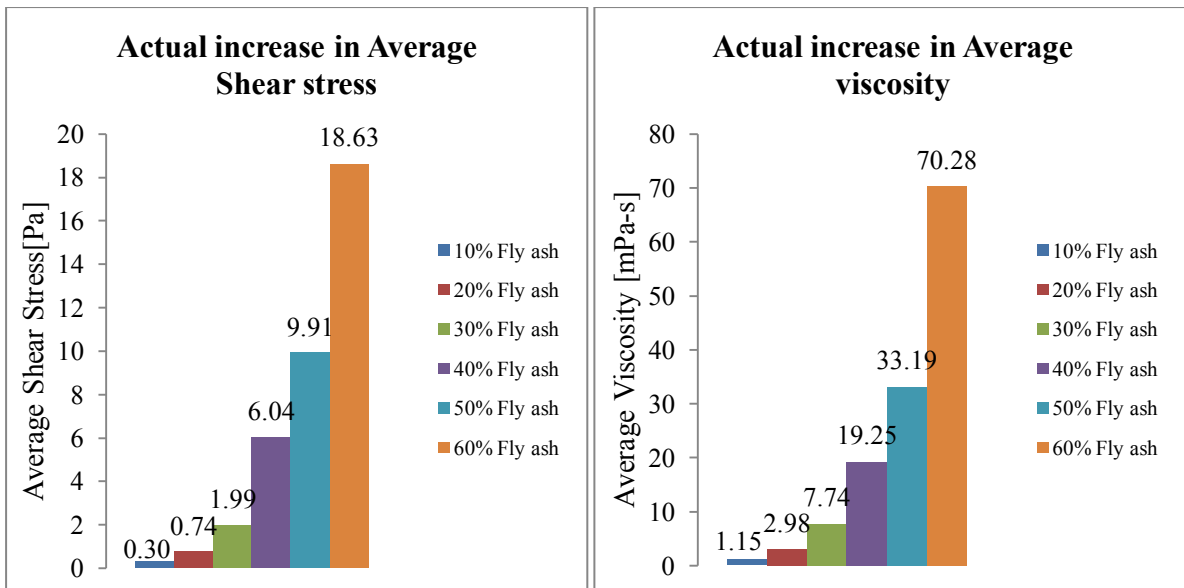


Figure 4.1.2 (c) Actual increase in average shear stress (d) Actual increase in Average viscosity

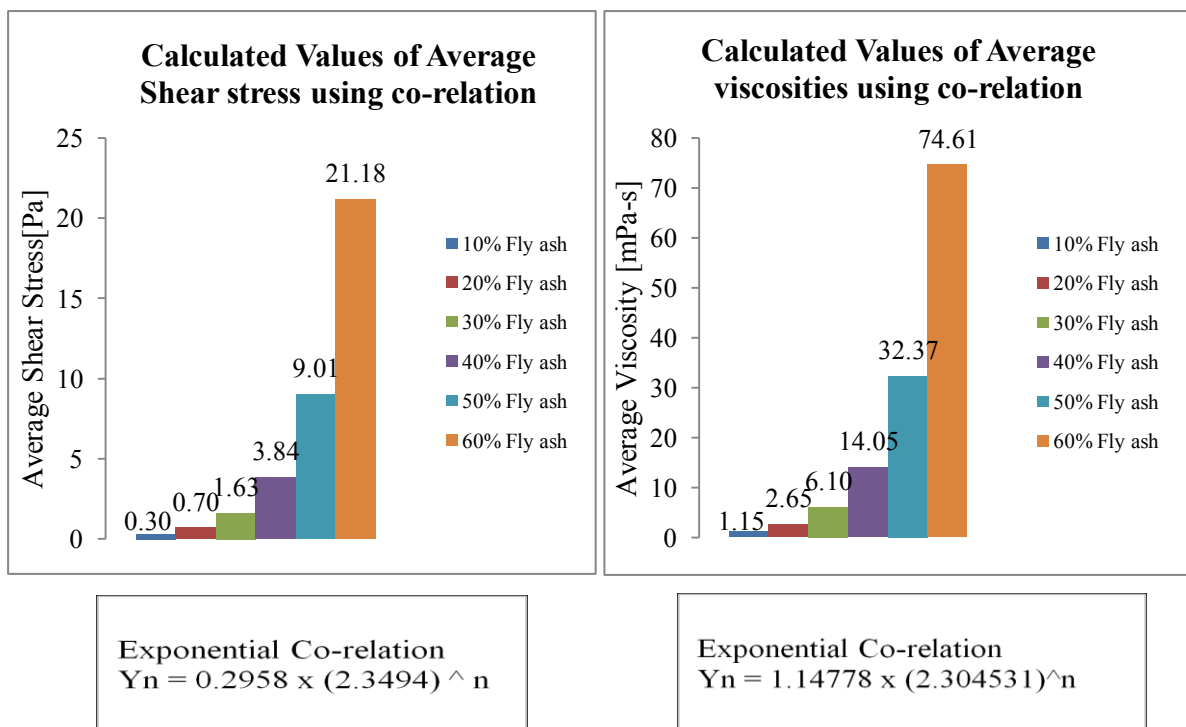


Figure 4.1.2 (e) Calculated average shear stress using co-relation (f) Calculated average Viscosity using co-relation.

Here,  $n$  is the power index and its value is 0 at 10%, 1 at 20% till 5 at 60% fly ash concentration.

#### 4.1.3 Modelling using Oswald de Waele rheological model

From figure 4.1.2b it is observed that even at high concentrations of fly ash in slurry (such as 40%, 50% and 60%) the apparent viscosity points still represents approximately a straight line. This is an indication that if viscosity lines are straight then there is a possibility that

shear stress curve can be approximated using a power law model. In this section, Oswald de Waele rheological model is used to calculate values of apparent viscosities. Another way to find the applicability of this model is to plot the shear stress vs shear strain values on logarithmic scale as shown in figure 4.1.3a and observe whether these points together form a straight line or not. It can be observed that lines are straight on log-log plot with good coefficient of regression 'r' ('r' defines the strength of regression).

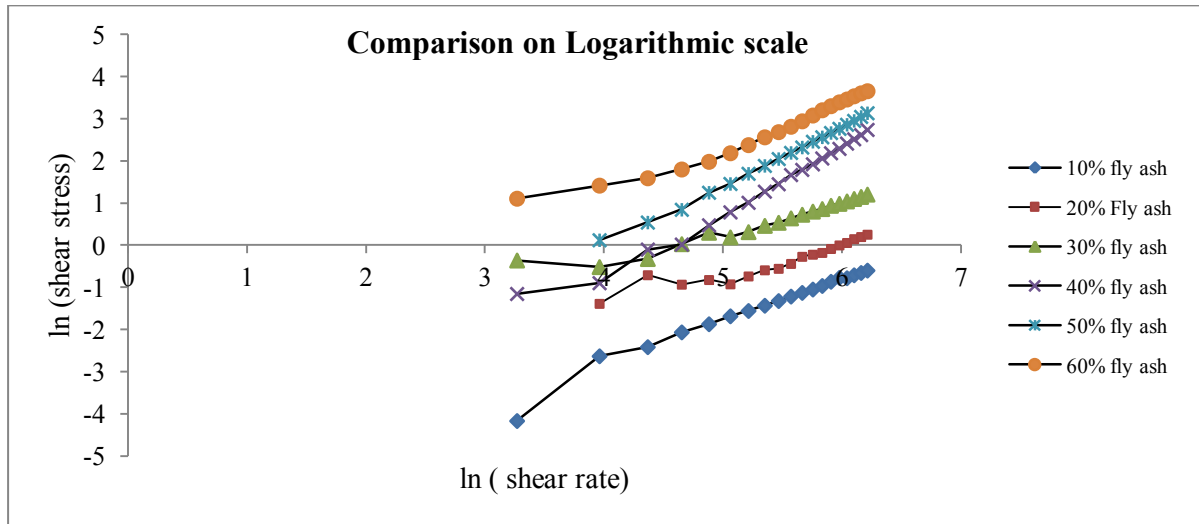
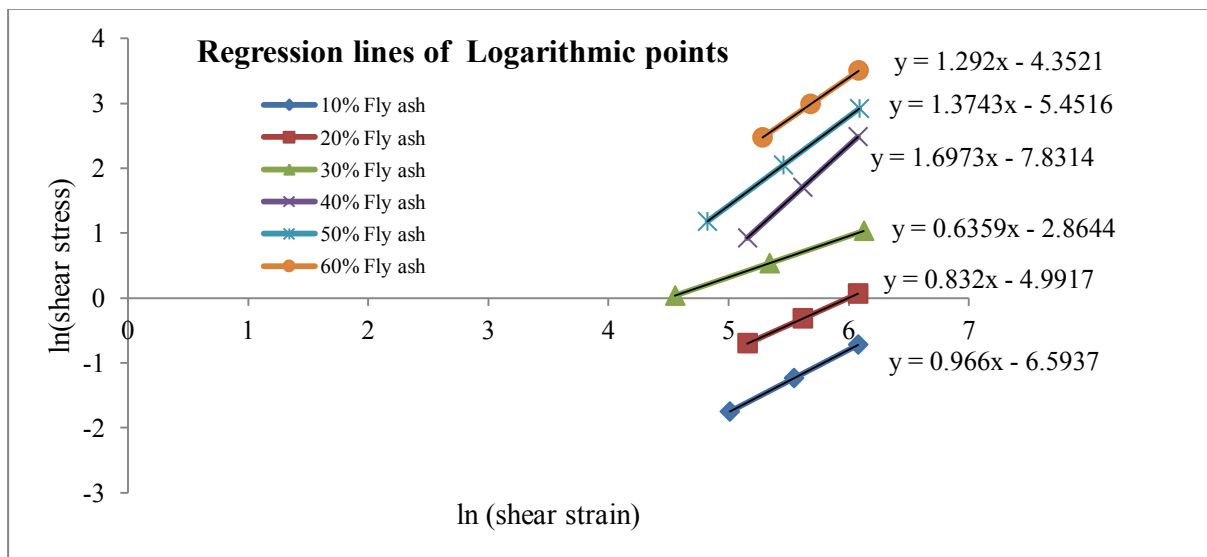


Figure 4.1.3a Comparison of shear stress vs shear strain on logarithmic scale



COEFFICIENT OF CORRELATION 'r'					
r1 (10% fly ash )	r2 (20% fly ash )	r3 (30% fly ash )	r4 (40% fly ash )	r5 (50% fly ash )	r5 (60% fly ash )
0.999184367	0.976561217	0.96282542	0.99961203	0.9987823	0.99939599

Figure 4.1.3b Regression lines with points plotted in the range of one standard deviation.

SLOPE (n) of Regression Lines					
10% fly ash on log	20% fly ash on log	30% fly ash on log	40% fly ash on log	50% fly ash on log	60% fly ash on log
n = 0.96596587	n = 0.8320407	n = 0.63589812	n = 1.6972993	n = 1.37430358	n = 1.29197702
ln (K)= -6.5937	ln (K)= -4.9917	ln (K)= -2.8644	ln (K)= -7.8314	ln (K)= -5.4516	ln (K)= -4.3521
K= 0.00136897	K= 0.0067941	K= 0.05701733	K= 0.00039707	K= 0.00428944	K= 0.01287974

Table 4.1.3c Table showing the modelling parameters calculated using experimental data

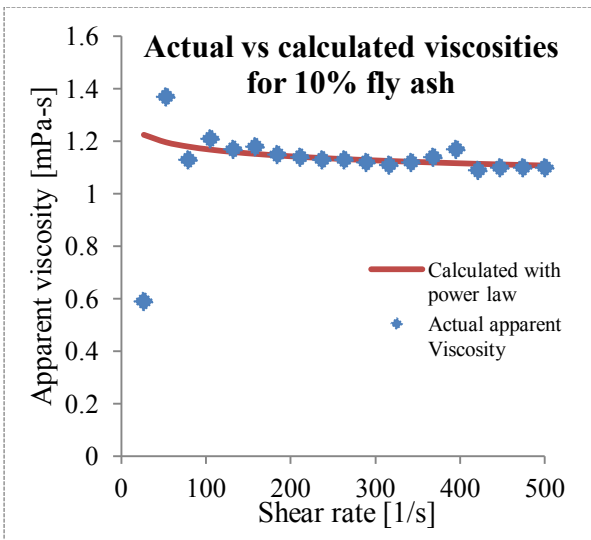


Figure 4.1.3d 10% fly ash slurry

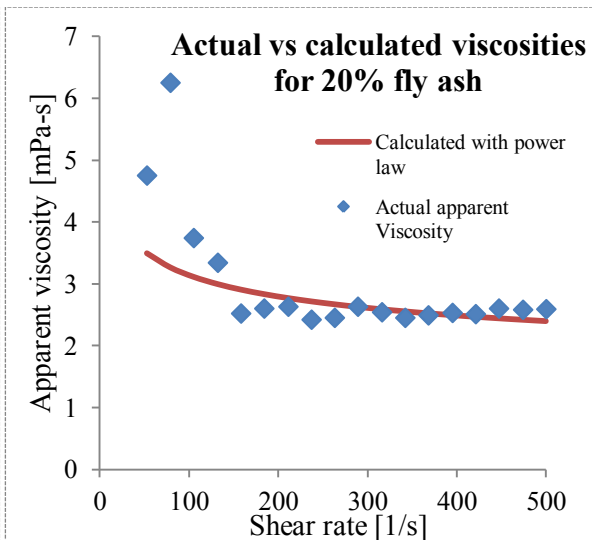


Figure 4.1.3e 20% fly ash slurry

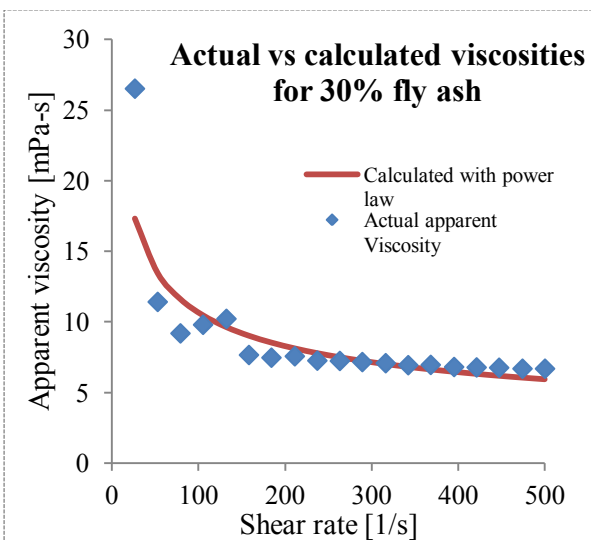


Figure 4.1.3f 30% fly ash slurry

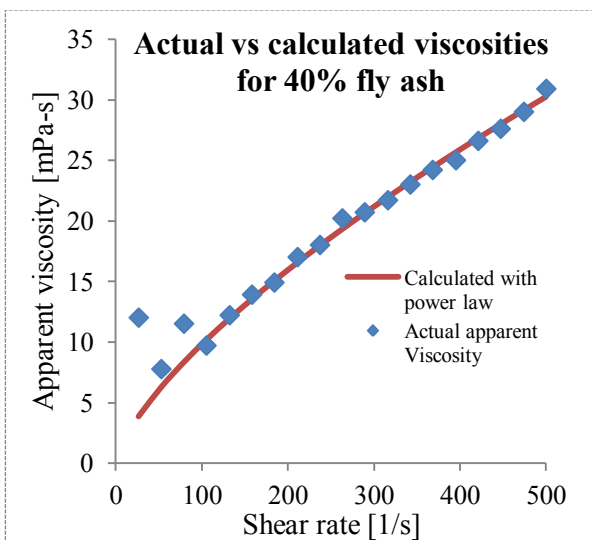


Figure 4.1.3g 40% fly ash slurry

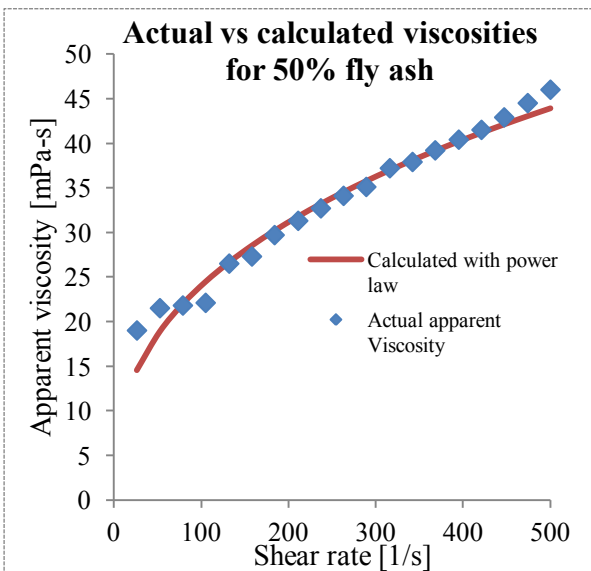


Figure 4.1.3h 50% fly ash slurry

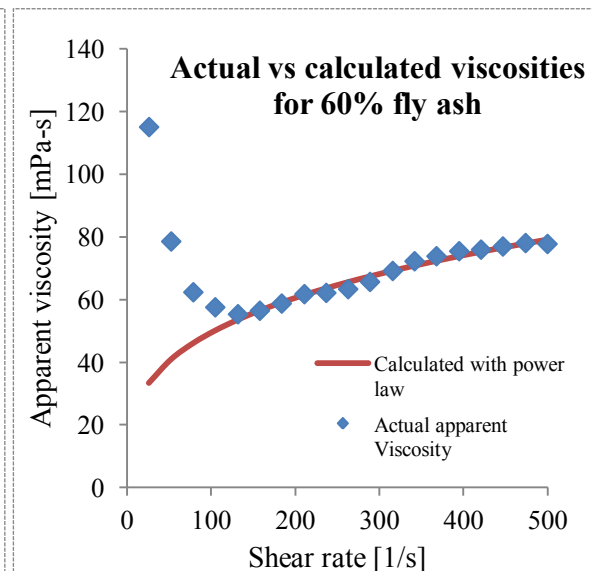


Figure 4.1.3i 60% fly ash slurry

It is observed from table 4.1.3c that value of viscosity index 'n' has changed from 0.63 (less than 1) at 30% concentration to 17 (greater than 1) at 40%. This increase signifies a sudden change in flow behaviour from pseudoplastic to dilatant.

Every model has a certain minimum 'x' value below which it cannot predict accurate values. Above figures (4.1.3d to 4.1.3i) shows the accuracy of modelling by comparing it with actual viscosity values. It is observed that viscosity values at very low shear rates (less than  $50\text{s}^{-1}$ ) are quite unpredictable using this model. The model works very well for higher shear rates ( $100\text{s}^{-1}$  to  $500\text{s}^{-1}$ ). It can be observed from figures 4.1.3g and 4.1.3h, that the model worked very well for the wide range of shear rate (0 to  $500\text{s}^{-1}$ ) at 40% and 50% concentrations. From figure 4.1.3i we can observe that at high concentration (60%) the ' $x_{\min}$ ' of the model has increased and is not predicting the viscosity values less than  $130\text{ s}^{-1}$  shear rate. It can be concluded that no matter, how the concentration of fly ash is varied the model is highly capable of predicting accurate viscosity values greater than  $100\text{ s}^{-1}$ , and at higher shear rates it works even better. The accuracy of model also highly depends on the method of selection of data points used for regression. A careless selection process can adversely deviate the calculated values from actual viscosity values. The modelling data is listed in Annexure A

Finally, from this study of flow behaviour of slurry it can be concluded that the exponential rise in viscosity makes the use of higher concentrations unfavourable, even after addition of additive the drag reduction will not be much. On the other hand, 40% concentration lies in the middle and additives can reduce its drag properties to an appreciable extent. It would not be unwise to experiment with this concentration of fly ash in slurry and see the results of additives on it. Also from modelling analysis we can observe that at 40% concentration of fly ash, the model worked well at all the shear rates. This shows the smooth flow behaviour and predictability of 40% fly ash slurry. Based on the above thoughts, experiments are done with 40% fly ash concentration slurry. The results are discussed below.

## **4.2 Effect of Additives on Drag Reduction of 40% Fly Ash Slurry**

### **4.2.1 Effect of CPC on drag reduction**

In this section the effect of 3 different concentrations (0.5%, 1% and 1.5% by weight) of CPC is studied. Figure 4.2.1a and 4.2.1b compare the viscosity and shear stress values of slurry with and without CPC. It can be observed from these figures that appreciable amount of reduction in viscosity is obtained in the shear rate range of 0 to  $260\text{s}^{-1}$ . Also in this range the effect produced by the 3 different dosages of additives is almost the same. It can be observed that at higher shear rates ( $260$  to  $500\text{s}^{-1}$ ) there is a change in the pattern of viscosity curve,

and we can see an increase in viscosity in this range. If we observe closely, the change is not sudden and starts building up at  $230\text{s}^{-1}$  and finally ready to flourish at  $260\text{s}^{-1}$ .

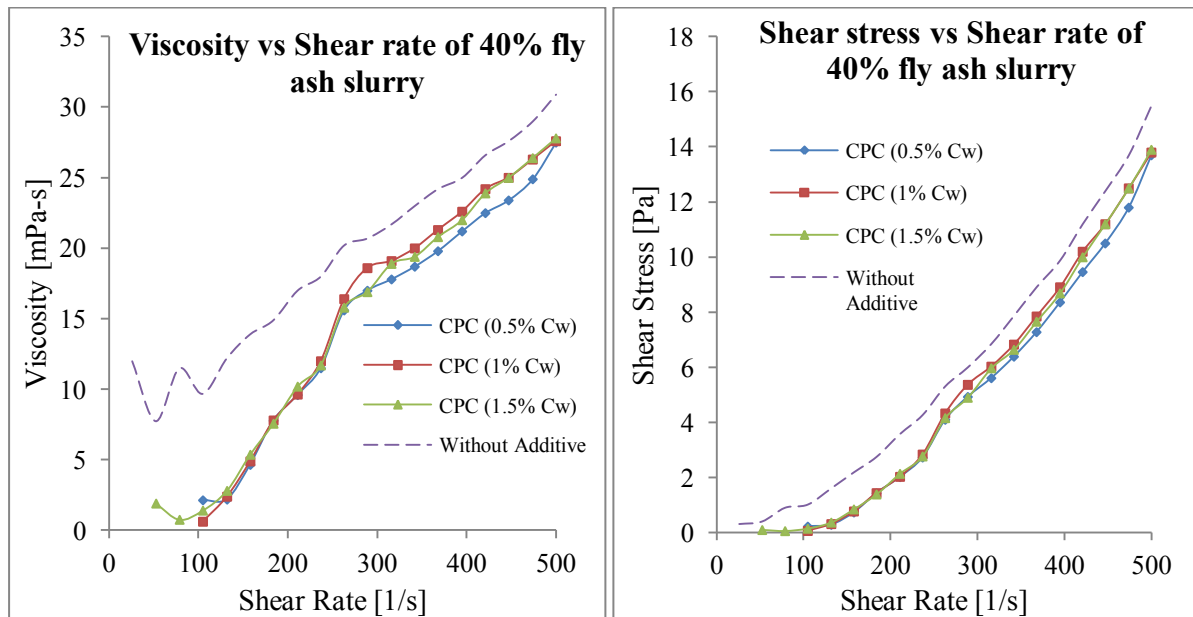


**Figure 4.2.1 (a) Viscosity reduction with addition of CPC (b) Shear stress plot of slurry with and without CPC with 40% (by weight) fly ash concentration**

This phenomenon of increase in viscosity in the shear range of  $260$  to  $500\text{s}^{-1}$  is associated with aggregation of micelles induced by the high shear rate flow [29]. It is observed that the process of micelle aggregation started at  $230\text{s}^{-1}$ , which created a bend and disrupted the straight line smooth pattern of viscosity increase. It is noticed that at high shear rates, slurry with  $0.5\%$  CPC has less viscosity than slurries with  $1\%$  and  $1.5\%$  CPC. This is because with increase in the dosage of additive, more micelles are generated [24, 29] and aggregated under the high shear flow. Even after increase in viscosity at high shear rates, the slurries with CPC bear less viscosity than slurry without CPC for the whole range of shear rates ( $0$  to  $500\text{s}^{-1}$ ). It can be observed that best and optimal dosage of CPC is  $0.5\%$ . Related data values are listed in Annexure B

#### 4.2.2 Modelling of slurries containing CPC

In order to analyse the flow behaviour of slurries (pseudoplastic or dilatant) modelling is necessary. The applicability of the model is estimating by observing the log-log plot as shown in figure 4.2.2a. Data points following a straight line patterns conforms the reliability of the model. Figure 4.2.2b shows the regression lines of data points drawn up to one standard deviation.

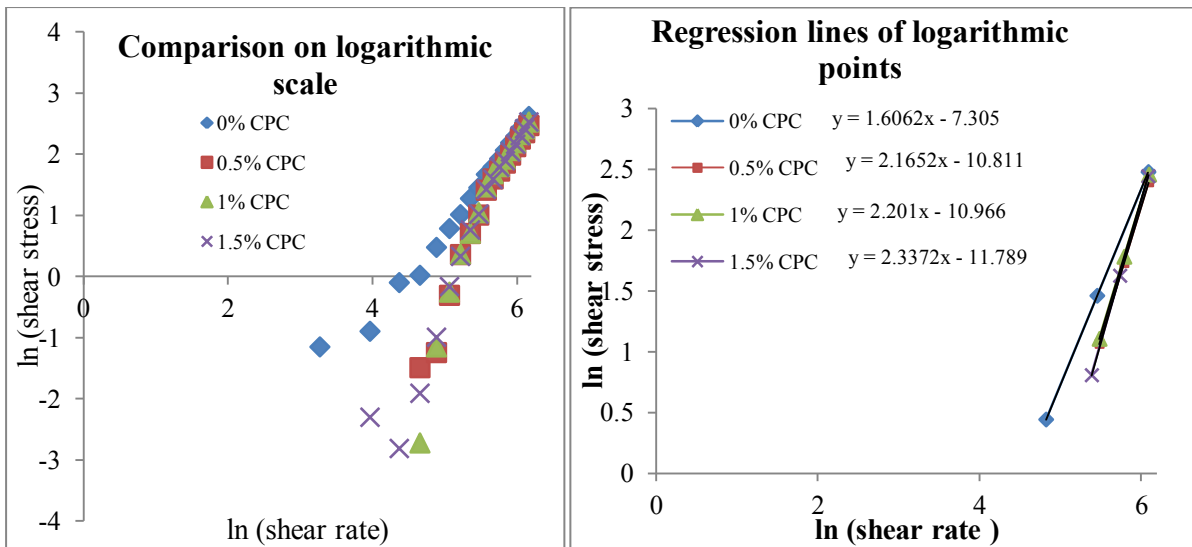


Figure 4.2.2 (a) Data points on log-log plot (b) Regression lines of points with equations on display

COEFFICIENT OF CORRELATION 'r'			
r1 (0% CPC )	r2 (0.5% CPC )	r3 (1% CPC )	r4 (1.5% CPC )
0.997944642	0.993180152	0.990122135	0.992293414

Table 4.2.2c Coefficient of correlation 'r' of regression lines

slope = viscosity index (n)							
0% CPC		0.5% CPC		1% CPC		1.5% CPC	
slope =	1.60619	slope =	2.165245386	slope =	2.201008006	slope =	2.337201478
ln (K) =	-7.305	ln (K) =	-10.811	ln (K) =	-10.966	ln (K) =	-11.789
K =	0.00067	K =	2.01763E-05	K =	1.72793E-05	K =	7.58756E-06

Table 4.2.2d Modelling parameters of slurries

Figures 4.2.2e to 4.2.2f compare the actual apparent viscosity values with modelled values. The model worked well even with slurries containing additive. It can be observed from table 4.2.2d that viscosity index 'n' increases with increase in the dosage of CPC conforming an increase in dilatant behaviour of slurry to increase in additive.

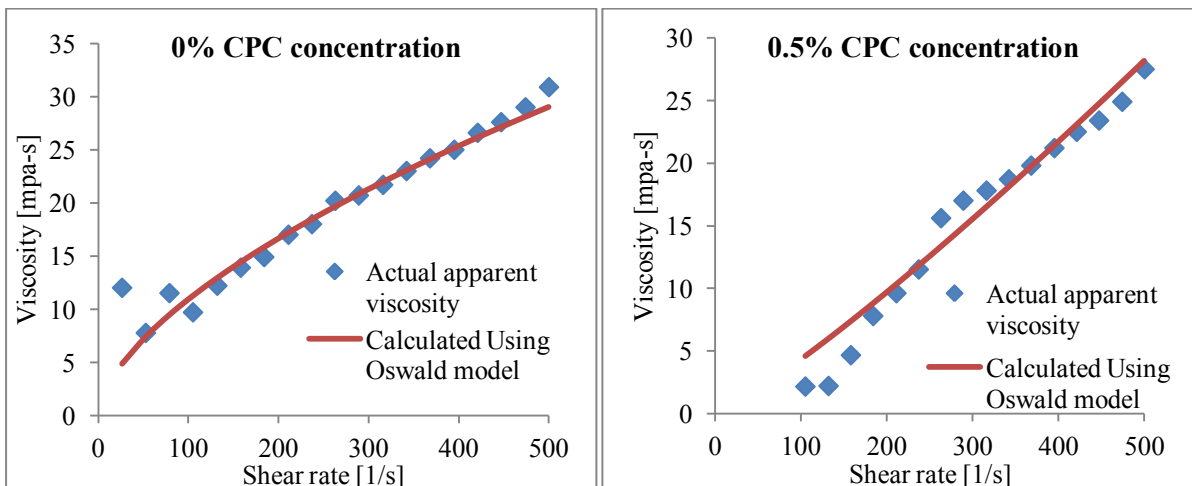
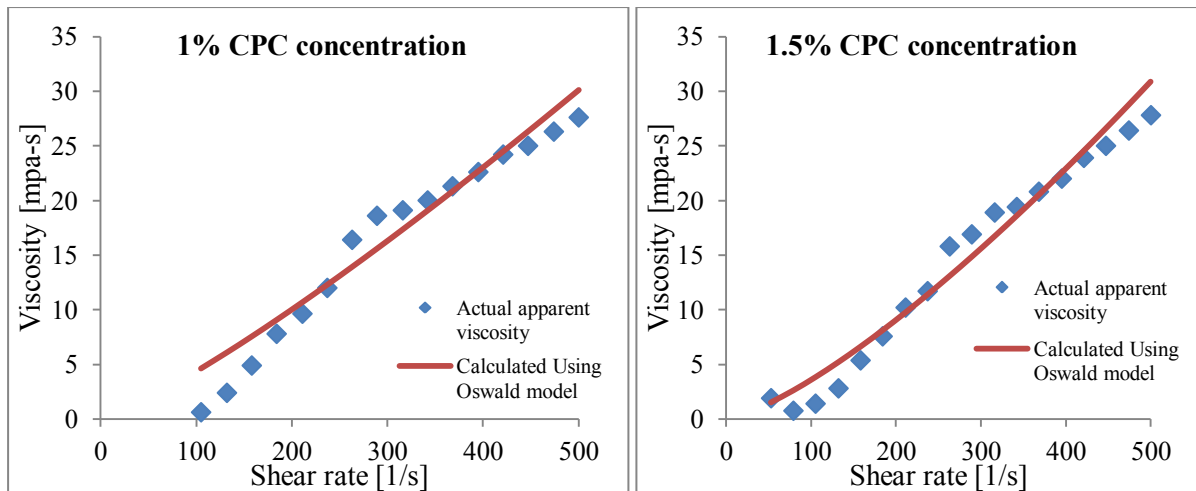


Figure 4.2.2e 40% slurry without CPC

Figure 4.2.1.2f 40% slurry with 0.5% CPC



**Figure 4.2.2g 40% fly ash with 1% CPC**

**Figure 4.2.2h 40% fly ash with 1.5% CPC**

From table 4.2.2d we can see that the value of consistency coefficient ‘K’ (another parameter which indicates viscosity level) also decreases with increase in CPC dosage indicating smooth flow behaviour attained with each increase in CPC concentration.

#### 4.2.3 Effect of SDS on drag reduction

SDS is anionic in nature with a long hydrophobic tail. Figures 4.2.3a and 4.2.3b display the effect of different dosages of SDS on Viscosity and shear stresses. It is observed that viscosity of slurry decreases with increase in the dosage of SDS. The same phenomenon of aggregation of micelles at higher shear rates (more than  $260\text{s}^{-1}$ ) is observed. Results obtained from 1.5% of SDS are better as compared to 0.5 and 1% of SDS. At this dosage the viscosity of slurry has reduced appreciably at low as well as high shear rates. The use of high dosage of SDS is also economical, as it is derived from inexpensive coconut and palm oil and hence has its cheap manufacturing cost.

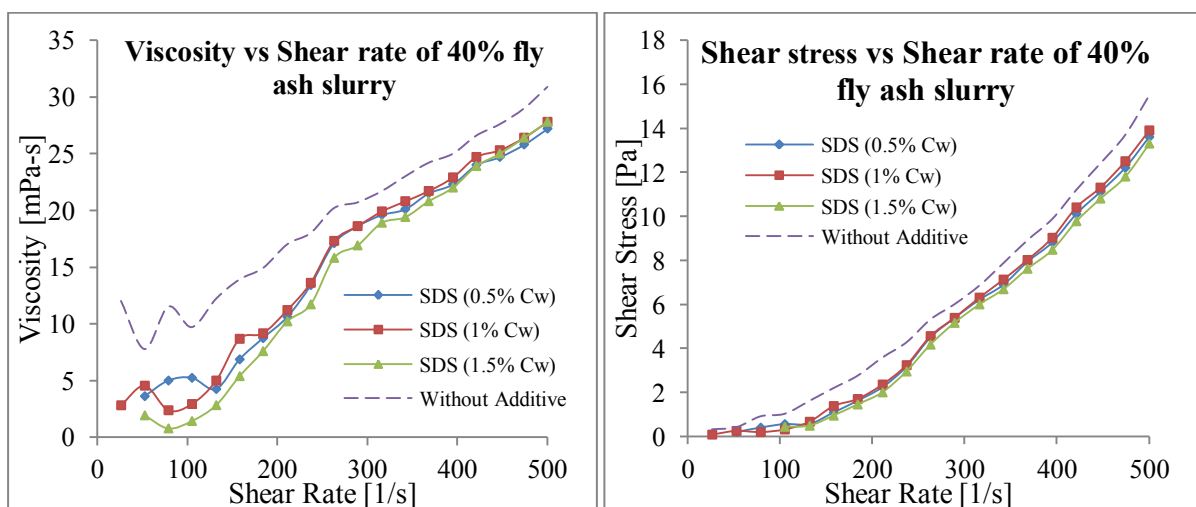


**Figure 4.2.3 (a) Effect of SDS on viscosity (b) Reduction in shear stress of slurry using SDS with 40% (by weight) fly ash concentration**

The similarity in the process of drag reduction between SDS and CPC can be accounted from the fact that both of these additives have hydrophobic tail, only the charge on the head is different. The action of these charged heads on the surface of fly ash particles increases the hydrophobic nature of the surface and hence induces repulsion between particles due to hydrophobic forces. The process of repulsion is entropic in origin and hence purely natural. The data is listed in Annexure B

#### 4.2.4 Modelling of slurries containing SDS

It is observed from log-log plot of shear stress and shear strain in figure 4.2.4a that the points approximate a straight line. Regression lines are plotted as in figure 4.2.4b.

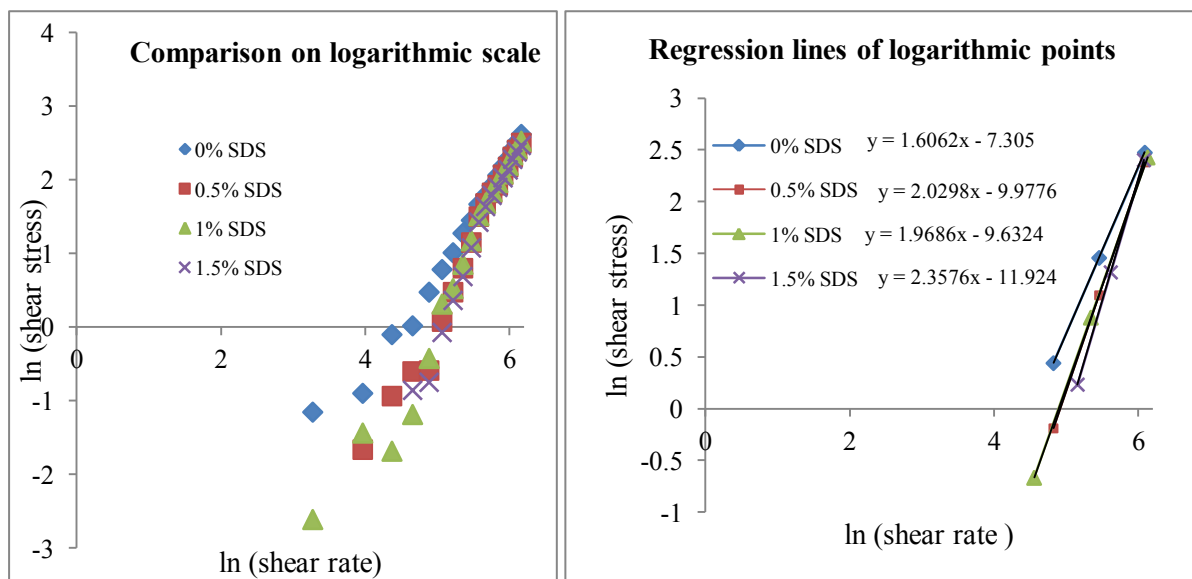


**Figure 4.2.4 (a) Shear stress on logarithmic plot (b) Regression lines with equations on display**

COEFFICIENT OF CORRELATION 'r'			
r1 (0% SDS )	r2 (0.5% SDS )	r3 (1% SDS )	r4 (1.5% SDS )
0.997944642	0.991158604	0.981618615	0.992116152

**Table 4.2.4c Coefficient of correlation 'r' showing the strength of regression**

slope = viscosity index (n)							
0% SDS		0.5% SDS		1% SDS		1.5% SDS	
slope =	1.60619	slope =	2.029817583	slope =	1.9685602	slope =	2.357599
ln (K) =	-7.305	ln (K) =	-9.9776	ln (K) =	-9.6324	ln (K) =	-11.924
K =	0.00067	K =	4.64284E-05	K =	6.557E-05	K =	6.63E-06

**Table 4.2.4d Modelling parameters of slurries containing SDS**

From the following figures (4.2.4e to 4.2.4h), we can observe that with increase in concentration of SDS in slurry, the modelled values start to deviate from actual values, it can

be observed that at 1.5% SDS the modelled values are not as approximately close to real viscosity values and even though viscosity is reduced flow behaviour is not so smooth.

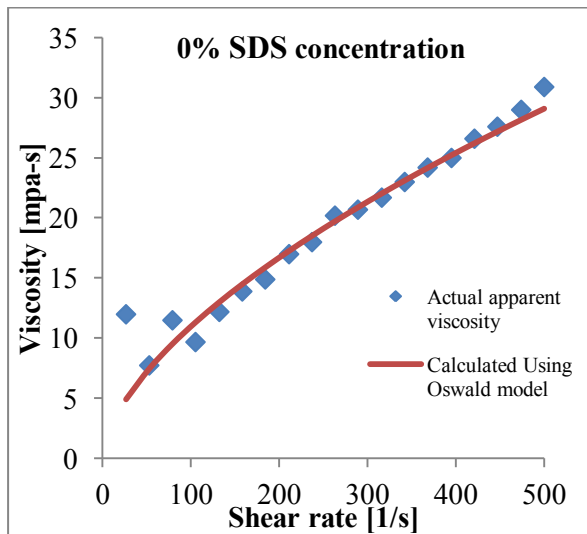


Figure 4.2.4e 40% fly ash slurry

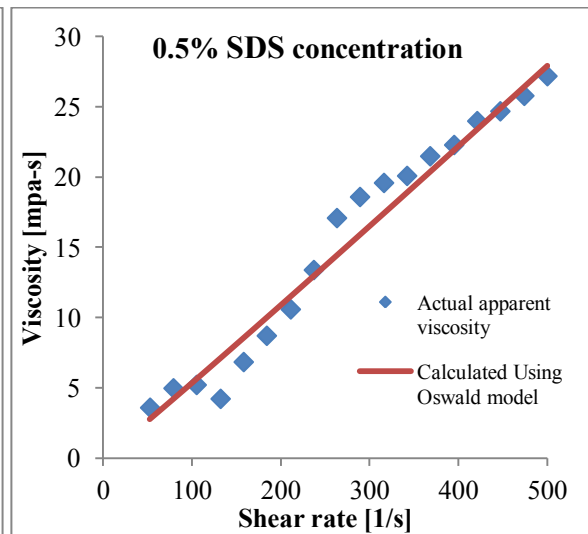


Figure 4.2.4f 40% fly ash slurry

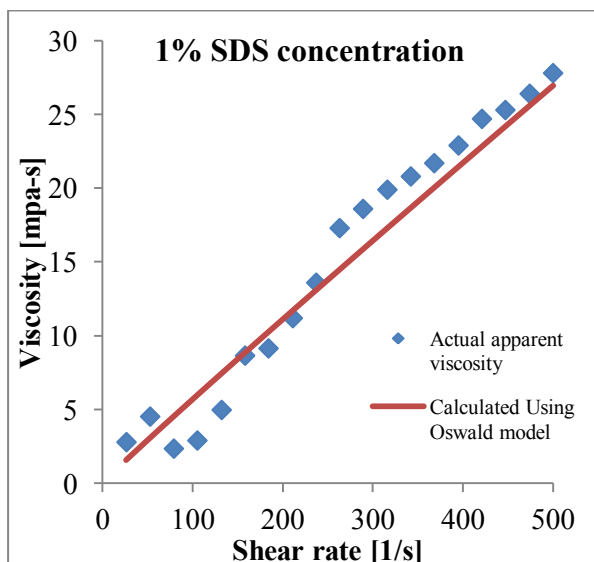


Figure 4.2.4g 40% fly ash slurry

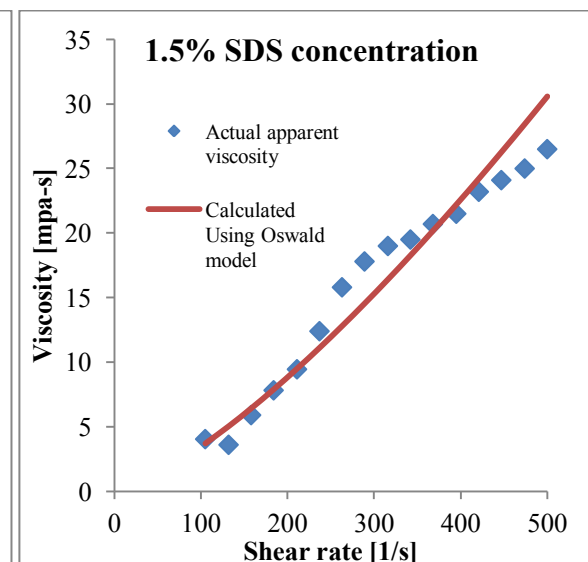


Figure 4.2.4h 40% fly ash slurry

The data involved is listed in Annexure B

#### 4.2.5 Effect of Triton x-100 on drag reduction

Triton x-100 is a non-ionic additive with hydrophobic hydrocarbon tail and polymer hydrophilic head with no charge. Figure 4.2.5a display the effect of triton on viscosity of slurry. we can notice an appreciable decrease in viscosity at very low shear rates (less than  $100\text{s}^{-1}$ ), as the shear rates increased viscosity increased and come closer and closer to the viscosity of slurry without additive, after  $260\text{s}^{-1}$  shear rate, we can see that viscosity of slurries containing triton even exceeded the viscosity of slurry without additive. Studies indicate [36, 38] that when a polymer additive like triton is dissolved in a solvent, the

polymer chains adopt various forms such as random coil, an extended configuration or a helix. These polymeric chains can expand leading to significant increase in viscosity of solution. At higher shear rates ( $300\text{s}^{-1}$  to  $500\text{s}^{-1}$ ) the stretching of polymer chains increase effective viscosity in the buffer layer of turbulent flow by increasing elongational viscosity [37]. This increase in viscosity at buffer layer results in reduction of wall friction. So, ironically, we can say that even though the viscosity of slurry is increased, the friction at wall is reduced.

The reduction in wall friction accompanies with itself smooth flow behaviour, one way to check the theory is to study the modelling behaviour of slurries containing triton, in general, if smooth flow behaviour is attained (which is related to reduction in wall friction) then modelled values of viscosities will lie very close to the actual values.

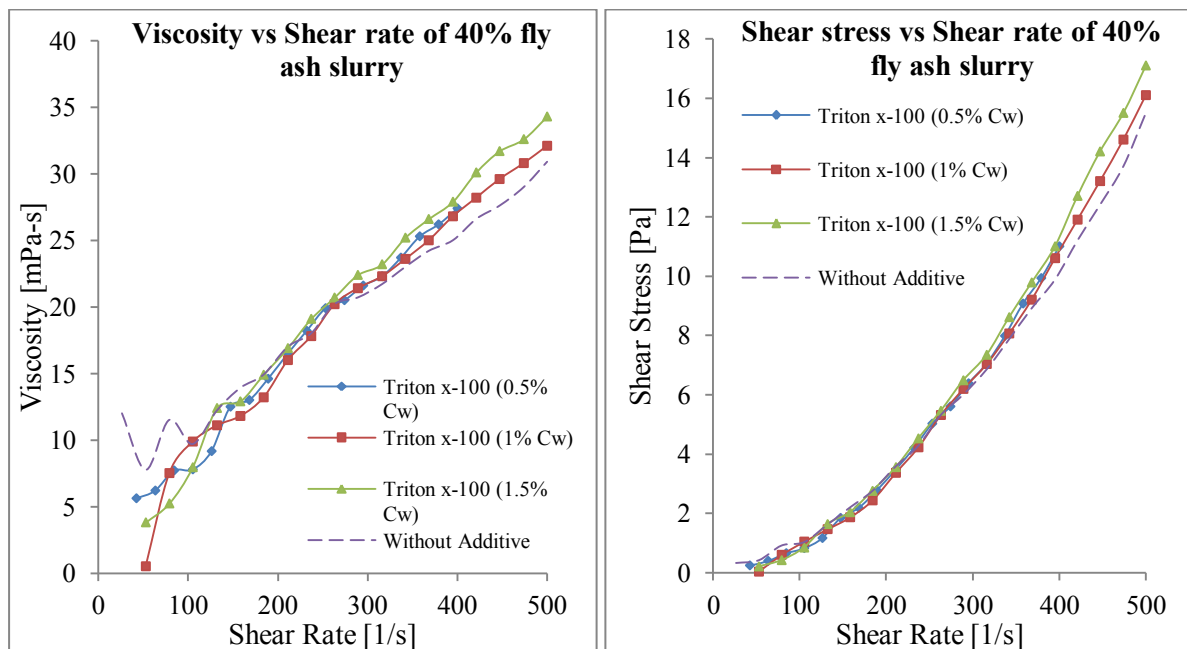


**Figure 4.2.5 (a) Viscosity change with Triton x-100 (b) change in shear stresses of slurry using triton with 40% (by weight) fly ash concentration**

The increase in viscosity at higher shear rates can also be accounted from the fact that micelles aggregate during high shear conditions, clearly the increase in viscosity with increase in the dosage of triton indicate increase in population of micelles, the highly populated micelles when undergo aggregation, they increase the viscosity. The measurement data is listed in Annexure B

#### 4.2.6 Modelling of slurries containing triton

As previously stated, modelling of slurries containing triton is a one way tool to conclude the reliability of the theory of reduction in wall friction. Figures 4.2.6a shows the data points of shear stress and shear strain on logarithmic plot.

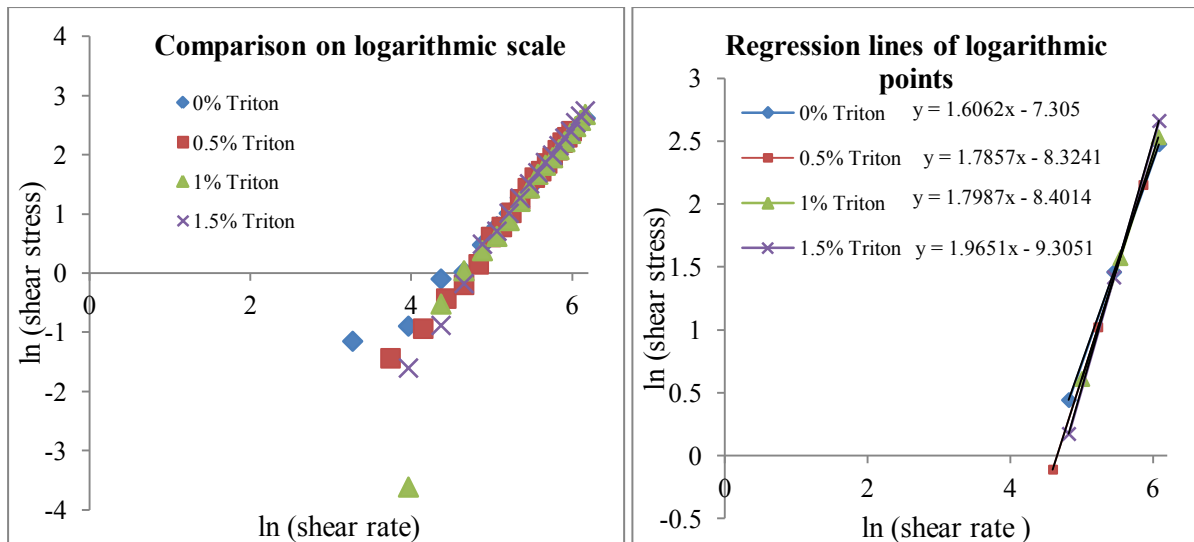


Figure 4.2.6(a) log-log plot of shear stresses (b) Regression lines of logarithmic plot

COEFFICIENT OF CORRELATION 'r'			
r1 (0% Triton )	r2 (0.5% Triton )	r3 (1% Triton )	r4 (1.5% Triton )
0.997944642	0.997525848	0.999221356	0.998070434

Table 4.2.6c Coefficient of regression 'r' of data points

slope = viscosity index (n)							
0% Triton		0.5% Triton		1% Triton		1.5% Triton	
slope =	1.606187	slope =	1.785695	slope =	1.798672	slope =	1.965052367
ln (K) =	-7.305	ln (K) =	-8.3241	ln (K) =	-8.4014	ln (K) =	-9.3051
K =	0.000672	K =	0.000243	K =	0.000225	K =	9.09592E-05

Table 4.2.6d Modelling parameters for slurries containing Triton x-100

Results of modelling are shown below, which indicates smooth flow behaviour of slurry. From figure 4.2.6f, apparent viscosity values of slurry containing triton lies very close to modelled values even at low shear rates such as  $30\text{s}^{-1}$ . Modelling data is listed in Annexure B.

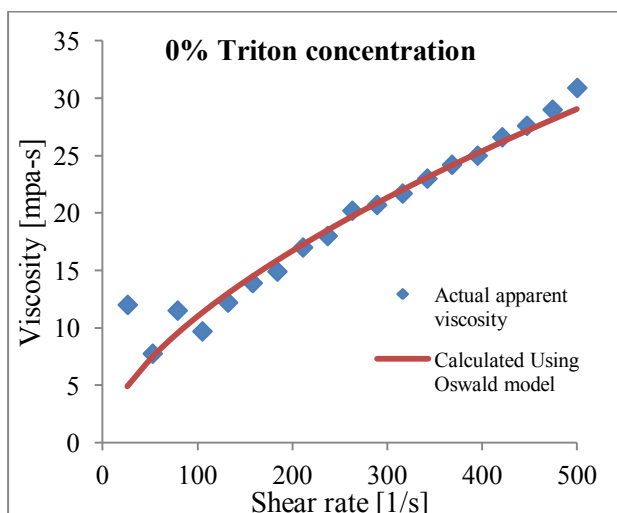


Figure 4.2.6e 40% fly ash slurry

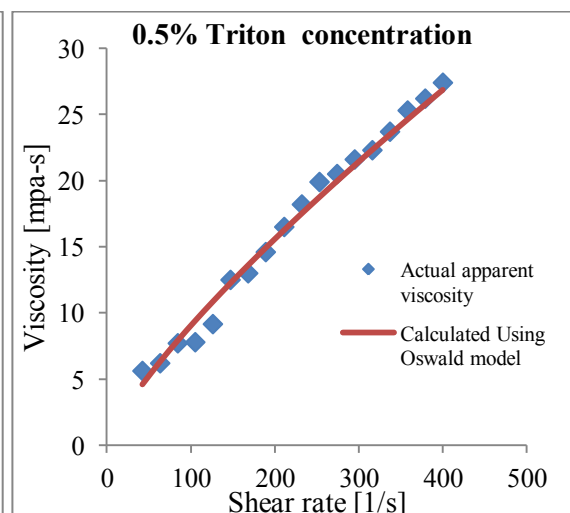


Figure 4.2.6f 40% fly ash slurry

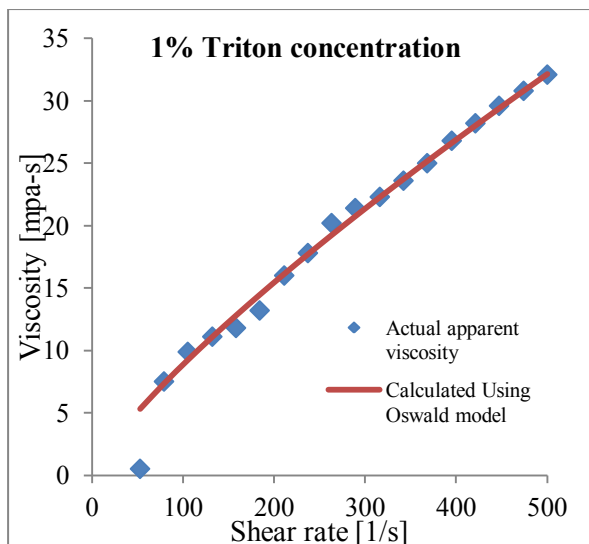


Figure 4.2.6g 40% fly ash slurry

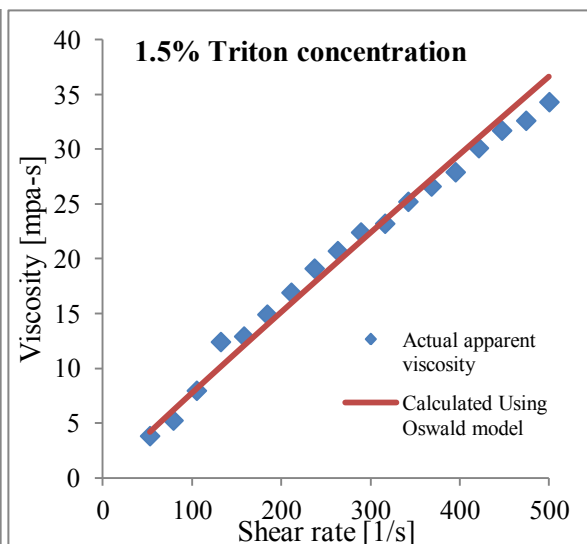


Figure 4.2.6h 40% fly ash slurry

### 4.3 Comparison between Drag Reduction Capabilities of CPC, SDS and Triton x-100

From figure 4.3a, we can observe that 0.5% concentration CPC is more effective as compared to SDS and Triton in reducing drag and improving flow. From figure 4.3b we can observe that use of 1.5% of SDS have resulted more decrease viscosity at higher shear rates (400 to  $500\text{s}^{-1}$ ) than 1.5% CPC. It is well known through studies that raw fly ash has a surface which mostly possess some charge; positive, negative or both. From the actions of CPC and SDS we can conclude that the charge on fly ash used is mostly positive. Viscosity is decreased with increase in concentration of anionic SDS, because more positively charged surface is available for the reaction at each time. While in case of CPC no significant effect is observed with higher concentrations. Due to lack of reactive surface micelles were generated which increases the viscosity at higher shear rates. Other factor which play important role in determining the effectiveness of additives is the temperature range required for effective reaction. CPC and SDS have a wide range of favourable temperature range in which they can maintain hydrophobic forces even at higher shear rates.

In case of Triton x-100, the weak bonds (Vanderwaal forces) formed between surface of fly ash and polymer head are not able to withstand high shear rates and undergo permanent degradation and breakage. But, by observing the results of modelling of slurries with Triton x-100, it is likely that they increase good flow behaviour and reduce wall friction even after increasing viscosity of slurry.

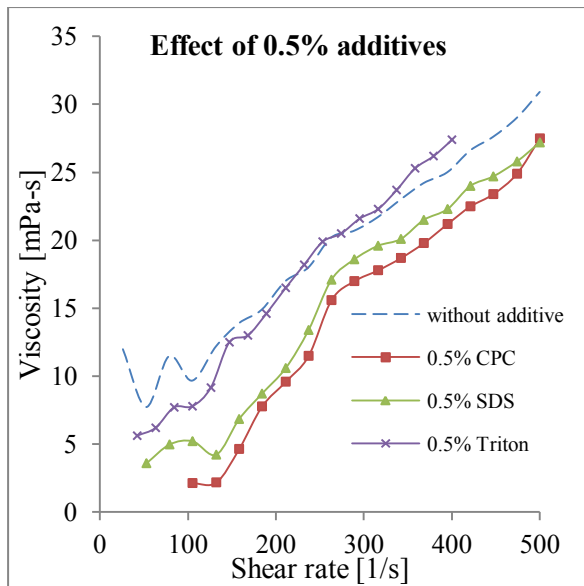


Figure 4.3a 40% fly ash slurry

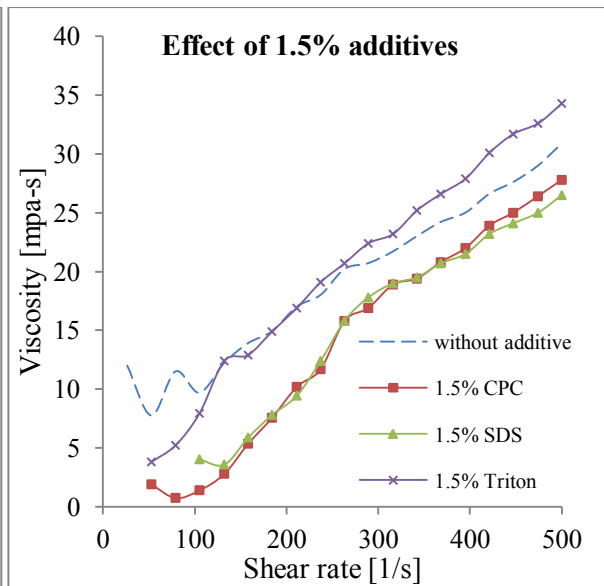


Figure 4.3b 40% fly ash slurry

#### 4.4 Effect of Particle Size (PS) on Drag Properties of Slurry

##### 4.4.1 Flow behaviour of slurries containing different particle size range fly ash at 50% concentration.

The size of particles plays an important role in determining the smooth flow behaviour of slurry. Studies indicate [2, 7] that small particles in a solution bear more stability, all the theories of entropic forces which create repulsion or attraction between particles are very well satisfied for small particle size solution. Also the drag reducing effect created by additives is strong on small particles due to their less mass and inertial force. In this section a study of the effect on drag properties with change in particle size range is done. Figures 4.4.1a to 4.4.1e shows the stress behaviour of slurry with change in particle size. It can be observed that in particle size range of 255 $\mu\text{m}$  to 106 $\mu\text{m}$ , unpredictable results are obtained. At particle size below 100 $\mu\text{m}$  smooth flow behaviour is obtained.

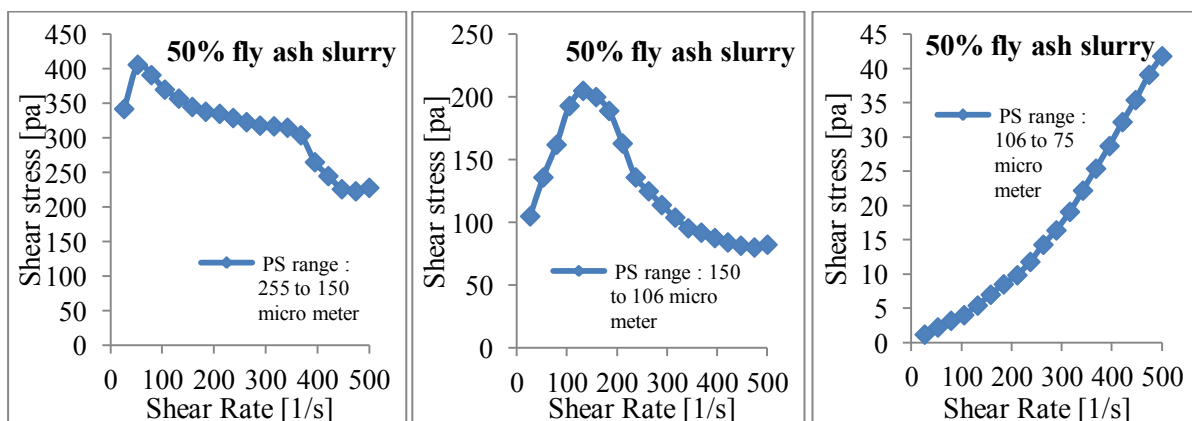
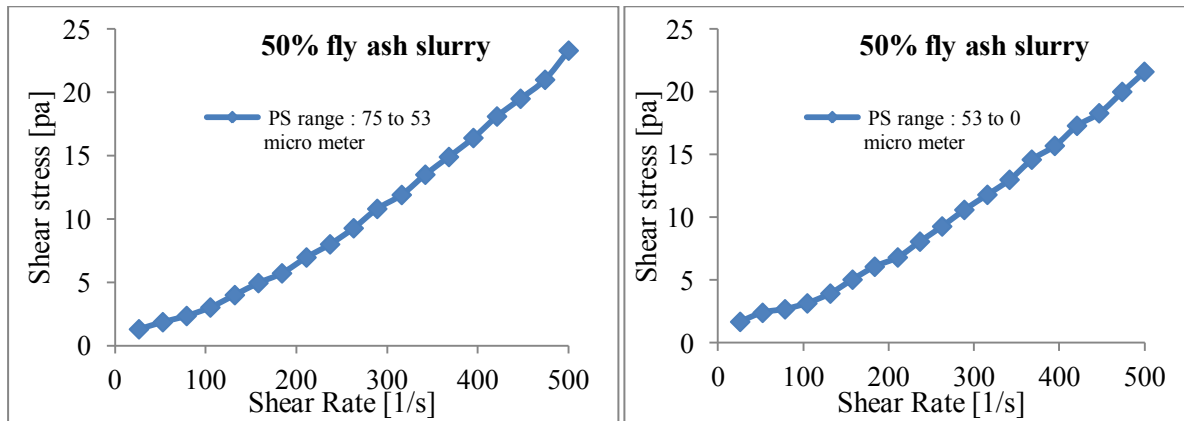
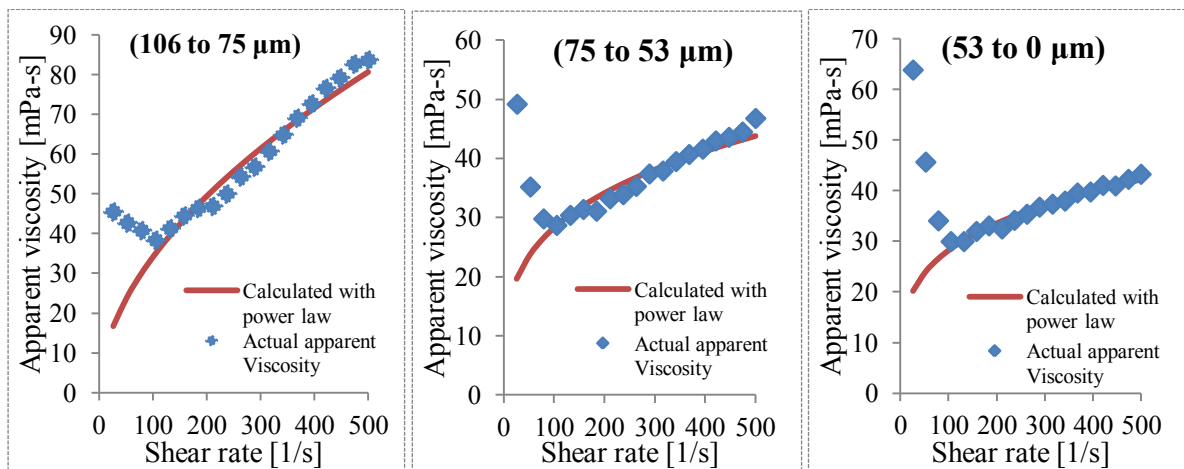


Figure 4.4.1 (a) PS range: 255 - 150 $\mu\text{m}$  (b) PS range: 150 - 106 $\mu\text{m}$  (c) PS range: 106 - 75  $\mu\text{m}$  (at 50%  $C_w$  fly ash slurry)



**Figure 4.4.1 (d) PS range: 75 to 53 $\mu$ m (e) PS range: 53 to 0 $\mu$ m (at 50%  $C_w$  fly ash slurry)**

It is observed that large particle size (more than 100 $\mu$ m) adversely affect flow behaviour. But, these particles are present in very small quantities as discussed in the section of particle size distribution. From above figures it is also observed that power law modelling is only possible for slurries with less than 100 $\mu$ m particle size, the results of modelling are discussed below. Modelling and Measurement data is listed in Annexure C.



**Figure 4.4.1f 50% slurry      Figure 4.4.1g 50% slurry      Figure 4.4.1h 50% slurry**

It is observed that as the particle size reduces, the flow behaviour of slurry is improved. Actual apparent viscosity points in figure 4.4.1h lie very close on modelled values. The model is predicting well at shear rates above 100 $s^{-1}$ .

	106 to 75	75 to 53	53 to 0
slope =	1.53535	1.27341	1.25152
r1=	0.99747	0.99791	0.99925
ln (K) =	-5.8447	-4.8275	-4.7281
K =	0.0029	0.00801	0.00884

**Table 4.4.1i Modelling parameters of slurries with different particle sizes**

From table 4.4.1i, it is observed that viscosity index is approaching the value 1 with decrease in particle size, it means dilatant behaviour of slurry is a function of large particle size.

#### 4.4.2 Effect of 0.5% $C_w$ of CPC on different particle size slurries

In this section the effect of minimum dosage of CPC on drag properties of different particle size slurries is discussed. Figures 4.4.2a to 4.4.2d compare the effect of 0.5% additive on viscosities of slurries.

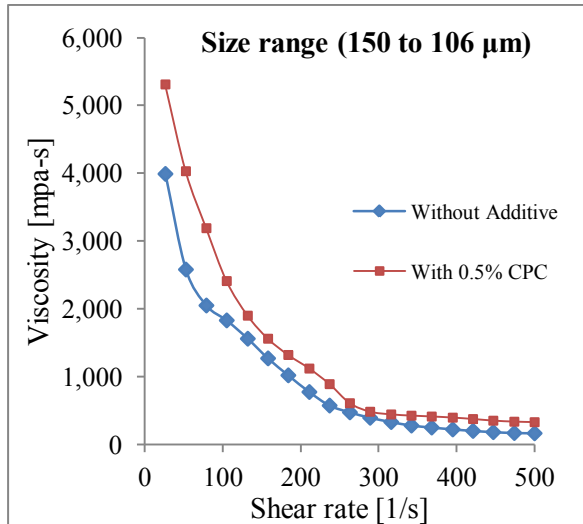


Figure 4.4.2a 50% fly ash slurry

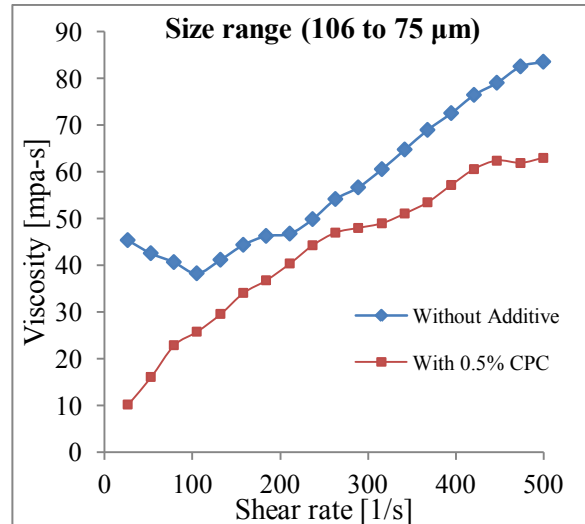


Figure 4.4.2b 50% fly ash slurry

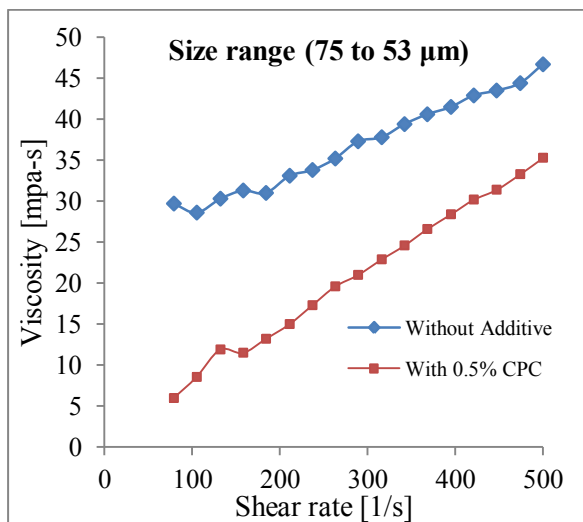


Figure 4.4.2c 50% fly ash slurry

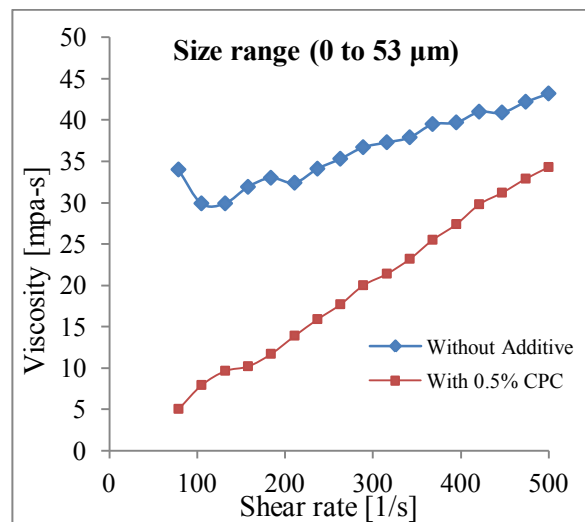


Figure 4.4.2d 50% fly ash slurry

In the particle size range of 150 to 106 $\mu$ m, addition of CPC has increased the viscosity; we can conclude that in high particle size solution like this, the repulsive forces created by CPC's hydrophobic tail are not enough as compared to inertial and gravitational forces created by the large particles, all the CPC molecules remain in water solution and form rapid micelles which aggregate at higher shear rates as shown in Figure 4.4.2i. From figures 4.4.2b to 4.4.2d we observe that flow behaviour is improved with CPC for particles less than 100 $\mu$ m size. Table 4.4.2e below shows a comparison between the flow properties of slurries with and without CPC.

106 to 75	106 to 75 (with CPC)	75 to 53	75 to 53 (with CPC)	53 to 0	53 to 0 (with CPC)
slope = 1.53535	slope = 1.61462	slope = 1.27341	slope = 1.9255091	slope = 1.25152	slope = 2.01141
r1= 0.99747	r2= 0.99957	r1= 0.99791	r2= 0.9989767	r1= 0.99925	r2= 0.99918
ln(K) = -5.8447	ln(K) = -6.528	ln(K) = -4.8275	ln(K) = -9.1038	ln(K) = -4.7281	ln(K) = -9.6551
K = 0.0029	K = 0.00146	K = 0.00801	K = 0.0001112	K = 0.00884	K = 6.4E-05

**Table 4.4.2e Flow parameters of slurries with different particle sizes, with and without CPC**

After addition of CPC the dilatant behaviour of all the slurries have increased, but the consistency coefficient 'K' decreased dramatically, indicating a large decrease in viscosity and increase in smooth flow. The modelling results shown below indicate that addition of CPC to low particle size range slurries has increased the flow behaviour to such an extent that there is little or no difference between modelled and actual viscosity values, this observation conform the effectiveness of repulsive forces created by CPC between small particles. Modelling and measurement data is listed in Annexure C

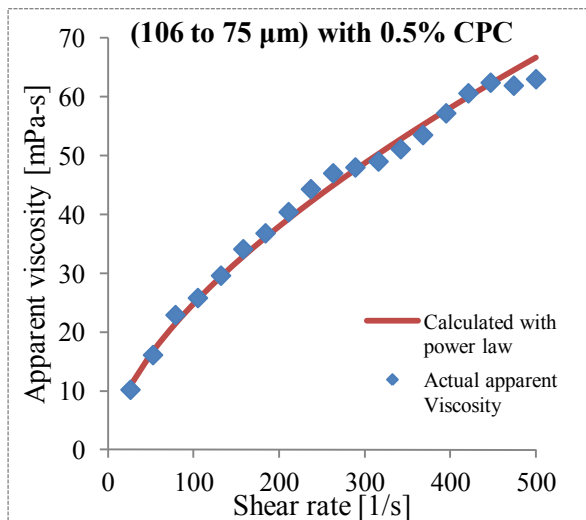


**Figure 4.4.2f 50% fly ash slurry**

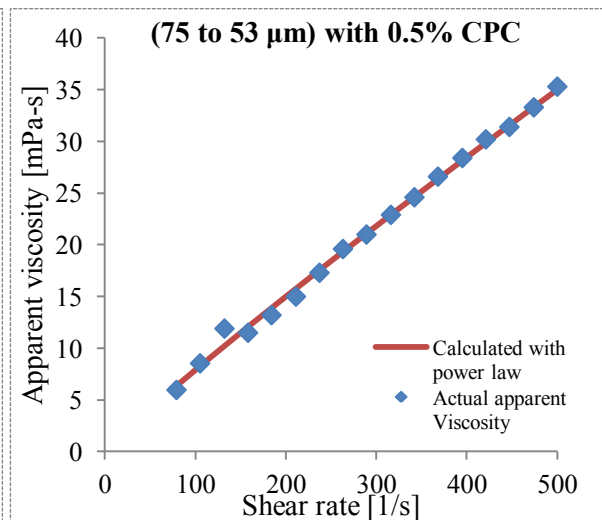


**Figure 4.4.2g 50% fly ash slurry**

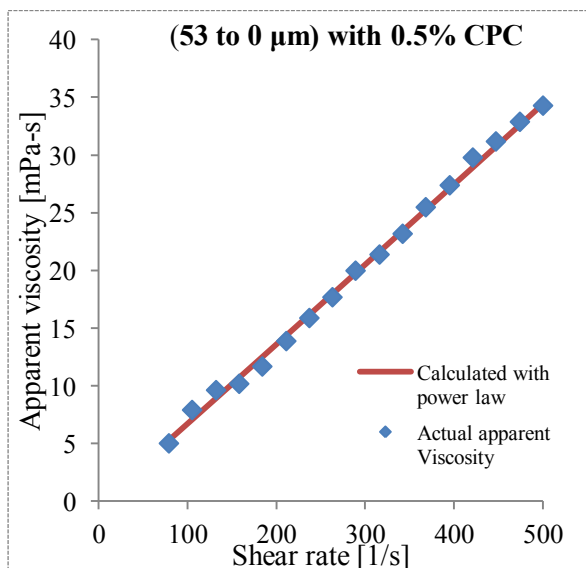


**Figure 4.4.2h 50% fly ash slurry**

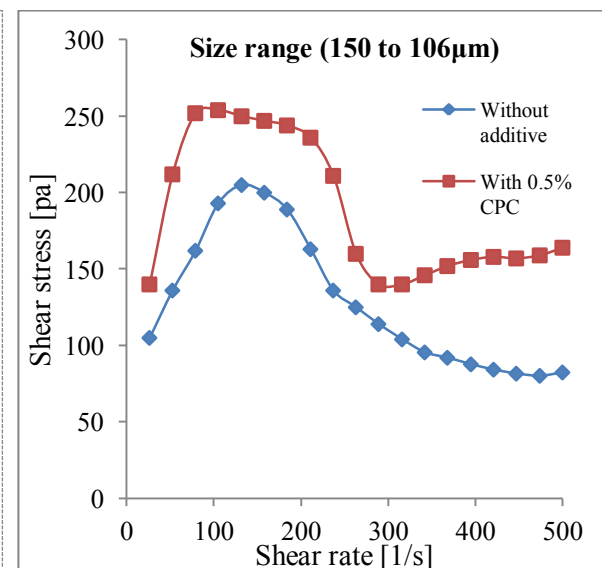


**Figure 4.4.2i Unpredictable results obtained**

#### 4.5 Effect of Additives on Settling Characteristics of 30% Fly Ash Slurry

Fly ash slurry is not a stable solution and ultimately all the fly ash settles down, but fly ash takes considerable amount of time to settle in an ash pond. If fly ash remains suspended in water for extended periods of time, it can degrade water quality adversely. Figures 4.5a and 4.5b display the settling behaviour of 30% concentration (by weight) fly ash slurry.

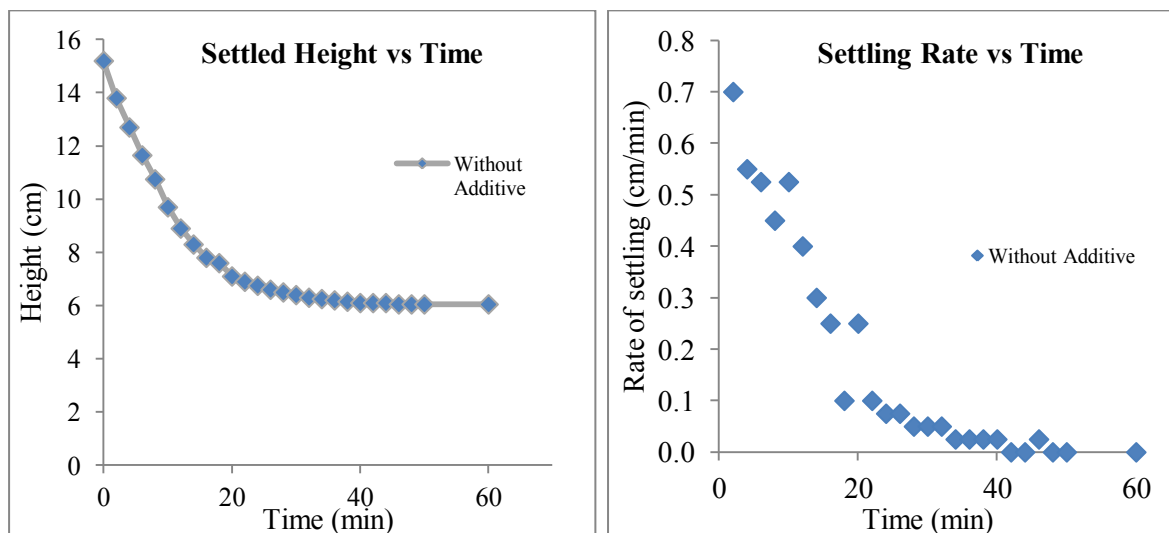


**Figure 4.5 (a) Height Vs time for 30%  $C_w$  slurry (b) Rate of settling of fly ash in slurry**

It is observed that height of fly ash in slurry is decreasing continuously with time. In about 1 hour it almost settled down, although the process of settling is very slow after 1 hour and it can continue up to 8 hours, most of the observable data which can be analysed is obtained in this 1 hour period. In order to make out some sense of the data points in figure 4.5b some analysis is required. Due to the smooth nature of the curve of settled height, the data points in (Figure 4.5b) represents almost a straight line, a linear regression analysis is possible for majority of points which follow a linear pattern. These linear patterns of settling rate of slurries at different concentration of additives can be compared to make out some conclusions. Using above methodology the effect of different additives at different concentrations have been analysed and some logical conclusions are made.

##### 4.5.1 Effect of CPC on settling rate

Figures 4.5.1a to 4.5.1d represents the settling rate obtained for slurries at 30% fly ash containing 4 different concentrations (0.01%, 0.02%, 0.04% and 0.06%) of CPC. A linear regression analysis shows that coefficient of regression 'r' is around -0.90 in each case, so quality of regression is good. Figure 4.5.1e represents a comparative graph between settling rate of different slurries showing the regression lines drawn up to one standard deviation up and sideways.

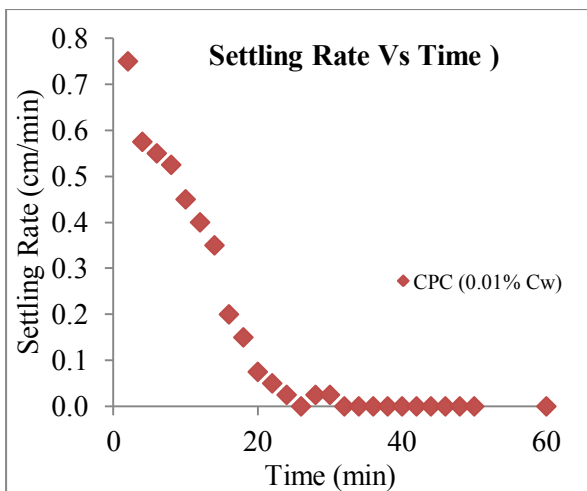


Figure 4.5.1a 30% C<sub>w</sub> fly ash slurry

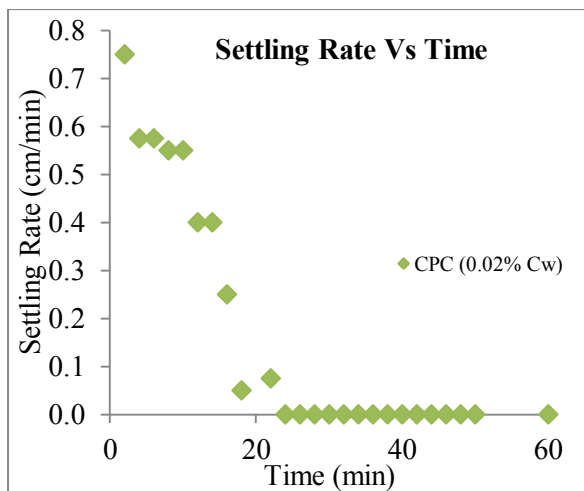


Figure 4.5.1b 30% C<sub>w</sub> fly ash slurry

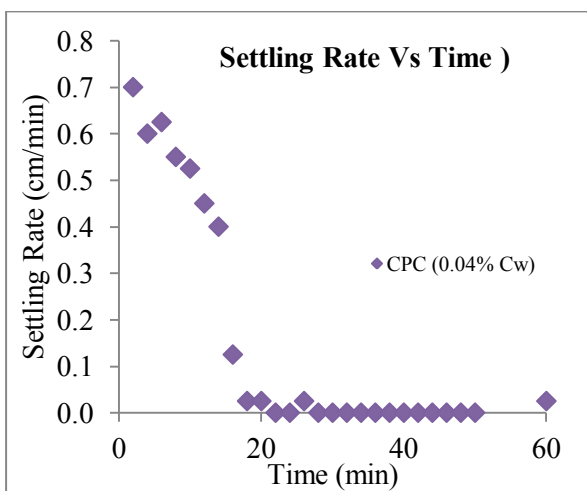


Figure 4.5.1c 30% C<sub>w</sub> fly ash slurry

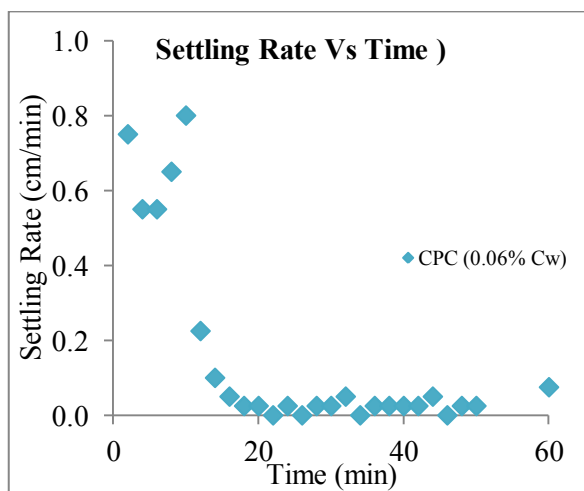


Figure 4.5.1d 30% C<sub>w</sub> fly ash slurry

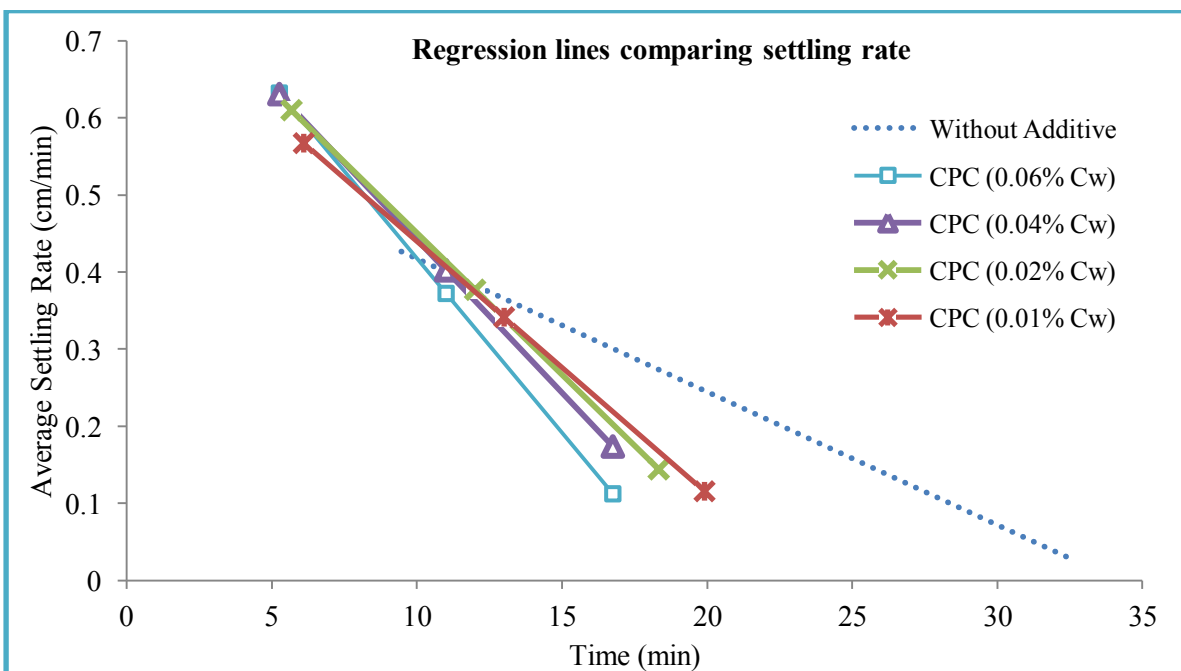


Figure 4.5.1e Regression lines of settling rate drawn up to one standard deviation for 30% fly ash slurry

Clearly from figure 4.5.1e we can observe that after addition of additive settling rate has increased for the first 12 or 14 minutes. It is during this initial 12 to 14 minutes of time, in which large amount of settling takes place. We can see after this period the settling rates are quite low than the rate of settling for the slurry without additive. Table 4.5.1f shows the strength of the regression lines obtained above.

COEFFICIENT OF CORRELATION 'r'				
r1 (without additive)	r2 (0.01% CPC)	r3 (0.02% CPC)	r4 (0.04% CPC)	r5 (0.06% CPC)
-0.92616704	-0.987700548	-0.959427681	-0.950287341	-0.862777123

**Table 4.5.1f Values of the coefficient of correlation of different regression lines**

To analyse and compare the effect of different concentrations of CPC on settling characteristics of slurry, one way is to compare the slopes of the regression lines, which is basically the acceleration at which settling took place. Table 4.5.1g shows the slope of these regression lines, it also shows the % increase in acceleration of settling process after the addition of additive.

SLOPE of regression lines = acceleration of settling process									
without additive		0.01% CPC		0.02% CPC		0.04% CPC		0.06% CPC	
acc. =	-0.017293233	acc. =	-0.03269231	acc. =	-0.036818182	acc. =	-0.0397727	acc. =	-0.0452273
increase in %acc. :			89.05 % increase		112.91 % increase		129.99 % increase		161.53 % increase

**Table 4.5.1g Acceleration of settling process**

Although comparing the average settling rate will not be a true comparison of settling rate (since value of settling rate is continuously decreasing, and not lying around a common average), but still in order to get some idea on the effect created by CPC, average settling rates are compared in Figure 4.5.1h.

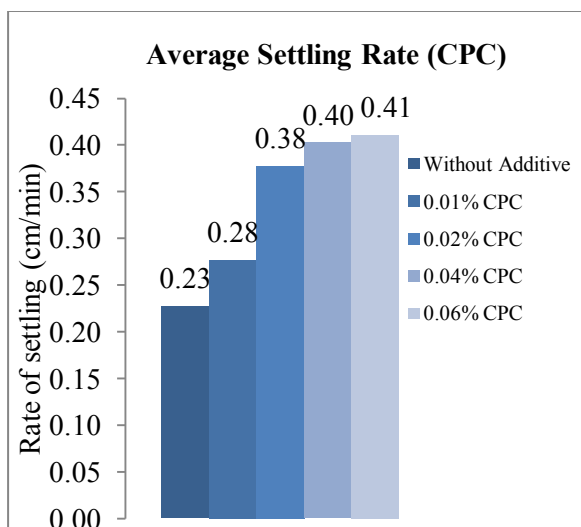


**Figure 4.5.1h 30% fly ash slurry**

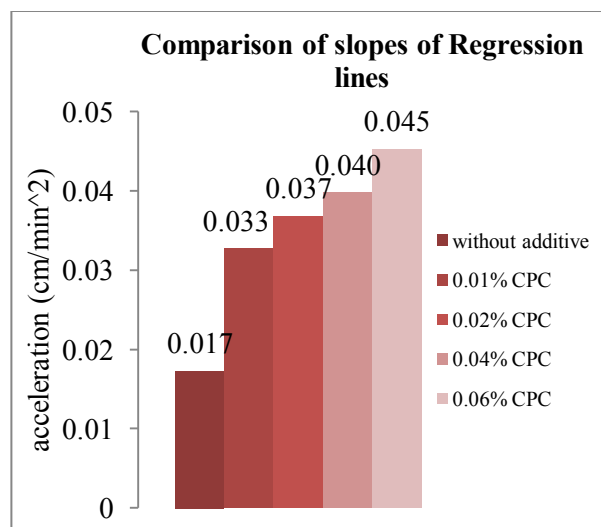


**Figure 4.5.1i Acceleration of settling process**

The true comparison of the effect of additives on settling process would be to compare the change in acceleration of settling process with addition of additives, we can see from figure

4.5.1i that with increase in CPC concentration the acceleration of settling process is increasing. We can see the effect of CPC on settling in terms of percentage increase in acceleration of the process from figure 4.5.1j. We can observe that this graph is almost linear and so the effect of any concentration of CPC which lie in between or nearby these points can be predicted through this graph. From graph we can see that addition of 0.06% of CPC has increased the acceleration of settling process to 161.53%. All the measurement and analysis data is listed in Annexure D

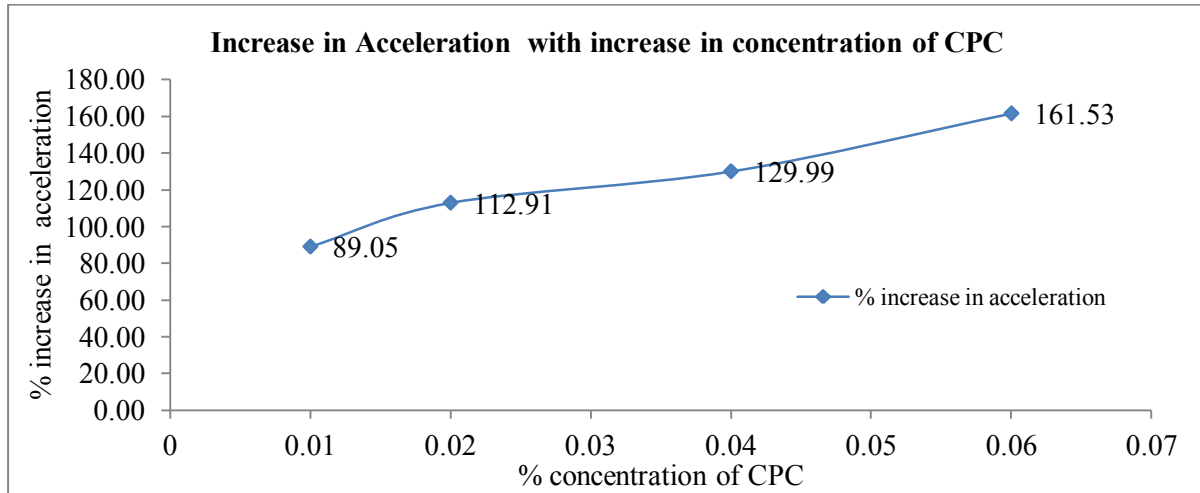


**Figure 4.5.1j Comparison of slopes of regression lines on percentage scale**

#### 4.5.2 Effect of SDS on settling rate

Figures 4.5.2a to 4.5.2d shows the settling rates of slurries with different concentrations of SDS. Figure 4.5.2e compares the regression lines of these settling rates; we can observe that at low concentrations of SDS such as 0.01%, settling rate has increased for the first 12 or 13 minutes, as the concentration of SDS is increasing settling rates are slowing down and reaching the settling rate of slurry without additive. The quality or strength of regression lines, given by the values of the coefficient of regression are shown in Table 4.5.2f

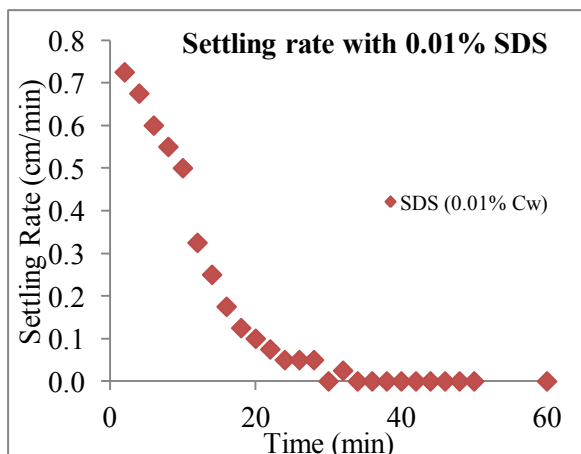


**Figure 4.5.2a 30% fly ash slurry**

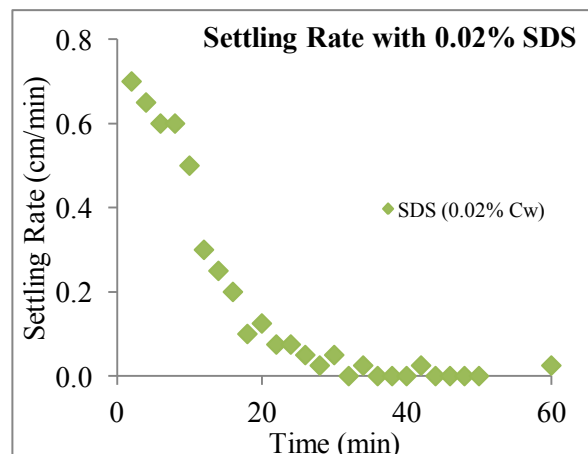


**Figure 4.5.2b 30% fly ash slurry**

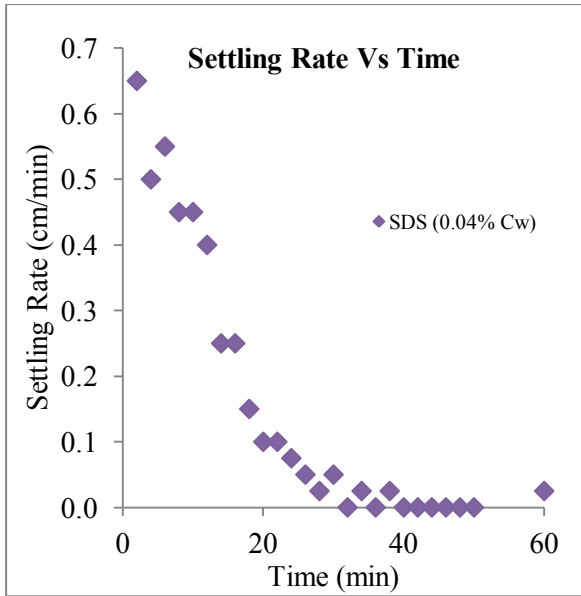


Figure 4.5.2c 30% fly ash slurry

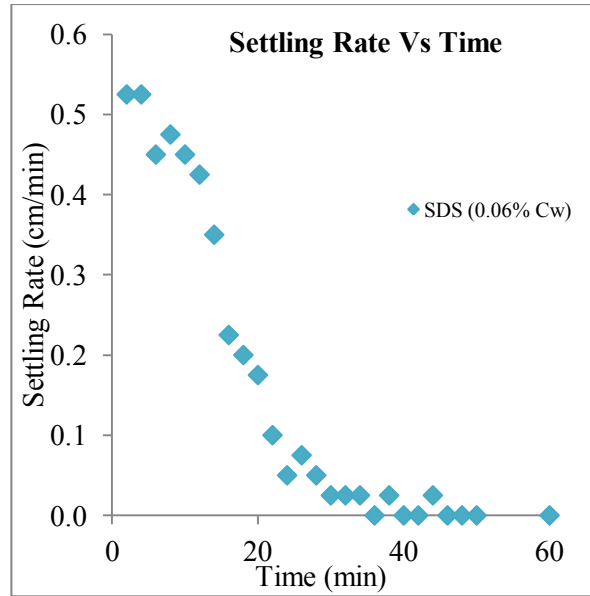


Figure 4.5.2d 30% fly ash slurry

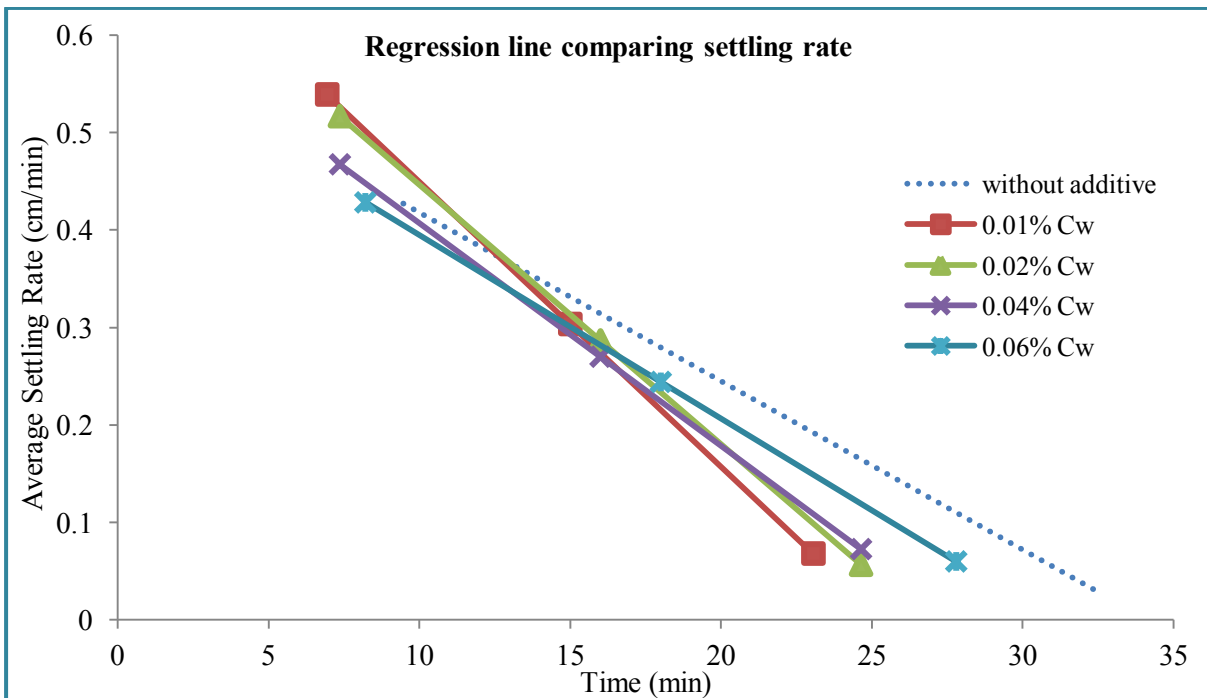


Figure 4.5.2e Regression line drawn up to one standard deviation up and sideways

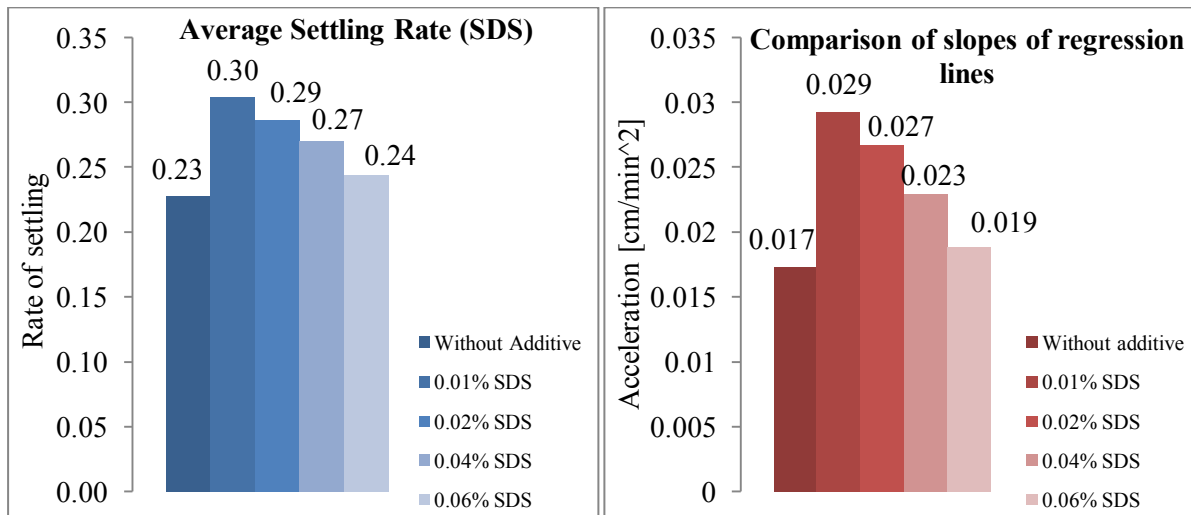
COEFFICIENT OF CORRELATION 'r'				
r1 (without additive)	r2 (0.01% SDS)	r3 (0.02% SDS)	r4 (0.04% SDS)	r5 (0.06% SDS)
-0.92616704	-0.961489399	-0.948210121	-0.967395591	-0.968516908

Table 4.5.2f Coefficient of co-relation of regression lines

SLOPE of regression lines = acceleration of settling process				
without additive	0.01% SDS	0.02% SDS	0.04% SDS	0.06% SDS
-0.01729323	-0.02923077	-0.0266518	-0.02285714	-0.0188113
% increase in acceleration	69.03 % increase	54.12 % increase	32.17 % increase	8.78 % increase

Table 4.5.2g Acceleration of settling process obtained for different slurries

From above table we can observe that % increase in acceleration of settling process is decreasing with increase in concentration of SDS, From average settling rate graph shown in Figure 4.5.2h below we can observe that average settling rates are high at low concentration of SDS, so 0.01% of SDS is best among the 4 concentrations. Figure 4.5.2i with indicates the acceleration process of settling is in harmony with the graph of average settling rate as shown below.



**Figure 4.5.2h 30% fly ash slurry**

**Figure 4.5.2i Acceleration of settling process**

The results obtained in figure 4.5.2i can be expressed as percentage increase in acceleration process in the form of a graph as shown in figure 4.5.2j below.

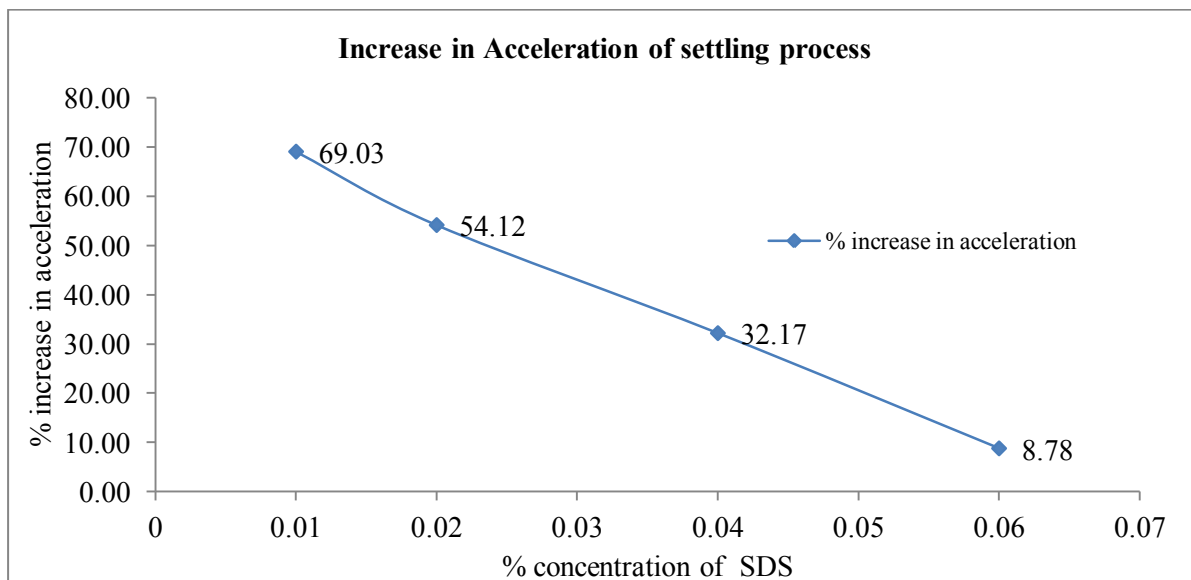


**Figure 4.5.2j Slope of regression lines expressed in percentage increase**

We can observe that points are aligned to form a straight line, so increase in acceleration of settling of any slurry with concentration of SDS lying in between or nearby these points can be calculated using this graph, increase in settling rate with 0.01% of SDS in slurry is 69.03%

as compared to a slurry with 0.06% of SDS where increase is only 8.78%. Clearly lower concentration of SDS is better than higher concentrations in improving settling rate

#### 4.5.3 Effect of Triton x-100 on settling rate

Figures 4.5.3a to 4.5.3d represents the settling rate data obtained for slurries containing 4 different concentrations of triton x-100.

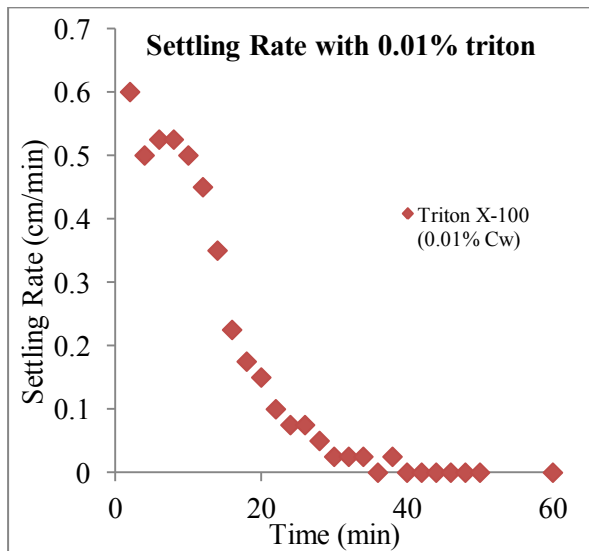


Figure 4.5.3a 30% fly ash slurry

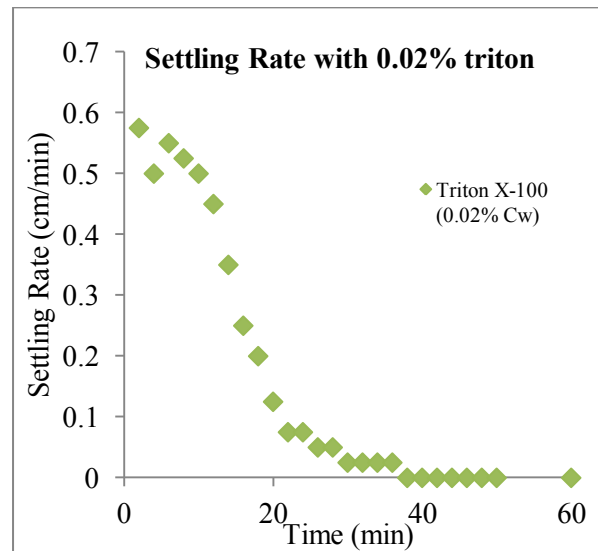


Figure 4.5.3b 30% fly ash slurry

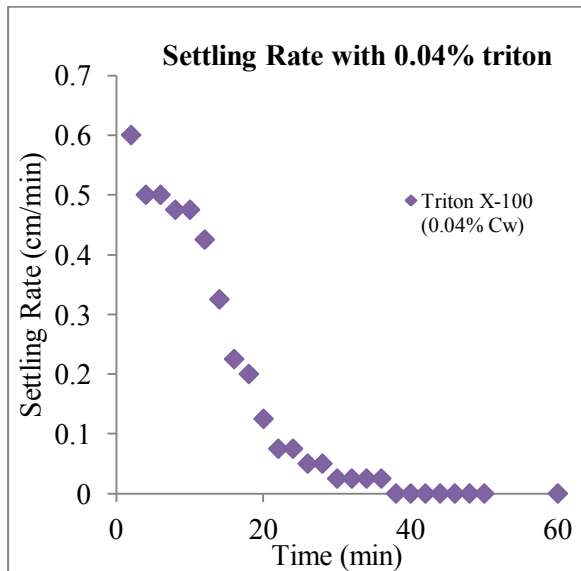


Figure 4.5.3c 30% fly ash slurry

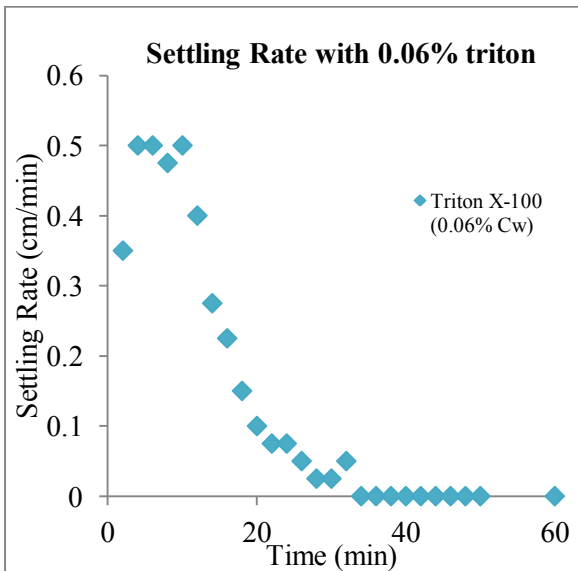


Figure 4.5.3d 30% fly ash slurry

SLOPE of regression lines = acceleration of the settling process				
without additive	0.01% of Triton x-100	0.02% of Triton x-100	0.04% of Triton x-100	0.06% of Triton x-100
-0.01729323	-0.020465686	-0.019414345	-0.01870485	-0.018327206
% increase in acceleration	18.35 % increase	12.27 % increase	8.16 % increase	5.98 % increase

Table 4.5.3e Coefficient of co-relation of regression lines

We can observe from above table, that there is 18.35% increase in acceleration of settling process at concentration of 0.01% triton. From figure 4.5.3f we can see that the increase in settling rate at 0.01% triton lasted for about 11 or 12 minutes. Triton has very little effect on settling rate of slurry, maximum increase in settling rate is obtained only at low concentration such as 0.01%. In fact, by observing the regression lines we can notice that it is making the slurry more and more stable with increase in concentration of triton. From figure 4.5.3f, the regression line at 0.06% of triton is almost parallel to the one without additive, but settling rates at this concentration are quite low than that of without additive. It indicates the stability attained by the slurry with higher concentration of triton.

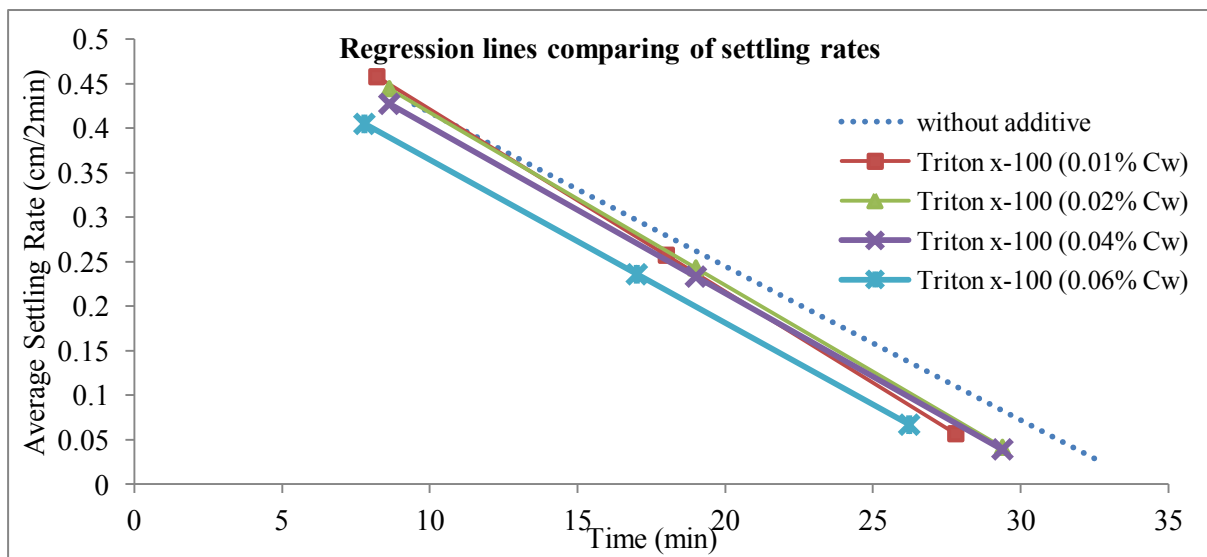


Figure 4.5.3f Regression lines drawn up to one standard deviation up and sideways

COEFFICIENT OF CORRELATION 'r'				
r1 (without additive)	r2 (0.01% Triton x-100)	r3 (0.02% Triton x-100)	r4 (0.04% Triton x-100)	r5 (0.06% Triton x-100)
-0.92616704	-0.961295376	-0.951247936	-0.955614862	-0.916603852

Table 4.5.3g Coefficient of co-relation for regression lines

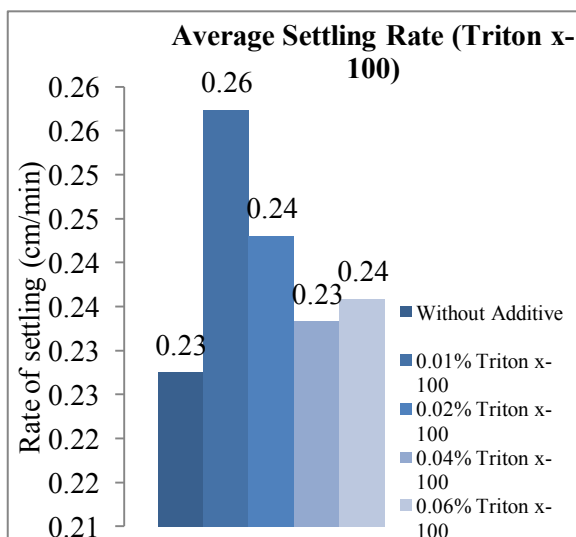


Figure 4.5.3h 30% fly ash

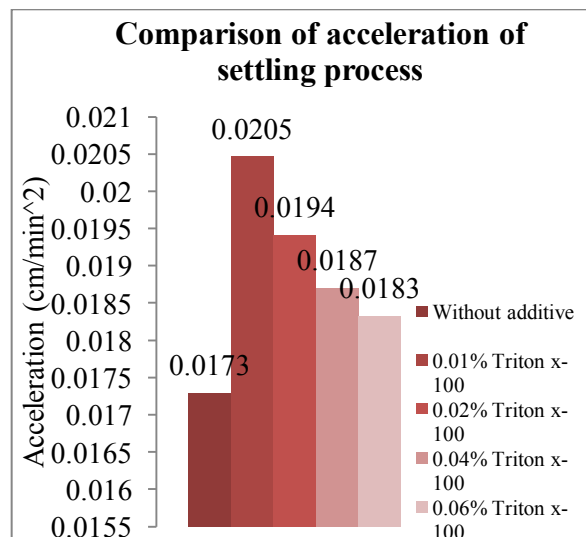
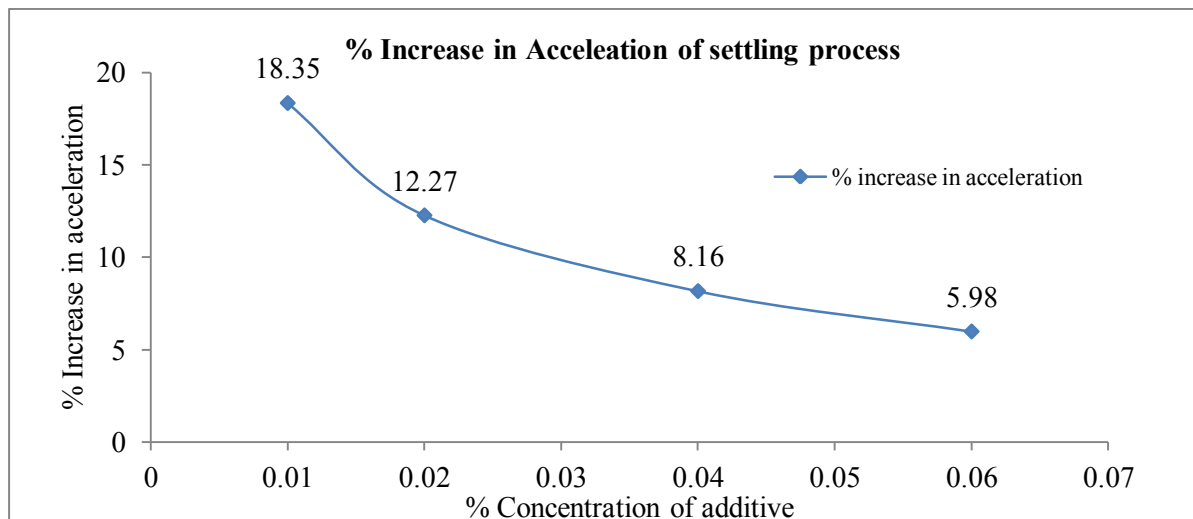


Figure 4.5.3i 30% fly ash

From figure 4.5.3h we can observe a bit increase in average settling rate at 0.01%, with increase in concentration of triton there is approximately negligible effect on average settling of slurry. The same figure 4.5.3i is shown below in terms of percentage increase in acceleration for better understanding.



**Figure 4.5.3j Slope of regression lines expressed as percentage increase**

#### 4.5.4 Comparison between settling behaviour of slurries containing CPC, SDS and Triton x-100

Sno.	Effects produced on 30% fly ash slurry	CPC	SDS	Triton x100
1	Effect on settling rate with increase in additive	Increased	Decreased	Decreased
2	Best dosage	0.06%	0.01%	0.01%
3	Maximum increase in acceleration	161.53%	69.03%	18.35%
4	Time period (minutes) of increase in settling rate	12 to 14	12 to 14	10 to 11
5	Maximum average settling rate achieved (cm/min)	0.41	0.30	0.26

**Table 4.5.4 Comparison between slurries containing CPC, SDS and Triton x-100**

#### 4.6 Effect of Different Concentration of Additives on pH of Slurry

Figure 4.6a shows the change in pH of slurry at 40% fly ash concentration with addition of additives. It can be observed that with increase in dosage of additives pH is increasing, so the slurries containing additives are alkaline in nature. Acidic slurries affect the soil fertility adversely. We can also observe that increase in pH is small in case of CPC as compared to SDS and Triton x-100. In case of CPC, pH has increased to a maximum of 8.04 as compared

to 8.31 for triton and 8.68 in case of SDS. Measurement data and weight concentrations are listed in Annexure E

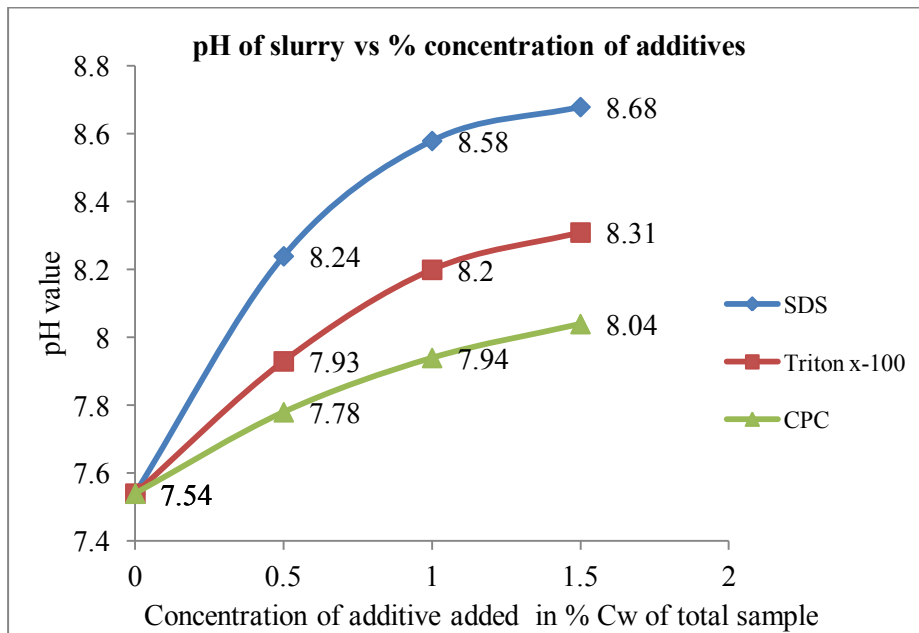


**Figure 4.6a Effect on pH of slurry with addition of CPC, Triton x-100 and SDS**

## CHAPTER 5

### CONCLUSIONS AND RECOMMENDATIONS

#### 5.1 Conclusions

1. The study of flow behaviour of slurry at different concentrations of fly ash indicates that viscosity increases exponentially with increase in concentration. Due to this exponential increase in viscosity, slurries with large fly ash concentrations (more than 50%) produce excessive drag making the process of transportation inappropriate.
2. At 10%, 20% and 30% fly ash concentration, slurries exhibited constant viscosities at approximately all the shear rates, so there is no necessity of a model to predict the values of apparent viscosities. At 40%, 50% and 60%, the behaviour of slurry is dilatant in nature. It is observed that at higher concentrations modelling is necessary in order to predict the smooth flow behaviour of slurry.
3. Even with small dosage of CPC (such as 0.5%  $C_w$ ), viscosity of slurry at 40% fly ash reduced drastically, also consistency coefficient 'K' decreases with each increase in CPC dosage. Optimal CPC dosage is observed to be 0.5%, in which aggregation of micelles is minimum and decrease in viscosity is maximum both at low and high shear rates.
4. Viscosity of slurry at 40% fly ash reduces with addition of SDS, Viscosity decreases with increase in dosage of SDS. Best dosage of SDS is 1.5%, at which viscosity is minimum both at low and high shear rates. Being cheap in price and easily available high dosage of SDS is also economical.
5. Flow behaviour of slurries containing triton x-100 is improved, and is confirmed by the modelling results, in which the predicted smooth behaviour values lie very close to actual values. The increase in viscosity at high shear rates is expected to be a result of elongation and twisting of polymer heads and breakage of weak bonds.
6. A comparative study between the effects created by the additives shows that CPC is more effective in reducing viscosity as compared to SDS or triton.
7. Large particles in fly ash adversely affect the flow behaviour and increase the drag properties, particles size ranging from 255 to 106 $\mu\text{m}$  exhibit unpredictable flow behaviour under shear flow. Particles less than 100 $\mu\text{m}$  exhibited smooth flow behaviour as conformed by the results of modelling.
8. Addition of 0.5% CPC with slurries made from different particle size range at 50% fly ash concentration showed that flow behaviour is improved with particles less than

100 $\mu$ m size. The modelled values calculated lie very close to the actual data points and conformed the smooth flow attained using CPC.

9. Settling rate of slurry at 30% concentration of fly ash is improved with addition of CPC, settling rate increases with increase in CPC dosage, best CPC dosage is 0.06%  $C_w$  of total sample. In case of SDS best dosage is 0.01%; there is no significant effect of Triton x-100 on settling rate of slurry. CPC is more effective in improving settling rate than SDS or triton.
10. The pH of slurry containing SDS, triton or CPC is alkaline in nature and hence not a threat to fertility of soil. The change in pH is minimal in case of CPC. Slurries containing SDS are most alkaline in nature. The alkalinity of slurries containing triton lies in the middle of CPC and SDS.

## 5.2 Recommendations for Future Work

Some recommendations for future work are as follows

1. In this work the study of CPC on 40% and 50% fly ash slurries is carried out without the use of any counterion. Cationic surfactants like CPC give better results when used in conjunction with counter ion like sodium Salicylate, due to time limitation a study on counter ions is not carried out. Now since the effect of CPC on high concentration slurries have been conformed, it is recommended to see the effect of CPC in conjunction with an appropriate counter ion, to increase its effect of viscosity reduction and prevent micelle aggregation.
2. Based on time limitations a simple rheological model (Oswald de Waele model) is used to predict the flow behaviour, after practically examining this model certain limitations are observed, such as the model worked very well at high shear rates but mostly gave unpredicted results less than  $100\text{s}^{-1}$  shear rate. It is recommended to study the shortcomings of this model and select another model which can give more accurate results at lower shear rates.
3. The study involved in this work deals with mainly the effect on viscosity of slurry, however flow behaviour is not fully defined by just viscosity. It also deals with surface tension and turbidity of the flow, due to time limitation a detail study on these parameters is not carried out, it is recommended to work on these parameters and flourish the study of flow behaviour of slurry to its full extent.
4. It is recommended to study the effect of different concentrations of additives on different particle size range slurries, as in this work the effect of only one concentration of CPC is studied on different particle size range slurries.

**REFERENCES**

1. Roh N.S., Shin D.H., Kim D.C., Kim, J.D., (1994), Rheological behaviour of coal-water mixtures, *Fuel*, 74 No. 8, 1220-1225.
2. Turian R.M., Ma T.W., Hsu F.L.G., Sung D.J., (1997), Characterization, settling, and rheology of concentrated fine particulate mineral slurries, *Powder Technology* 93, 219-233.
3. Aomari N., Gaudu R., Cabioc'h F., Omari A., (1998), Rheology of water in crude oil emulsions, *Colloids and surfaces A: Physicochemical and Engineering Aspects* 139, 13-20.
4. Aktas Z., Woodburn E.T., (2000), Effect of addition of surface active agent on the viscosity of a high concentration slurry of a low-rank British coal in water, *Fuel Processing Technology* 62, 1-15.
5. Turian R.M., Attal F.J., Sung D.J., Wedgewood L.E., (2002), Properties and rheology of coal-water mixtures using different coals, *Fuel* 81, 2019-2033.
6. Atesok G., Boylu F., Sirkeci A.A., Dincer H., (2002), The effect of coal properties on the viscosity of coal-water slurries, *Fuel* 81, 1855-1858.
7. Kumar U., Mishra R., Singh S.N., Seshadri V., (2003), Effect of particle gradation on flow characteristics of ash disposal pipelines, *Powder Technology* 132, 39-51.
8. K.T. Kaushal, K.B. Sibendra, C.B. Kumaresh, Banerjee S., Mishra K.K., (2003), High concentration coal-water slurry from Indian coals using newly developed additives, *Fuel Processing Technology* 85, 31-42.
9. Lu. Ping, Zhang M., (2005), Rheology of coal-water paste, *Powder Technology* 150, 189-195.
10. X. Renfu., H. Baixing., H. Qihui., C. Jun., P. Yi., S. Jian., (2006), Effect of compound inorganic nano-stabilizer on the stability of high concentration coal water mixtures, *Fuel* 85, 2524-2529.
11. Gurses A., A Metin, Dogar C., Karaca S., Bayarak R., (2006), An investigation on effects of various parameters on viscosities of coal-water mixture prepared with Erzurum-Askale lignite coal, *Fuel Processing Technology* 87, 821-827.
12. Chandra S., Kukade S., Kumar M.S., Kundu G., (2008), Coal-oil-water multiphase fuel: Rheological behaviour and prediction of optimum particle size, *Fuel* 87, 3428-3432.
13. Chandel S., Singh S.N., Seshadri V., (2009), Deposition characteristics of coal ash slurries at higher concentrations, *Advanced Powder Technology* 20, 383-389.

14. Liu Meng, Duan F.Y., (2009), Resistance properties of coal-water slurry flowing through local piping fitting, *Experimental Thermal and Fluid Science* 33, 828-837.
15. Chandel S., Singh S.N., Seshadri V., (2010), Deposition characteristics of coal ash slurries at higher concentrations, *Advanced Powder Technology* 20, 383-389.
16. Senapati P.K., Mishra B.K., Parida A., (2010), Modelling of viscosity for power plant ash slurry at higher concentrations: Effect of Solids volume fraction, particle size and hydrodynamic interactions, *Powder Technology* 197, 1-8.
17. Masalova I., Foudazi R., Malkin A.Y., (2011), The rheology of highly concentrated emulsions stabilized with different surfactants, *Colloids and Surfaces A: Physicochemical and Engineering Aspects* 375, 76-86.
18. He Qihui., Wang R., Wang W., Xu Renfu., Hu Baixing., (2011), Effect of particle size distribution of petroleum coke on the properties of petroleum coke-oil slurry, *Fuel* 90, 2896-2901.
19. Chen R., Wilson M., Leong Y.K., Bryant P., Yang H., Zhang D.K., (2011), Preparation and rheology of biochar, lignite char and coal slurry fuels, *Fuel* 90, 1689-1695.
20. Anton paar German manufactured user manual of rheometer, Rheolab QC Rotational rheometer for quality control.
21. Usui H., Li Lei, Suzuki H., (2001), Rheology and pipeline transportation of dense fly ash-water slurry, *Korea-Australia Rheology Journal*, 13, No. 1, 47-54.
22. Naik H.K., Mishra M.K., Rao U.M., (2011), Evaluation of flow characteristics of fly ash slurry at 40% solid concentration with and without an additive, *World of Coal Ash (WOCA) conference –May 9-12*.
23. Cengel A.Y., Cimbala J.M., (2006), *Fluid Mechanics, Fundamentals and application (in SI units)*, The Tata-McGraw Hill companies publications, ISBN 978-0-07-070034-5.
24. Sumer M. Peker., Serife S. Helvacı., (2008), *Solid-Liquid Two phase flow*, The Elsevier science and technology publications, ISBN 978-0-444-52237-5.
25. Naik H.K., Mishra M.K., Rao U.M., (2009), Rheological characteristics of fly ash slurry at varying temperature environment with and without an additive, *World of Coal Ash (WOCA) Conference – May 4-7*.
26. Chatterjee A.K., (2010), *Indian Fly Ashes, Their Characteristics, and Potential for Mechano-Chemical Activation for Enhanced Usability*, 2<sup>nd</sup> International Conference on Sustainable Construction Materials and Technologies, June 28-30.

27. Biswas A., Gandhi B.K., Singh S.N., Seshadri V., (2000), Indian journal of Engineering and Material Science 7, 1-7.
28. Matras Z., Malcher T., Gzyl-Malcher B., (2007), The influence of polymer surfactant aggregates on drag reduction, Thin solid films, DOI: 10. 1016/j.tsf.2007.11.057.
29. Derkach R.S., (2009), Rheology of emulsions, Advances in Colloid and Interface Science 151, 1-23.
30. Sheen S., Addy M., An in vitro evaluation of the availability of Cetylpyridinium chloride and chlorhexidine in some commercially available mouth rinse products, British Dental Journal 194, No. 4.
31. Final report on the safety assessment of sodium lauryl sulfate and ammonium lauryl sulfate, International journal of toxicology 2, No. 7, 127-181, doi: 10.3109/10915818309142005.
32. Freedman D., Pisani R., Purves R., (2009), Statistics, Viva Books private limited, ISBN -13: 978-81-309-1055-0.
33. Turian R.M., Ma T.W., Hsu F.L.G., Sung D.J., (1997), Characterization, settling, and rheology of concentrated fine particulate mineral slurries, Powder Technology 93, 219-233.
34. L Chahine., N Sempson., C Wagoner., (1997), The effect of sodium lauryl sulfate on recurrent aphthous ulcers: a clinical study, Compend Contic Educ Dent 18, No. 12. 1238-40. PMID 9656847.
35. Hinch E.J., (1977), Mechanical models of dilute polymer solutions in strong flows, Physics of Fluids 20, No. 10, S22-S30
36. Lumley J.L., (1973), Drag reduction in turbulent flow by polymer additives, Journal of Polymer Science 7, 263-290.
37. White C., Mungal M., (2008), Mechanics and prediction of turbulent drag reduction with polymer additives, Annual review of fluid mechanics 40, 235-256.
38. Choi D.G., Kim W.J., Yang S.M., (2000), Shear-induced microstructure and rheology of Cetylpyridinium chloride/sodium Salicylate micellar solutions, Korea-Australia Rheology Journal 12, No. ¾, 143-149.
39. S. Ezrahi., E. Tuval., A. Aserin., (2006) Properties, main applications and perspectives of worm micelles, Advances in Colloid and Interface science, December, 77-102.
40. Marksberry. A., [www.caer.uky.edu](http://www.caer.uky.edu), (2007),  
<http://www.caer.uky.edu/kyasheducation/index.html>

## ANNEXURE A

## FLOW BEHAVIOUR OF SLURRY

10 % Fly ash				
Meas. Pts.	Time [s]	Viscosity [mPa·s]	Shear Rate [1/s]	Shear Stress [Pa]
1	6	#####	0.000014	0.024
2	12	0.59	26.3	0.015
3	18	1.37	52.6	0.072
4	24	1.13	78.9	0.089
5	30	1.21	105	0.127
6	36	1.17	132	0.154
7	42	1.18	158	0.186
8	48	1.15	184	0.211
9	54	1.14	211	0.239
10	60	1.13	237	0.267
11	66	1.13	263	0.297
12	72	1.12	289	0.324
13	78	1.11	316	0.351
14	84	1.12	342	0.382
15	90	1.14	368	0.422
16	96	1.17	395	0.463
17	102	1.09	421	0.459
18	108	1.1	447	0.492
19	114	1.1	474	0.52
20	120	1.1	500	0.55

Table A.1 data for 10% fly ash slurry

20 %Fly ash				
Meas. Pts.	Time [s]	Viscosity [mPa·s]	Shear Rate [1/s]	Shear Stress [Pa]
1	6	#####	2E-05	-0.0118
2	12	46.7	26.2	1.23
3	18	4.75	52.6	0.25
4	24	6.25	78.9	0.493
5	30	3.74	105	0.394
6	36	3.34	132	0.44
7	42	2.52	158	0.397
8	48	2.6	184	0.479
9	54	2.63	211	0.554
10	60	2.42	237	0.574
11	66	2.45	263	0.645
12	72	2.63	289	0.763
13	78	2.54	316	0.802
14	84	2.45	342	0.837
15	90	2.49	368	0.919
16	96	2.53	395	1
17	102	2.51	421	1.06
18	108	2.6	447	1.16
19	114	2.58	474	1.22
20	120	2.59	500	1.29

Table A.2 data for 20% fly ash slurry

%Fly ash 30				
Meas. Pts.	Time [s]	Viscosity [mPa·s]	Shear Rate [1/s]	Shear Stress [Pa]
1	6	#####	-2E-05	0.294
2	12	26.5	26.3	0.699
3	18	11.4	52.6	0.598
4	24	9.17	78.9	0.724
5	30	9.78	105	1.03
6	36	10.2	132	1.35
7	42	7.64	158	1.21
8	48	7.45	184	1.37
9	54	7.55	211	1.59
10	60	7.24	237	1.71
11	66	7.22	263	1.9
12	72	7.14	289	2.07
13	78	7.06	316	2.23
14	84	6.92	342	2.37
15	90	6.94	368	2.56
16	96	6.79	395	2.68
17	102	6.76	421	2.84
18	108	6.74	447	3.01
19	114	6.67	474	3.16
20	120	6.67	500	3.34

Table A.3 rheometer data for 30% fly ash

%Fly ash 40				
Meas. Pts.	Time [s]	Viscosity [mPa·s]	Shear Rate [1/s]	Shear Stress [Pa]
1	6	#####	2.4E-06	-
2	12	12	26.3	0.316
3	18	7.75	52.6	0.408
4	24	11.5	78.9	0.905
5	30	9.69	105	1.02
6	36	12.2	132	1.61
7	42	13.9	158	2.19
8	48	14.9	184	2.75
9	54	17	211	3.58
10	60	18	237	4.27
11	66	20.2	263	5.31
12	72	20.7	289	6
13	78	21.7	316	6.85
14	84	23	342	7.87
15	90	24.2	368	8.91
16	96	25	395	9.88
17	102	26.6	421	11.2
18	108	27.6	447	12.4
19	114	29	474	13.7
20	120	30.9	500	15.5

Table A.4 rheometer data for 40% fly ash

%Fly ash 50				
Meas. Pts.	Time [s]	Viscosity [mPa·s]	Shear Rate [1/s]	Shear Stress [Pa]
1	6	#####	1.5E-06	-1.89
2	12	19	26.3	0.499
3	18	21.5	52.6	1.13
4	24	21.8	78.9	1.72
5	30	22.1	105	2.33
6	36	26.5	132	3.49
7	42	27.3	158	4.3
8	48	29.7	184	5.47
9	54	31.3	211	6.6
10	60	32.7	237	7.76
11	66	34.1	263	8.98
12	72	35.1	289	10.2
13	78	37.2	316	11.7
14	84	37.9	342	13
15	90	39.2	368	14.4
16	96	40.4	395	15.9
17	102	41.5	421	17.5
18	108	42.9	447	19.2
19	114	44.5	474	21.1
20	120	46	500	23

Table A.5 rheometer data for 50% fly ash

60 %Fly ash				
Meas. Pts.	Time [s]	Viscosity [mPa·s]	Shear Rate [1/s]	Shear Stress [Pa]
1	6	#####	3.7E-06	0.256
2	12	115	26.3	3.03
3	18	78.5	52.6	4.13
4	24	62.3	78.9	4.92
5	30	57.5	105	6.06
6	36	55.3	132	7.27
7	42	56.4	158	8.91
8	48	58.7	184	10.8
9	54	61.7	211	13
10	60	62.1	237	14.7
11	66	63.3	263	16.7
12	72	65.6	289	19
13	78	69.1	316	21.8
14	84	72.2	342	24.7
15	90	73.8	368	27.2
16	96	75.4	395	29.8
17	102	75.9	421	31.9
18	108	76.9	447	34.4
19	114	78	474	36.9
20	120	77.7	500	38.8

Table A.6 rheometer data for 60% fly ash

	Y0	Y1	Y2	Y3	Y4	Y5	
concentration of fly ash	10%	20%	30%	40%	50%	60%	average ratio
Average Shear stress	0.2958 4	0.737611 1	1.9856 7	6.0352 1	9.9094 2	18.632 6	
ratio (Y <sub>n+1</sub> /Y <sub>n</sub> )		2.493303 8	2.6920 2	3.0393 9	1.6419 3	1.8802 9	2.3493888 8

Average Shear Stress increases exponentially with increase in concentration with common ratio of 2.349388  
9

**exponential co-relation :**

$$Y_n = 0.2958 \times (2.3494)^n$$

here n = 0 at 10%, 1 at 20%, 2 at 30%..

Y axis values	real values	calculated values	error %
Y0	0.29584	0.2958368	0
Y1	0.73761	0.6950358	5.77206
Y2	1.98567	1.6329093	17.7652
Y3	6.03521	3.8363391	36.434
Y4	9.90942	9.0130523	9.04562
Y5	18.6326	21.175165	13.6456

**Table A.7 Calculations involved in the process of estimating an exponential co-relation which describes the change in average shear stress with change in % concentration of fly ash in slurry**

	Y0	Y1	Y2	Y3	Y4	Y5																													
concentration of fly ash	10%	20%	30%	40%	50%	60%	average ratio																												
Average Viscosity	1.14778	2.978889	7.741111	19.2547	33.1947	70.2842																													
ratio (Y <sub>n+1</sub> /Y <sub>n</sub> )		2.595353	2.598657	2.48734	1.72398	2.11733		2.30453065																											
<p>Viscosity increases exponentially with increase in concentration with common ratio of 2.304531</p> <p><b>exponential co-relation :</b></p> <p><math>Y_n = 1.14778 \times (2.304531)^n</math> here n =0 at 10%, 1 at 20%, 2 at 30%...</p> <table border="1"> <thead> <tr> <th>Y axis values</th> <th>real values</th> <th>calculated values</th> <th>error %</th> </tr> </thead> <tbody> <tr> <td>Y0</td> <td>1.14778</td> <td>1.147778</td> <td>0</td> </tr> <tr> <td>Y1</td> <td>2.97889</td> <td>2.645089</td> <td>11.20551</td> </tr> <tr> <td>Y2</td> <td>7.74111</td> <td>6.095689</td> <td>21.25563</td> </tr> <tr> <td>Y3</td> <td>19.2547</td> <td>14.0477</td> <td>27.04288</td> </tr> <tr> <td>Y4</td> <td>33.1947</td> <td>32.37336</td> <td>2.474422</td> </tr> <tr> <td>Y5</td> <td>70.2842</td> <td>74.6054</td> <td>6.148163</td> </tr> </tbody> </table>								Y axis values	real values	calculated values	error %	Y0	1.14778	1.147778	0	Y1	2.97889	2.645089	11.20551	Y2	7.74111	6.095689	21.25563	Y3	19.2547	14.0477	27.04288	Y4	33.1947	32.37336	2.474422	Y5	70.2842	74.6054	6.148163
Y axis values	real values	calculated values	error %																																
Y0	1.14778	1.147778	0																																
Y1	2.97889	2.645089	11.20551																																
Y2	7.74111	6.095689	21.25563																																
Y3	19.2547	14.0477	27.04288																																
Y4	33.1947	32.37336	2.474422																																
Y5	70.2842	74.6054	6.148163																																

**Table A.8** Calculations involved in the process of estimating an exponential co-relation which describes the change in average viscosity with change in %concentration of fly ash in slurry.

REGRESSION DATA											
10% fly ash		20% fly ash		30% fly ash		40% fly ash		50% fly ash		60% fly ash	
ln( $\ddot{Y}$ )	ln( $\tau$ )	ln( $\ddot{Y}$ )	ln( $\tau$ )	ln( $\ddot{Y}$ )	ln( $\tau$ )	ln( $\ddot{Y}$ )	ln( $\tau$ )	ln( $\ddot{Y}$ )	ln( $\tau$ )	ln( $\ddot{Y}$ )	ln( $\tau$ )
5.00922	-1.7550139	5.1569943	-0.700823	4.55455	0.031847	5.15699	0.921599	4.82266	1.1762411	5.2815	2.47144417
5.5435	-1.238916	5.6169575	-0.318115	5.34062	0.53171	5.61696	1.702294	5.45568	2.0462005	5.68116	2.98779028
6.07778	-0.722818	6.0769208	0.064593	6.1267	1.031574	6.07692	2.482989	6.0887	2.9161599	6.08081	3.50413638

**Table A.9** Regression data calculated for 10%,20%,30%,40%,50% and 60% fly ash slurry, data points are calculated within one standard deviation up and sideways.

10 % fly ash						20 % fly ash					
Shear Rate ( $\dot{\gamma}$ ) [1/s]	Shear Stress ( $\tau$ ) [Pa]	$\ln(\dot{\gamma})$	$\ln(\tau)$	actual apparent Viscosity	Calculated viscosity	Shear Rate ( $\dot{\gamma}$ ) [1/s]	Shear Stress ( $\tau$ ) [Pa]	$\ln(\dot{\gamma})$	$\ln(\tau)$	actual apparent Viscosity	Calculated viscosity
0.0000141	0.0241	-11.169	-3.7255	1710000	2.002094	0.0000202	-0.0118	-10.81	#NUM!	#####	41.748623
26.3	0.0155	3.26957	-4.1669	0.59	1.224801	26.2	1.23	3.26576	0.20701	46.70	3.925684
52.6	0.072	3.96272	-2.6311	1.37	1.196245	52.6	0.25	3.96272	-1.3863	4.75	3.4920195
78.9	0.0894	4.36818	-2.4146	1.13	1.179851	78.9	0.493	4.36818	-0.7072	6.25	3.2621243
105	0.127	4.65396	-2.0636	1.21	1.168431	105	0.394	4.65396	-0.9314	3.74	3.1092431
132	0.154	4.8828	-1.8708	1.17	1.159366	132	0.44	4.8828	-0.821	3.34	2.9920036
158	0.186	5.0626	-1.682	1.18	1.152293	158	0.397	5.0626	-0.9238	2.52	2.9030019
184	0.211	5.21494	-1.5559	1.15	1.146335	184	0.479	5.21494	-0.7361	2.60	2.8296649
211	0.239	5.35186	-1.4313	1.14	1.141005	211	0.554	5.35186	-0.5906	2.63	2.7653326
237	0.267	5.46806	-1.3205	1.13	1.136501	237	0.574	5.46806	-0.5551	2.42	2.7118843
263	0.297	5.57215	-1.214	1.13	1.132482	263	0.645	5.57215	-0.4385	2.45	2.664883
289	0.324	5.66643	-1.127	1.12	1.128854	289	0.763	5.66643	-0.2705	2.63	2.6230197
316	0.351	5.75574	-1.047	1.11	1.125428	316	0.802	5.75574	-0.2206	2.54	2.5839644
342	0.382	5.83481	-0.9623	1.12	1.122404	342	0.837	5.83481	-0.1779	2.45	2.5498755
368	0.422	5.90808	-0.8627	1.14	1.119608	368	0.919	5.90808	-0.0845	2.49	2.5186871
395	0.463	5.97889	-0.77	1.17	1.116914	395	1	5.97889	0	2.53	2.4889123
421	0.459	6.04263	-0.7787	1.09	1.114493	421	1.06	6.04263	0.05827	2.51	2.4624059
447	0.492	6.10256	-0.7093	1.1	1.112222	447	1.16	6.10256	0.14842	2.60	2.4377459
474	0.52	6.16121	-0.6539	1.1	1.110004	474	1.22	6.16121	0.19885	2.58	2.4138505
500	0.55	6.21461	-0.5978	1.1	1.107989	500	1.29	6.21461	0.25464	2.59	2.3922971

Table A.10 Modelling data for 10% and 20% fly ash slurry with actual viscosity values and modelled viscosity values

30 % fly ash						40 % fly ash					
Shear Rate ( $\dot{\gamma}$ ) [1/s]	Shear Stress ( $\tau$ ) [Pa]	$\ln(\dot{\gamma})$	$\ln(\tau)$	actual apparent Viscosity	Calculated viscosity	Shear Rate ( $\dot{\gamma}$ ) [1/s]	Shear Stress ( $\tau$ ) [Pa]	$\ln(\dot{\gamma})$	$\ln(\tau)$	actual apparent Viscosity	Calculated viscosity
-0.0000183	0.294	#NUM!	-1.2242	#####	#NUM!	0.00000239	-0.209	-12.944	#NUM!	#####	4.774E-05
26.3	0.699	3.26957	-0.3581	26.50	17.3379732	26.3	0.316	3.26957	-1.152	12.00	3.8815067
52.6	0.598	3.96272	-0.5142	11.40	13.4707799	52.6	0.408	3.96272	-0.8965	7.75	6.2937335
78.9	0.724	4.36818	-0.323	9.17	11.621912	78.9	0.905	4.36818	-0.0998	11.50	8.3501958
105	1.03	4.65396	0.02956	9.78	10.473409	105	1.02	4.65396	0.0198	9.69	10.191546
132	1.35	4.8828	0.3001	10.20	9.63611404	132	1.61	4.8828	0.47623	12.20	11.954761
158	1.21	5.0626	0.19062	7.64	9.02550907	158	2.19	5.0626	0.7839	13.90	13.551527
184	1.37	5.21494	0.31481	7.45	8.53851722	184	2.75	5.21494	1.0116	14.90	15.070306
211	1.59	5.35186	0.46373	7.55	8.12327722	211	3.58	5.35186	1.27536	17.00	16.580084
237	1.71	5.46806	0.53649	7.24	7.78675568	237	4.27	5.46806	1.45161	18.00	17.979456
263	1.9	5.57215	0.64185	7.22	7.49715428	263	5.31	5.57215	1.66959	20.20	19.333017
289	2.07	5.66643	0.72755	7.14	7.24418203	289	6	5.66643	1.79176	20.70	20.6466
316	2.23	5.75574	0.802	7.06	7.01239094	316	6.85	5.75574	1.92425	21.70	21.973349
342	2.37	5.83481	0.86289	6.92	6.8133895	342	7.87	5.83481	2.06306	23.00	23.218856
368	2.56	5.90808	0.94001	6.94	6.63402145	368	8.91	5.90808	2.18717	24.20	24.435998
395	2.68	5.97889	0.98582	6.79	6.46518567	395	9.88	5.97889	2.29051	25.00	25.672699
421	2.84	6.04263	1.0438	6.76	6.31685403	421	11.2	6.04263	2.41591	26.60	26.839614
447	3.01	6.10256	1.10194	6.74	6.18051883	447	12.4	6.10256	2.5177	27.60	27.984901
474	3.16	6.16121	1.15057	6.67	6.04993852	474	13.7	6.16121	2.6174	29.00	29.153088
500	3.34	6.21461	1.20597	6.67	5.9334438	500	15.5	6.21461	2.74084	30.90	30.259106

Table A.11 Modelling data for 30% and 40% fly ash slurry with actual viscosity values and modelled viscosity values

50 % fly ash						60 % fly ash					
Shear Rate ( $\dot{\gamma}$ ) [1/s]	Shear Stress ( $\tau$ ) [Pa]	$\ln(\dot{\gamma})$	$\ln(\tau)$	actual apparent Viscosity	Calculated viscosity	Shear Rate ( $\dot{\gamma}$ ) [1/s]	Shear Stress ( $\tau$ ) [Pa]	$\ln(\dot{\gamma})$	$\ln(\tau)$	actual apparent Viscosity	Calculated viscosity
0.00000145	-1.89	-13.444	#N/MI	#####	0.0279885	0.00000371	0.256	-12.504	-1.3626	#####	0.33441747
26.3	0.499	3.26957	-0.6951	19.00	14.584606	26.3	3.03	3.26957	1.10856	115.00	33.4581123
52.6	1.13	3.96272	0.12222	21.50	18.904767	52.6	4.13	3.96272	1.41828	78.50	40.963332
78.9	1.72	4.36818	0.54232	21.80	22.003051	78.9	4.92	4.36818	1.59331	62.30	46.1115666
105	2.33	4.65396	0.84587	22.10	24.487169	105	6.06	4.65396	1.80171	57.50	50.1242417
132	3.49	4.8828	1.2499	26.50	26.677099	132	7.27	4.8828	1.98376	55.30	53.5877897
158	4.3	5.0626	1.45862	27.30	28.534181	158	8.91	5.0626	2.18717	56.40	56.4760523
184	5.47	5.21494	1.69928	29.70	30.208531	184	10.8	5.21494	2.37955	58.70	59.0448123
211	6.6	5.35186	1.88707	31.30	31.797094	211	13	5.35186	2.56495	61.70	61.4531363
237	7.76	5.46806	2.04898	32.70	33.210621	237	14.7	5.46806	2.68785	62.10	63.5739115
263	8.98	5.57215	2.195	34.10	34.530136	263	16.7	5.57215	2.81541	63.30	65.5357774
289	10.2	5.66643	2.32239	35.10	35.77034	289	19	5.66643	2.94444	65.60	67.3647351
316	11.7	5.75574	2.45959	37.20	36.986396	316	21.8	5.75574	3.08191	69.10	69.1445848
342	13	5.83481	2.56495	37.90	38.097391	342	24.7	5.83481	3.2068	72.20	70.7594386
368	14.4	5.90808	2.66723	39.20	39.156712	368	27.2	5.90808	3.30322	73.80	72.289561
395	15.9	5.97889	2.76632	40.40	40.208306	395	29.8	5.97889	3.39451	75.40	73.7995425
421	17.5	6.04263	2.8622	41.50	41.179244	421	31.9	6.04263	3.46261	75.90	75.1860127
447	19.2	6.10256	2.95491	42.90	42.113349	447	34.4	6.10256	3.53806	76.90	76.5131145
474	21.1	6.16121	3.04927	44.50	43.048062	474	36.9	6.16121	3.60821	78.00	77.8346137
500	23	6.21461	3.13549	46.00	43.917168	500	38.8	6.21461	3.65842	77.70	79.0577057

Table A.12 Modelling data for 50% and 60% fly ash slurry with actual viscosity values and modelled viscosity values

## ANNEXURE B

## ADDITIVES WITH 40% FLY ASH SLURRY

slurry without additive				
Meas. Pts.	Time [s]	Viscosity [mPa·s]	Shear Rate [1/s]	Shear Stress [Pa]
1	6	##### #	2.4E -06	-0.209
2	12	12	26.3	0.316
3	18	7.75	52.6	0.408
4	24	11.5	78.9	0.905
5	30	9.69	105	1.02
6	36	12.2	132	1.61
7	42	13.9	158	2.19
8	48	14.9	184	2.75
9	54	17	211	3.58
10	60	18	237	4.27
11	66	20.2	263	5.31
12	72	20.7	289	6
13	78	21.7	316	6.85
14	84	23	342	7.87
15	90	24.2	368	8.91
16	96	25	395	9.88
17	102	26.6	421	11.2
18	108	27.6	447	12.4
19	114	29	474	13.7
20	120	30.9	500	15.5
Average		19.2547		6.03521

Table B.1 40% slurry without additive

% 0.5 SDS				
Meas. Pts.	Time [s]	Viscosity [mPa·s]	Shear Rate [1/s]	Shear Stress [Pa]
1	6	##### #	-3E- 06	-0.657 -
2	12	-1.93	26.3	0.0508
3	18	3.6	52.6	0.19
4	24	4.98	78.9	0.393
5	30	5.22	105	0.549
6	36	4.23	132	0.556
7	42	6.85	158	1.08
8	48	8.72	184	1.61
9	54	10.6	211	2.23
10	60	13.4	237	3.16
11	66	17.1	263	4.49
12	72	18.6	289	5.37
13	78	19.6	316	6.2
14	84	20.1	342	6.88
15	90	21.5	368	7.92
16	96	22.3	395	8.81
17	102	24	421	10.1
18	108	24.7	447	11.1
19	114	25.8	474	12.2
20	120	27.2	500	13.6
Average		16.87		5.99094

Table B.2 40% slurry with 0.5%SDS

% 1 SDS				
Meas. Pts.	Time [s]	Viscosity [mPa·s]	Shear Rate [1/s]	Shear Stress [Pa]
1	6	#####	-1E-05	-0.562
2	12	2.8	26.3	0.0736
3	18	4.53	52.6	0.238
4	24	2.36	78.9	0.186
5	30	2.91	105	0.306
6	36	4.98	132	0.655
7	42	8.66	158	1.37
8	48	9.15	184	1.69
9	54	11.2	211	2.35
10	60	13.6	237	3.23
11	66	17.3	263	4.55
12	72	18.6	289	5.38
13	78	19.9	316	6.3
14	84	20.8	342	7.12
15	90	21.7	368	8.01
16	96	22.9	395	9.02
17	102	24.7	421	10.4
18	108	25.3	447	11.3
19	114	26.4	474	12.5
20	120	27.8	500	13.9
Average		17.2438		6.13006

Table B.3 40% slurry with 1% SDS

1.5 % SDS				
Meas. Pts.	Time [s]	Viscosity [mPa·s]	Shear Rate [1/s]	Shear Stress [Pa]
1	6	#####	#####	-0.854
2	12	0.182	26.3	0.00479
3	18	-1.79	52.6	-0.094
4	24	-0.382	78.9	-0.0302
5	30	4.04	105	0.425
6	36	3.6	132	0.474
7	42	5.9	158	0.932
8	48	7.82	184	1.44
9	54	9.45	211	1.99
10	60	12.4	237	2.94
11	66	15.8	263	4.16
12	72	17.8	289	5.15
13	78	19	316	5.99
14	84	19.5	342	6.68
15	90	20.7	368	7.61
16	96	21.5	395	8.47
17	102	23.2	421	9.77
18	108	24.1	447	10.8
19	114	25	474	11.8
20	120	26.5	500	13.3
Average		14.1188		5.10038

Table B.4 40% slurry with 1.5% SDS

% Triton x-100				
0.5				
Meas. Pts.	Time [s]	Viscosity [mPa·s]	Shear Rate [1/s]	Shear Stress [Pa]
1	6	#####	-1E-05	-1.61
2	12	-1.5	21.1	-0.03
3	18	5.62	42.1	0.23
4	24	6.2	63.2	0.39
5	30	7.71	84.2	0.65
6	36	7.79	105	0.82
7	42	9.16	126	1.16
8	48	12.5	147	1.84
9	54	13	168	2.18
10	60	14.6	189	2.77
11	66	16.5	211	3.48
12	72	18.2	232	4.2
13	78	19.9	253	5.02
14	84	20.5	274	5.6
15	90	21.6	295	6.38
16	96	22.3	316	7.05
17	102	23.7	337	7.98
18	108	25.3	358	9.07
19	114	26.2	379	9.93
20	120	27.4	400	11
Average		16.566		4.431

Table B.5 40% slurry with 0.5% triton

1 % Triton x-100				
Meas. Pts.	Time [s]	Viscosity [mPa·s]	Shear Rate [1/s]	Shear Stress [Pa]
1	6	1.15E+09	#####	-0.165
2	12	-3.34	26.3	0.088
3	18	0.51	52.6	0.026
4	24	7.51	78.9	0.593
5	30	9.88	105	1.04
6	36	11.1	132	1.46
7	42	11.8	158	1.86
8	48	13.2	184	2.43
9	54	16	211	3.36
10	60	17.8	237	4.22
11	66	20.2	263	5.31
12	72	21.4	289	6.19
13	78	22.3	316	7.03
14	84	23.6	342	8.06
15	90	25	368	9.2
16	96	26.8	395	10.6
17	102	28.2	421	11.9
18	108	29.6	447	13.2
19	114	30.8	474	14.6
20	120	32.1	500	16.1
Average		19.3222		6.51

Table B.6 40% slurry with 1% triton

1.5 % Triton x-100				
Meas. Pts.	Time [s]	Viscosity [mPa·s]	Shear Rate [1/s]	Shear Stress [Pa]
1	6	#####	-2E-06	-1.53
2	12	-5.6	26.3	-0.147
3	18	3.81	52.6	0.201
4	24	5.23	78.9	0.413
5	30	7.95	105	0.837
6	36	12.4	132	1.63
7	42	12.9	158	2.03
8	48	14.9	184	2.75
9	54	16.9	211	3.55
10	60	19.1	237	4.52
11	66	20.7	263	5.45
12	72	22.4	289	6.48
13	78	23.2	316	7.34
14	84	25.2	342	8.61
15	90	26.6	368	9.78
16	96	27.9	395	11
17	102	30.1	421	12.7
18	108	31.7	447	14.2
19	114	32.6	474	15.5
20	120	34.3	500	17.1
Average		20.4383		6.89394

Table B.7 40% slurry with 1.5% triton

0.5 % CPC				
Meas. Pts.	Time [s]	Viscosity [mPa·s]	Shear Rate [1/s]	Shear Stress [Pa]
1	6	#####	#####	-0.904
2	12	-3.11	26.3	-0.0818
3	18	-0.36	52.6	-0.0189
4	24	-0.246	78.9	-0.0195
5	30	2.14	105	0.225
6	36	2.19	132	0.288
7	42	4.65	158	0.735
8	48	7.78	184	1.43
9	54	9.6	211	2.02
10	60	11.5	237	2.73
11	66	15.6	263	4.1
12	72	17	289	4.93
13	78	17.8	316	5.61
14	84	18.7	342	6.39
15	90	19.8	368	7.28
16	96	21.2	395	8.36
17	102	22.5	421	9.46
18	108	23.4	447	10.5
19	114	24.9	474	11.8
20	120	27.5	500	13.7
Average		15.3913		5.59738

Table B.8 40% slurry, 0.5% CPC

% 1 CPC				
Meas. Pts.	Time [s]	Viscosity [mPa·s]	Shear Rate [1/s]	Shear Stress [Pa]
1	6	#####	2.1E-05	-2.02
2	12	-6.13	26.3	-0.161
3	18	-0.501	52.6	-0.0264
4	24	-0.0278	78.9	-0.0022
5	30	0.624	105	0.0657
6	36	2.4	132	0.316
7	42	4.9	158	0.774
8	48	7.8	184	1.44
9	54	9.64	211	2.03
10	60	12	237	2.84
11	66	16.4	263	4.33
12	72	18.6	289	5.37
13	78	19.1	316	6.03
14	84	20	342	6.83
15	90	21.3	368	7.85
16	96	22.6	395	8.91
17	102	24.2	421	10.2
18	108	25	447	11.2
19	114	26.3	474	12.5
20	120	27.6	500	13.8
Average		16.154		5.90536

Table B.9 40% slurry with 1% CPC

% 1.5 CPC				
Meas. Pts.	Time [s]	Viscosity [mPa·s]	Shear Rate [1/s]	Shear Stress [Pa]
1	6	#####	-1E-05	-2.38
2	12	-3.53	26.3	-0.09
3	18	1.91	52.6	0.1
4	24	0.76	78.9	0.06
5	30	1.41	105	0.148
6	36	2.81	132	0.37
7	42	5.37	158	0.848
8	48	7.57	184	1.39
9	54	10.2	211	2.14
10	60	11.7	237	2.77
11	66	15.8	263	4.16
12	72	16.9	289	4.9
13	78	18.9	316	5.97
14	84	19.4	342	6.64
15	90	20.8	368	7.66
16	96	22	395	8.69
17	102	23.9	421	10
18	108	25	447	11.2
19	114	26.4	474	12.5
20	120	27.8	500	13.9
Average		14.368		5.191

Table B.10 40% slurry with 1.5% CPC

0% additive					0.5% additive						
Shear Rate ( $\dot{\gamma}$ ) [1/s]	Shear Stress ( $\tau$ ) [Pa]	$\ln(\dot{\gamma})$	$\ln(\tau)$	Actual apparent viscosity	Calculated Viscosity	Shear Rate ( $\dot{\gamma}$ ) [1/s]	Shear Stress ( $\tau$ ) [Pa]	$\ln(\dot{\gamma})$	$\ln(\tau)$	Actual apparent viscosity	Calculated Viscosity
0.00000239	-0.209	-12.944	#NUM!	#####	0.0002629	0.00	-0.904	#NUM!	#NUM!	#####	#NUM!
26.3	0.316	3.26957	-1.152	12.00	4.8779503	26.30	-0.0818	3.26957	#NUM!	-3.11	0.910834
52.6	0.408	3.96272	-0.8965	7.75	7.4253651	52.60	-0.0189	3.96272	#NUM!	-0.36	2.0427398
78.9	0.905	4.36818	-0.0998	11.50	9.4942798	78.90	-0.0195	4.36818	#NUM!	-0.25	3.2764427
105	1.02	4.65396	0.0198	9.69	11.290087	105.00	0.225	4.65396	-1.4917	2.14	4.571133
132	1.61	4.8828	0.47623	12.20	12.970088	132.00	0.288	4.8828	-1.2448	2.19	5.9680348
158	2.19	5.0626	0.7839	13.90	14.463584	158.00	0.735	5.0626	-0.3079	4.65	7.3589759
184	2.75	5.21494	1.0116	14.90	15.862867	184.00	1.43	5.21494	0.35767	7.78	8.7884214
211	3.58	5.35186	1.27536	17.00	17.235678	211.00	2.02	5.35186	0.7031	9.60	10.308649
237	4.27	5.46806	1.45161	18.00	18.493544	237.00	2.73	5.46806	1.0043	11.50	11.803394
263	5.31	5.57215	1.66959	20.20	19.698097	263.00	4.1	5.57215	1.41099	15.60	13.325534
289	6	5.66643	1.79176	20.70	20.856567	289.00	4.93	5.66643	1.59534	17.00	14.872782
316	6.85	5.75574	1.92425	21.70	22.01691	316.00	5.61	5.75574	1.72455	17.80	16.504075
342	7.87	5.83481	2.06306	23.00	23.097886	342.00	6.39	5.83481	1.85473	18.70	18.096917
368	8.91	5.90808	2.18717	24.20	24.146941	368.00	7.28	5.90808	1.98513	19.80	19.709912
395	9.88	5.97889	2.29051	25.00	25.205884	395.00	8.36	5.97889	2.12346	21.20	21.404995
421	11.2	6.04263	2.41591	26.60	26.19897	421.00	9.46	6.04263	2.24707	22.50	23.055522
447	12.4	6.10256	2.5177	27.60	27.168177	447.00	10.5	6.10256	2.35138	23.40	24.722989
474	13.7	6.16121	2.6174	29.00	28.151437	474.00	11.8	6.16121	2.4681	24.90	26.471632
500	15.5	6.21461	2.74084	30.90	29.077633	500.00	13.7	6.21461	2.6174	27.50	28.171158

Table B.11 Modelling data of 40% fly ash concentration slurry with 0% additive and 0.5% CPC

1% additive				Actual				1.5% additive				Actual					
Shear Rate ( $\dot{\gamma}$ ) [1/s]	Shear Stress ( $\tau$ ) [Pa]	$\ln(\dot{\gamma})$	$\ln(\tau)$	apparent viscosity	Calculated Viscosity	Shear Rate ( $\dot{\gamma}$ ) [1/s]	Shear Stress ( $\tau$ ) [Pa]	$\ln(\dot{\gamma})$	$\ln(\tau)$	apparent viscosity	Calculated Viscosity	Shear Rate ( $\dot{\gamma}$ ) [1/s]	Shear Stress ( $\tau$ ) [Pa]	$\ln(\dot{\gamma})$	$\ln(\tau)$	apparent viscosity	Calculated Viscosity
0.00	-2.02	-10.757	#NUM!	#####	4.235E-08	0.00	-2.38	#NUM!	#NUM!	#####	#NUM!	0.00	-2.38	#NUM!	#NUM!	#####	#NUM!
26.30	-0.161	3.26957	#NUM!	-6.13	0.8768089	26.30	-0.0928	3.26957	#NUM!	-3.53	0.6009928	26.30	-0.0928	3.26957	#NUM!	-3.53	0.6009928
52.60	-0.0264	3.96272	#NUM!	-0.50	2.0157857	52.60	0.1	3.96272	-2.3026	1.91	1.5184729	52.60	0.1	3.96272	-2.3026	1.91	1.5184729
78.90	-0.0022	4.36818	#NUM!	-0.03	3.2804346	78.90	0.06	4.36818	-2.8134	0.76	2.6114188	78.90	0.06	4.36818	-2.8134	0.76	2.6114188
105.00	0.0657	4.65396	-2.7227	0.62	4.623717	105.00	0.148	4.65396	-1.9105	1.41	3.8268344	105.00	0.148	4.65396	-1.9105	1.41	3.8268344
132.00	0.316	4.8828	-1.152	2.40	6.0862947	132.00	0.37	4.8828	-0.9943	2.81	5.1968113	132.00	0.37	4.8828	-0.9943	2.81	5.1968113
158.00	0.774	5.0626	-0.2562	4.90	7.5532085	158.00	0.848	5.0626	-0.1649	5.37	6.6092147	158.00	0.848	5.0626	-0.1649	5.37	6.6092147
184.00	1.44	5.21494	0.36464	7.80	9.0696609	184.00	1.39	5.21494	0.3293	7.57	8.1025197	184.00	1.39	5.21494	0.3293	7.57	8.1025197
211.00	2.03	5.35186	0.70804	9.64	10.690759	211.00	2.14	5.35186	0.76081	10.20	9.7305253	211.00	2.14	5.35186	0.76081	10.20	9.7305253
237.00	2.84	5.46806	1.0438	12.00	12.291885	237.00	2.77	5.46806	1.01885	11.70	11.366306	237.00	2.77	5.46806	1.01885	11.70	11.366306
263.00	4.33	5.57215	1.46557	16.40	13.928776	263.00	4.16	5.57215	1.42552	15.80	13.063837	263.00	4.16	5.57215	1.42552	15.80	13.063837
289.00	5.37	5.66643	1.68083	18.60	15.598568	289.00	4.9	5.66643	1.58924	16.90	14.818989	289.00	4.9	5.66643	1.58924	16.90	14.818989
316.00	6.03	5.75574	1.79675	19.10	17.364845	316.00	5.97	5.75574	1.78675	18.90	16.69889	316.00	5.97	5.75574	1.78675	18.90	16.69889
342.00	6.83	5.83481	1.92132	20.00	19.094679	342.00	6.64	5.83481	1.89311	19.40	18.56119	342.00	6.64	5.83481	1.89311	19.40	18.56119
368.00	7.85	5.90808	2.06051	21.30	20.851173	368.00	7.66	5.90808	2.03601	20.80	20.471886	368.00	7.66	5.90808	2.03601	20.80	20.471886
395.00	8.91	5.97889	2.18717	22.60	22.701817	395.00	8.69	5.97889	2.16217	22.00	22.504835	395.00	8.69	5.97889	2.16217	22.00	22.504835
421.00	10.2	6.04263	2.32239	24.20	24.508149	421.00	10	6.04263	2.30259	23.90	24.507344	421.00	10	6.04263	2.30259	23.90	24.507344
447.00	11.2	6.10256	2.41591	25.00	26.337058	447.00	11.2	6.10256	2.41591	25.00	26.552015	447.00	11.2	6.10256	2.41591	25.00	26.552015
474.00	12.5	6.16121	2.52573	26.30	28.259074	474.00	12.5	6.16121	2.52573	26.40	28.718193	474.00	12.5	6.16121	2.52573	26.40	28.718193
500.00	13.8	6.21461	2.62467	27.60	30.130844	500.00	13.9	6.21461	2.63189	27.80	30.843882	500.00	13.9	6.21461	2.63189	27.80	30.843882

**Table B.12 Modelling data of 40% fly ash concentration slurry with 1% additive and 1.5% CPC**

REGRESSION LINE							
without CPC		0.5% CPC		1% CPC		1.5% CPC	
$\ln(\ddot{Y})$	$\ln(\tau)$	$\ln(\ddot{Y})$	$\ln(\tau)$	$\ln(\ddot{Y})$	$\ln(\tau)$	$\ln(\ddot{Y})$	$\ln(\tau)$
4.82266	0.44105407	5.4836264	1.0627003	5.48363	1.103593	5.38839	0.80482
5.45568	1.45779991	5.790151	1.7264013	5.79015	1.778257	5.73818	1.622357
6.0887	2.47454574	6.0966756	2.3901023	6.09668	2.45292	6.08798	2.439894

**Table B.13 Regression data calculated for 40% fly ash slurry with different concentrations of CPC**

REGRESSION LINE							
Without SDS		0.5% SDS		1% SDS		1.5% SDS	
$\ln(\ddot{Y})$	$\ln(\tau)$	$\ln(\ddot{Y})$	$\ln(\tau)$	$\ln(\ddot{Y})$	$\ln(\tau)$	$\ln(\ddot{Y})$	$\ln(\tau)$
4.82266	0.44105407	4.8226604	-0.188436	4.55455	0.666479	-	-
5.45568	1.45779991	5.4556788	1.0964756	5.34062	0.880957	5.15699	0.233903
6.0887	2.47454574	6.0886972	2.3813875	6.1267	2.428393	5.61696	1.318312
						6.07692	2.402721

**Table B.14 Regression data calculated for 40% fly ash slurry with different concentrations of SDS**

REGRESSION LINE							
Without Triton		0.5% Triton x-100		1% Triton x-100		1.5% Triton x-100	
$\ln(\ddot{Y})$	$\ln(\tau)$	$\ln(\ddot{Y})$	$\ln(\tau)$	$\ln(\ddot{Y})$	$\ln(\tau)$	$\ln(\ddot{Y})$	$\ln(\tau)$
4.82266	0.44105407	4.5989682	-0.111786	5.00922	0.608509	4.82266	0.171674
5.45568	1.45779991	5.23241	1.0193476	5.5435	1.569507	5.45568	1.415588
6.0887	2.47454574	5.8658518	2.1504816	6.07778	2.530505	6.0887	2.659502

**Table B.15 Regression data calculated for 40% fly ash slurry with different concentrations of Triton**

0.5% additive				Actual				1% additive				Actual					
Shear Rate ( $\dot{\gamma}$ ) [1/s]	Shear Stress ( $\tau$ ) [Pa]	$\ln(\dot{\gamma})$ #NUM!	$\ln(\tau)$ #NUM!	apparent viscosity #####	Calculated Viscosity #NUM!	Shear Rate ( $\dot{\gamma}$ ) [1/s]	Shear Stress ( $\tau$ ) [Pa]	$\ln(\dot{\gamma})$ #NUM!	$\ln(\tau)$ #NUM!	apparent viscosity #####	Calculated Viscosity #NUM!	Shear Rate ( $\dot{\gamma}$ ) [1/s]	Shear Stress ( $\tau$ ) [Pa]	$\ln(\dot{\gamma})$ #NUM!	$\ln(\tau)$ #NUM!	apparent viscosity #####	Calculated Viscosity #NUM!
0.00	-0.657	#NUM!	#NUM!	#####	#NUM!	0.00	-0.562	#NUM!	#NUM!	#####	#NUM!	0.00	-0.562	#NUM!	#NUM!	#####	#NUM!
26.30	-0.0508	3.26957	#NUM!	-1.93	1.3461045	26.30	0.0736	3.26957	-2.6091	2.80	1.5560174	26.30	0.0736	3.26957	-2.6091	2.80	1.5560174
52.60	0.19	3.96272	-1.6607	3.60	2.7484305	52.60	0.238	3.96272	-1.4355	4.53	3.0449498	52.60	0.238	3.96272	-1.4355	4.53	3.0449498
78.90	0.393	4.36818	-0.9339	4.98	4.172791	78.90	0.186	4.36818	-1.682	2.36	4.5095699	78.90	0.186	4.36818	-1.682	2.36	4.5095699
105.00	0.549	4.65396	-0.5997	5.22	5.6006658	105.00	0.306	4.65396	-1.1842	2.91	5.9476493	105.00	0.306	4.65396	-1.1842	2.91	5.9476493
132.00	0.556	4.8828	-0.587	4.23	7.0890444	132.00	0.655	4.8828	-0.4231	4.98	7.4234425	132.00	0.655	4.8828	-0.4231	4.98	7.4234425
158.00	1.08	5.0626	0.07696	6.85	8.5309835	158.00	1.37	5.0626	0.31481	8.66	8.83555	158.00	1.37	5.0626	0.31481	8.66	8.83555
184.00	1.61	5.21494	0.47623	8.72	9.9800472	184.00	1.69	5.21494	0.52473	9.15	10.240337	184.00	1.69	5.21494	0.52473	9.15	10.240337
211.00	2.23	5.35186	0.802	10.60	11.491331	211.00	2.35	5.35186	0.85442	11.20	11.692552	211.00	2.35	5.35186	0.85442	11.20	11.692552
237.00	3.16	5.46806	1.15057	13.40	12.952124	237.00	3.23	5.46806	1.17248	13.60	13.085447	237.00	3.23	5.46806	1.17248	13.60	13.085447
263.00	4.49	5.57215	1.50185	17.10	14.417712	263.00	4.55	5.57215	1.51513	17.30	14.473537	263.00	4.55	5.57215	1.51513	17.30	14.473537
289.00	5.37	5.66643	1.68083	18.60	15.887635	289.00	5.38	5.66643	1.68269	18.60	15.857311	289.00	5.38	5.66643	1.68269	18.60	15.857311
316.00	6.2	5.75574	1.82455	19.60	17.418273	316.00	6.3	5.75574	1.84055	19.90	17.29017	316.00	6.3	5.75574	1.84055	19.90	17.29017
342.00	6.88	5.83481	1.92862	20.10	18.895919	342.00	7.12	5.83481	1.96291	20.80	18.666319	342.00	7.12	5.83481	1.96291	20.80	18.666319
368.00	7.92	5.90808	2.06939	21.50	20.376922	368.00	8.01	5.90808	2.08069	21.70	20.039179	368.00	8.01	5.90808	2.08069	21.70	20.039179
395.00	8.81	5.97889	2.17589	22.30	21.918192	395.00	9.02	5.97889	2.19944	22.90	21.461617	395.00	9.02	5.97889	2.19944	22.90	21.461617
421.00	10.1	6.04263	2.31254	24.00	23.405354	421.00	10.4	6.04263	2.34181	24.70	22.828482	421.00	10.4	6.04263	2.34181	24.70	22.828482
447.00	11.1	6.10256	2.40695	24.70	24.89526	447.00	11.3	6.10256	2.4248	25.30	24.192694	447.00	11.3	6.10256	2.4248	25.30	24.192694
474.00	12.2	6.16121	2.50144	25.80	26.445206	474.00	12.5	6.16121	2.52573	26.40	25.606737	474.00	12.5	6.16121	2.52573	26.40	25.606737
500.00	13.6	6.21461	2.61007	27.20	27.940241	500.00	13.9	6.21461	2.63189	27.80	26.966015	500.00	13.9	6.21461	2.63189	27.80	26.966015

**Table B.16 Modelling data of 40% fly ash concentration slurry with 0.5% and 1% SDS**

1.5% SDS						0.5% Triton x-100					
Shear Rate ( $\dot{\gamma}$ ) [1/s]	Shear Stress ( $\tau$ ) [Pa]	$\ln(\dot{\gamma})$	$\ln(\tau)$	Actual apparent viscosity	Calculated Viscosity	Shear Rate ( $\dot{\gamma}$ ) [1/s]	Shear Stress ( $\tau$ ) [Pa]	$\ln(\dot{\gamma})$	$\ln(\tau)$	Actual apparent viscosity	Calculated Viscosity
0.00	-0.854	#NUM!	#NUM!	#####	#NUM!	0.00				#####	#NUM!
26.30	0.00479	3.26957	-5.341225	0.18	0.5613104	21.10	-0.0316	3.049273	#NUM!	-1.50	2.66300417
52.60	-0.094	3.96272	#NUM!	-1.79	1.4384049	42.10	0.237	3.740048	-1.4397	5.62	4.5822646
78.90	-0.0302	4.36818	#NUM!	-0.38	2.4942643	63.20	0.391	4.146304	-0.93905	6.20	6.30527896
105.00	0.425	4.65396	-0.855666	4.04	3.6765223	84.20	0.65	4.433195	-0.43078	7.71	7.8994713
132.00	0.474	4.8828	-0.746548	3.60	5.0160479	105.00	0.82	4.65396	-0.19845	7.79	9.3956818
158.00	0.932	5.0626	-0.070422	5.90	6.4027611	126.00	1.16	4.836282	0.14842	9.16	10.8427797
184.00	1.44	5.21494	0.3646431	7.82	7.8738483	147.00	1.84	4.990433	0.609766	12.50	12.2388445
211.00	1.99	5.35186	0.6881346	9.45	9.4823541	168.00	2.18	5.123964	0.779325	13.00	13.5926589
237.00	2.94	5.46806	1.0784096	12.40	11.1027	189.00	2.77	5.241747	1.018847	14.60	14.9105861
263.00	4.16	5.57215	1.4255151	15.80	12.787986	211.00	3.48	5.351858	1.247032	16.50	16.2580022
289.00	5.15	5.66643	1.6389967	17.80	14.533998	232.00	4.2	5.446737	1.435085	18.20	17.5162918
316.00	5.99	5.75574	1.7900914	19.00	16.40761	253.00	5.02	5.533389	1.61343	19.90	18.7503716
342.00	6.68	5.83481	1.899118	19.50	18.266862	274.00	5.6	5.613128	1.722767	20.50	19.962666
368.00	7.61	5.90808	2.0294632	20.70	20.177394	295.00	6.38	5.686975	1.853168	21.60	21.1551901
395.00	8.47	5.97889	2.1365305	21.50	22.213156	316.00	7.05	5.755742	1.953028	22.30	22.3296428
421.00	9.77	6.04263	2.2793165	23.20	24.221185	337.00	7.98	5.820083	2.076938	23.70	23.4874742
447.00	10.8	6.10256	2.3795461	24.10	26.274078	358.00	9.07	5.880533	2.204972	25.30	24.6299355
474.00	11.8	6.16121	2.4680995	25.00	28.451596	379.00	9.93	5.937536	2.29556	26.20	25.7581159
500.00	13.3	6.21461	2.587764	26.50	30.590855	400.00	11	5.991465	2.397895	27.40	26.8729715

**Table B.17 Modelling data of 40% fly ash concentration slurry with 1.5% SDS and 0.5% Triton x-100**

1% Triton x-100					1.5% Triton x-100						
Shear Rate ( $\dot{\gamma}$ ) [1/s]	Shear Stress ( $\tau$ ) [Pa]	$\ln(\dot{\gamma})$	$\ln(\tau)$	Actual apparent viscosity	Calculated Viscosity	Shear Rate ( $\dot{\gamma}$ ) [1/s]	Shear Stress ( $\tau$ ) [Pa]	$\ln(\dot{\gamma})$	$\ln(\tau)$	Actual apparent viscosity	Calculated Viscosity
0.00	-0.165	#NUM!	#NUM!	#####	#NUM!	0.00	-1.53	#NUM!	#NUM!	656000000.00	#NUM!
26.30	-0.0879	3.269569	#NUM!	-3.34	3.0577151	26.30	-0.147	3.269569	#NUM!	-5.60	2.1339197
52.60	0.0269	3.962716	-3.61563	0.51	5.31889235	52.60	0.201	3.962716	-1.6044504	3.81	4.16569801
78.90	0.593	4.368181	-0.52256	7.51	7.3529283	78.90	0.413	4.368181	-0.8843077	5.23	6.16062919
105.00	1.04	4.65396	0.039221	9.88	9.23815677	105.00	0.837	4.65396	-0.1779312	7.95	8.11708201
132.00	1.46	4.882802	0.378436	11.10	11.0907531	132.00	1.63	4.882802	0.48858001	12.40	10.1230483
158.00	1.86	5.062595	0.620576	11.80	12.8033569	158.00	2.03	5.062595	0.70803579	12.90	12.0410856
184.00	2.43	5.214936	0.887891	13.20	14.4598761	184.00	2.75	5.214936	1.01160091	14.90	13.9480732
211.00	3.36	5.351858	1.211941	16.00	16.1308517	211.00	3.55	5.351858	1.2669476	16.90	15.9184472
237.00	4.22	5.46806	1.439835	17.80	17.699581	237.00	4.52	5.46806	1.50851199	19.10	17.807499
263.00	5.31	5.572154	1.669592	20.20	19.2339669	263.00	5.45	5.572154	1.69561561	20.70	19.6893074
289.00	6.19	5.66427	1.822935	21.40	20.7380617	289.00	6.48	5.66427	1.86872051	22.40	21.5646148
316.00	7.03	5.755742	1.950187	22.30	22.2714265	316.00	7.34	5.755742	1.99333884	23.20	23.5058171
342.00	8.06	5.834811	2.086914	23.60	23.7232206	342.00	8.61	5.834811	2.15292432	25.20	25.3696402
368.00	9.2	5.908083	2.219203	25.00	25.1529399	368.00	9.78	5.908083	2.28033948	26.60	27.2285132
395.00	10.6	5.978886	2.360854	26.80	26.6162787	395.00	11	5.978886	2.39789527	27.90	29.1540296
421.00	11.9	6.042633	2.476538	28.20	28.0064824	421.00	12.7	6.042633	2.54160199	30.10	31.0038813
447.00	13.2	6.102559	2.580217	29.60	29.379496	447.00	14.2	6.102559	2.65324196	31.70	32.8497422
474.00	14.6	6.161207	2.681022	30.80	30.7884033	474.00	15.5	6.161207	2.74084002	32.60	34.762631
500.00	16.1	6.214608	2.778819	32.10	32.1299237	500.00	17.1	6.214608	2.83907846	34.30	36.6010722

**Table B.18 Modelling data of 40% fly ash concentration slurry with 1% and 1.5% Triton x-100**

## ANNEXURE C

## 50% FLY ASH SLURRY WITH DIFFERENT PARTICLE SIZE RANGE

Particle size of slurry 255 to 150 $\mu\text{m}$				
Meas. Pts.	Time [s]	Viscosity [mPa·s]	Shear Rate [1/s]	Shear Stress [Pa]
1	6	#####	0	0.151
2	12	13,000	26	342
3	18	7,720	53	406
4	24	4,950	79	391
5	30	3,520	105	370
6	36	2,720	132	357
7	42	2,190	158	345
8	48	1,830	184	338
9	54	1,590	211	335
10	60	1,390	237	329
11	66	1,230	263	323
12	72	1,100	289	318
13	78	1,000	316	317
14	84	921	342	315
15	90	825	368	304
16	96	670	395	265
17	102	581	421	245
18	108	505	447	226
19	114	471	474	223
20	120	457	500	228

Table C.1 50% slurry, size-255 to 150 $\mu\text{m}$ 

Particle size of slurry 150 to 106 $\mu\text{m}$				
Meas. Pts.	Time [s]	Viscosity [mPa·s]	Shear Rate [1/s]	Shear Stress [Pa]
1	6	#####	-6E-05	1.36
2	12	3,990	26.3	105
3	18	2,580	52.6	136
4	24	2,050	78.9	162
5	30	1,830	105	193
6	36	1,560	132	205
7	42	1,270	158	200
8	48	1,020	184	189
9	54	774	211	163
10	60	574	237	136
11	66	474	263	125
12	72	394	289	114
13	78	331	316	104
14	84	279	342	95.5
15	90	250	368	92
16	96	222	395	87.7
17	102	200	421	84.2
18	108	182	447	81.6
19	114	169	474	80.2
20	120	165	500	82.4

Table C.2 50% slurry, size-150 to 106 $\mu\text{m}$

Particle size of slurry 106 to 75 $\mu\text{m}$				
Meas. Pts.	Time [s]	Viscosity [mPa·s]	Shear Rate [1/s]	Shear Stress [Pa]
1	6	#####	4.59E-08	-0.42
2	12	45.4	26.3	1.19
3	18	42.6	52.6	2.24
4	24	40.7	78.9	3.21
5	30	38.3	105	4.03
6	36	41.2	132	5.43
7	42	44.4	158	7.01
8	48	46.3	184	8.53
9	54	46.8	211	9.85
10	60	49.9	237	11.8
11	66	54.2	263	14.3
12	72	56.7	289	16.4
13	78	60.6	316	19.1
14	84	64.8	342	22.2
15	90	69	368	25.4
16	96	72.6	395	28.7
17	102	76.5	421	32.2
18	108	79.1	447	35.4
19	114	82.6	474	39.1
20	120	83.6	500	41.8

Table C.3 50% fly ash, size-106 to 75 $\mu\text{m}$ 

Particle size of slurry 75 to 53 $\mu\text{m}$				
Meas. Pts.	Time [s]	Viscosity [mPa·s]	Shear Rate [1/s]	Shear Stress [Pa]
1	6	#####	2.3E-06	-0.377
2	12	49.1	26.3	1.29
3	18	35.1	52.6	1.85
4	24	29.7	78.9	2.34
5	30	28.6	105	3.01
6	36	30.3	132	3.99
7	42	31.3	158	4.94
8	48	31	184	5.71
9	54	33.1	211	6.96
10	60	33.8	237	8
11	66	35.2	263	9.27
12	72	37.3	289	10.8
13	78	37.8	316	11.9
14	84	39.4	342	13.5
15	90	40.6	368	14.9
16	96	41.5	395	16.4
17	102	42.9	421	18.1
18	108	43.5	447	19.5
19	114	44.4	474	21
20	120	46.7	500	23.3

Table C.4 50% fly ash, size-75 to 53 $\mu\text{m}$

Particle size of slurry 0 to 53 $\mu\text{m}$				
Meas. Pts.	Time [s]	Viscosity [mPa·s]	Shear Rate [1/s]	Shear Stress [Pa]
1	6	#####	-4E-06	-0.742
2	12	63.8	26.3	1.68
3	18	45.6	52.6	2.4
4	24	34	78.9	2.68
5	30	29.9	105	3.15
6	36	29.9	132	3.93
7	42	31.9	158	5.04
8	48	33	184	6.07
9	54	32.4	211	6.81
10	60	34.1	237	8.07
11	66	35.3	263	9.28
12	72	36.7	289	10.6
13	78	37.3	316	11.8
14	84	37.9	342	13
15	90	39.5	368	14.6
16	96	39.7	395	15.7
17	102	41	421	17.3
18	108	40.9	447	18.3
19	114	42.2	474	20
20	120	43.2	500	21.6

Table C.5 50% slurry, size-0 to 53 $\mu\text{m}$ 

Particle size 255 to 150 $\mu\text{m}$ with 0.5% CPC				
Meas. Pts.	Time [s]	Viscosity [mPa·s]	Shear Rate [1/s]	Shear Stress [Pa]
1	6	#####	0	12.5
2	12	11,100	26	291
3	18	7,070	53	372
4	24	4,550	79	359
5	30	3,310	105	348
6	36	2,540	132	335
7	42	2,070	158	326
8	48	1,720	184	316
9	54	1,450	211	306
10	60	1,250	237	296
11	66	1,040	263	275
12	72	721	289	209
13	78	546	316	172
14	84	475	342	163
15	90	446	368	164
16	96	424	395	167
17	102	407	421	171
18	108	388	447	174
19	114	368	474	174
20	120	352	500	176

Table C.6 50% slurry, (255-150 $\mu\text{m}$ ), 0.5% CPC

Particle size 150 to 106 $\mu\text{m}$ with 0.5% CPC				
Meas. Pts.	Time [s]	Viscosity [mPa·s]	Shear Rate [1/s]	Shear Stress [Pa]
1	6	#####	0.0003	5.96
2	12	5,310	26.3	140
3	18	4,030	52.6	212
4	24	3,190	78.9	252
5	30	2,410	105	254
6	36	1,900	132	250
7	42	1,560	158	247
8	48	1,320	184	244
9	54	1,120	211	236
10	60	890	237	211
11	66	609	263	160
12	72	483	289	140
13	78	443	316	140
14	84	425	342	146
15	90	412	368	152
16	96	396	395	156
17	102	375	421	158
18	108	351	447	157
19	114	336	474	159
20	120	329	500	164

Table C.7 50% fly ash,(150-106 $\mu\text{m}$ )

Particle size 106 to 75 $\mu\text{m}$ with 0.5% CPC				
Meas. Pts.	Time [s]	Viscosity [mPa·s]	Shear Rate [1/s]	Shear Stress [Pa]
1	6	#####	2.19E-07	0.706
2	12	10.2	26.3	0.268
3	18	16.1	52.6	0.848
4	24	22.9	78.9	1.81
5	30	25.8	105	2.71
6	36	29.6	132	3.89
7	42	34.1	158	5.39
8	48	36.8	184	6.79
9	54	40.4	211	8.51
10	60	44.3	237	10.5
11	66	47	263	12.4
12	72	48	289	13.9
13	78	49	316	15.5
14	84	51.1	342	17.5
15	90	53.5	368	19.7
16	96	57.2	395	22.6
17	102	60.6	421	25.5
18	108	62.4	447	27.9
19	114	61.9	474	29.3
20	120	63	500	31.5

Table C.8 50% fly ash,(106-75 $\mu\text{m}$ ),0.5%CPC

Particle size 75 to 53 $\mu\text{m}$ with 0.5% CPC				
Meas. Pts.	Time [s]	Viscosity [mPa·s]	Shear Rate [1/s]	Shear Stress [Pa]
1	6	#####	-3E-06	-0.58
2	12	-7.56	26.3	-0.199
3	18	-1.04	52.6	-0.055
4	24	5.97	78.9	0.472
5	30	8.54	105	0.899
6	36	11.9	132	1.57
7	42	11.5	158	1.81
8	48	13.2	184	2.42
9	54	15	211	3.16
10	60	17.3	237	4.1
11	66	19.6	263	5.15
12	72	21	289	6.07
13	78	22.9	316	7.25
14	84	24.6	342	8.43
15	90	26.6	368	9.8
16	96	28.4	395	11.2
17	102	30.2	421	12.7
18	108	31.4	447	14
19	114	33.3	474	15.8
20	120	35.3	500	17.6

Particle size 0 to 53 $\mu\text{m}$ with 0.5% CPC				
Meas. Pts.	Time [s]	Viscosity [mPa·s]	Shear Rate [1/s]	Shear Stress [Pa]
1	6	#####	3.97E-07	-0.82 0.0092
2	12	0.35	26.3	2
3	18	-1.83	52.6	-0.0962
4	24	5.04	78.9	0.398
5	30	7.93	105	0.835
6	36	9.65	132	1.27
7	42	10.2	158	1.6
8	48	11.7	184	2.16
9	54	13.9	211	2.92
10	60	15.9	237	3.76
11	66	17.7	263	4.65
12	72	20	289	5.78
13	78	21.4	316	6.74
14	84	23.2	342	7.95
15	90	25.5	368	9.4
16	96	27.4	395	10.8
17	102	29.8	421	12.5
18	108	31.2	447	14
19	114	32.9	474	15.6
20	120	34.3	500	17.1

Table C.9 50% fly ash,(75-53 $\mu\text{m}$ ),0.5%CPC Table C.10 50% fly ash,(53-0 $\mu\text{m}$ ),0.5%CPC

106 to 75 (without additive)						106 to 75 (with 0.5% CPC)					
Shear Rate ( $\dot{\gamma}$ ) [1/s]	Shear Stress ( $\tau$ ) [Pa]	$\ln(\dot{\gamma})$	$\ln(\tau)$	actual apparent Viscosity	Calculated viscosity	Shear Rate ( $\dot{\gamma}$ ) [1/s]	Shear Stress ( $\tau$ ) [Pa]	$\ln(\dot{\gamma})$	$\ln(\tau)$	actual apparent Viscosity	Calculated viscosity
4.59E-08	-0.42	-16.897	#NUM!	-9.14E+09	0.0	2.19E-07	0.706	-15.334	-0.3481	3.23E+09	0.0
26.3	1.19	3.26957	0.17395	45.4	16.7	26.3	0.268	3.26957	-1.3168	10.2	10.9
52.6	2.24	3.96272	0.80648	42.6	24.2	52.6	0.848	3.96272	-0.1649	16.1	16.7
78.9	3.21	4.36818	1.16627	40.7	30.0	78.9	1.81	4.36818	0.59333	22.9	21.4
105	4.03	4.65396	1.39377	38.3	35.0	105	2.71	4.65396	0.99695	25.8	25.5
132	5.43	4.8828	1.69194	41.2	39.5	132	3.89	4.8828	1.35841	29.6	29.4
158	7.01	5.0626	1.94734	44.4	43.5	158	5.39	5.0626	1.68455	34.1	32.8
184	8.53	5.21494	2.14359	46.3	47.2	184	6.79	5.21494	1.91545	36.8	36.1
211	9.85	5.35186	2.28747	46.8	50.8	211	8.51	5.35186	2.14124	40.4	39.2
237	11.8	5.46806	2.4681	49.9	54.1	237	10.5	5.46806	2.35138	44.3	42.1
263	14.3	5.57215	2.66026	54.2	57.2	263	12.4	5.57215	2.5177	47	44.9
289	16.4	5.66643	2.79728	56.7	60.1	289	13.9	5.66643	2.63189	48	47.6
316	19.1	5.75574	2.94969	60.6	63.1	316	15.5	5.75574	2.74084	49	50.3
342	22.2	5.83481	3.10009	64.8	65.8	342	17.5	5.83481	2.8622	51.1	52.8
368	25.4	5.90808	3.23475	69	68.4	368	19.7	5.90808	2.98062	53.5	55.2
395	28.7	5.97889	3.3569	72.6	71.1	395	22.6	5.97889	3.11795	57.2	57.7
421	32.2	6.04263	3.47197	76.5	73.5	421	25.5	6.04263	3.23868	60.6	60.0
447	35.4	6.10256	3.56671	79.1	75.9	447	27.9	6.10256	3.32863	62.4	62.2
474	39.1	6.16121	3.66612	82.6	78.4	474	29.3	6.16121	3.37759	61.9	64.5
500	41.8	6.21461	3.7329	83.6	80.6	500	31.5	6.21461	3.44999	63	66.6

**Table C.11 Modelling data of 50% fly ash concentration slurry with different particle size with and without 0.5% CPC**

75 to 53 (without additive)						75 to 53 (with 0.5% CPC)					
Shear Rate ( $\dot{\gamma}$ ) [1/s]	Shear Stress ( $\tau$ ) [Pa]	$\ln(\dot{\gamma})$	$\ln(\tau)$	actual apparent Viscosity	Calculated viscosity	Shear Rate ( $\dot{\gamma}$ ) [1/s]	Shear Stress ( $\tau$ ) [Pa]	$\ln(\dot{\gamma})$	$\ln(\tau)$	actual apparent Viscosity	Calculated viscosity
0.00000231	-0.377	-12.978	#NUM!	#####	0.23035692	-0.00000289	-0.58	#NUM!	#NUM!	#####	#NUM!
26.3	1.29	3.26957	0.25464	49.1	19.5736944	26.3	-0.199	3.26957	#NUM!	-7.56	2.2932527
52.6	1.85	3.96272	0.61519	35.1	23.6579587	52.6	-0.055	3.96272	#NUM!	-1.04	4.3556997
78.9	2.34	4.36818	0.85015	29.7	26.4315295	78.9	0.472	4.36818	-0.7508	5.97	6.3391642
105	3.01	4.65396	1.10194	28.6	28.5795758	105	0.899	4.65396	-0.1065	8.54	8.2584599
132	3.99	4.8828	1.38379	30.3	30.4248525	132	1.57	4.8828	0.45108	11.9	10.206585
158	4.94	5.0626	1.59737	31.3	31.957821	158	1.81	5.0626	0.59333	11.5	12.054442
184	5.71	5.21494	1.74222	31	33.3170189	184	2.42	5.21494	0.88377	13.2	13.879681
211	6.96	5.35186	1.94018	33.1	34.5879109	211	3.16	5.35186	1.15057	15	15.75486
237	8	5.46806	2.07944	33.8	35.7044367	237	4.1	5.46806	1.41099	17.3	17.5437
263	9.27	5.57215	2.22678	35.2	36.7351925	263	5.15	5.57215	1.639	19.6	19.317951
289	10.8	5.66643	2.37955	37.3	37.6943517	289	6.07	5.66643	1.80336	21	21.079162
316	11.9	5.75574	2.47654	37.8	38.626168	316	7.25	5.75574	1.981	22.9	22.895658
342	13.5	5.83481	2.60269	39.4	39.4702831	342	8.43	5.83481	2.1318	24.6	24.633959
368	14.9	5.90808	2.70136	40.6	40.2689773	368	9.8	5.90808	2.28238	26.6	26.362434
395	16.4	5.97889	2.79728	41.5	41.056105	395	11.2	5.97889	2.41591	28.4	28.147786
421	18.1	6.04263	2.89591	42.9	41.7779463	421	12.7	6.04263	2.5416	30.2	29.85843
447	19.5	6.10256	2.97041	43.5	42.4680859	447	14	6.10256	2.63906	31.4	31.561216
474	21	6.16121	3.04452	44.4	43.1545559	474	15.8	6.16121	2.76001	33.3	33.321704
500	23.3	6.21461	3.14845	46.7	43.7892465	500	17.6	6.21461	2.8679	35.3	35.009935

Table C.12 Modelling data of 50% fly ash concentration slurry with different particle size with and without 0.5% CPC

0 to 53 (without additive)						0 to 53 (with 0.5% CPC)					
Shear Rate ( $\dot{\gamma}$ ) [1/s]	Shear Stress ( $\tau$ ) [Pa]	$\ln(\dot{\gamma})$	$\ln(\tau)$	actual apparent Viscosity	Calculated Viscosity	Shear Rate ( $\dot{\gamma}$ ) [1/s]	Shear Stress ( $\tau$ ) [Pa]	$\ln(\dot{\gamma})$	$\ln(\tau)$	actual apparent Viscosity	Calculated Viscosity
-0.00000352	-0.742	#NUM!	#NUM!	21,10,00,000	#NUM!	3.97E-07	-0.82	-14.7393	#NUM!	#####	0.00
26.3	1.68	3.269569	0.518794	63.8	20.12632161	26.3	0.00922	3.269569	-4.68638	0.35	1.75
52.6	2.4	3.962716	0.875469	45.6	23.95965206	52.6	-0.0962	3.962716	#NUM!	-1.83	3.53
78.9	2.68	4.368181	0.985817	34	26.53209756	78.9	0.398	4.368181	-0.9213	5.04	5.32
105	3.15	4.65396	1.147402	29.9	28.50944327	105	0.835	4.65396	-0.18032	7.93	7.10
132	3.93	4.882802	1.368639	29.9	30.19856461	132	1.27	4.882802	0.239017	9.65	8.95
158	5.04	5.062595	1.617406	31.9	31.59555906	158	1.6	5.062595	0.470004	10.2	10.73
184	6.07	5.214936	1.803359	33	32.829708	184	2.16	5.214936	0.770108	11.7	12.52
211	6.81	5.351858	1.918392	32.4	33.98003083	211	2.92	5.351858	1.071584	13.9	14.38
237	8.07	5.46806	2.088153	34.1	34.98783927	237	3.76	5.46806	1.324419	15.9	16.17
263	9.28	5.572154	2.227862	35.3	35.91599016	263	4.65	5.572154	1.536867	17.7	17.96
289	10.6	5.666427	2.360854	36.7	36.77779944	289	5.78	5.666427	1.754404	20	19.76
316	11.8	5.755742	2.4681	37.3	37.61336107	316	6.74	5.755742	1.90806	21.4	21.63
342	13	5.834811	2.564949	37.9	38.36888795	342	7.95	5.834811	2.073172	23.2	23.43
368	14.6	5.908083	2.681022	39.5	39.08257038	368	9.4	5.908083	2.24071	25.5	25.23
395	15.7	5.978886	2.753661	39.7	39.78480946	395	10.8	5.978886	2.379546	27.4	27.11
421	17.3	6.042633	2.850707	41	40.42785588	421	12.5	6.042633	2.525729	29.8	28.91
447	18.3	6.102559	2.906901	40.9	41.04182967	447	14	6.102559	2.639057	31.2	30.72
474	20	6.161207	2.995732	42.2	41.65174697	474	15.6	6.161207	2.747271	32.9	32.60
500	21.6	6.214608	3.072693	43.2	42.21496836	500	17.1	6.214608	2.83908	34.3	34.40

Table C.13 Modelling data of 50% fly ash concentration slurry with different particle size with and without 0.5% CPC

REGRESSION LINE											
106 to 75 (without additive)		106 to 75 (with 0.5% CPC)		75 to 53 (without additive)		75 to 53 (with 0.5% CPC)		0 to 53 (without additive)		0 to 53 (with 0.5% CPC)	
$\ln(\bar{Y})$	$\ln(\tau)$	$\ln(\bar{Y})$	$\ln(\tau)$	$\ln(\bar{Y})$	$\ln(\tau)$	$\ln(\bar{Y})$	$\ln(\tau)$	$\ln(\bar{Y})$	$\ln(\tau)$	$\ln(\bar{Y})$	$\ln(\tau)$
5.15699	2.073100798	4.5545453	0.825824058	5.00922	1.551322248	5.00922	0.541500142	5.15699	1.725959707	5.00922	0.420478915
5.61696	2.779304277	5.3406204	2.095038431	5.5435	2.231681762	5.5435	1.570264609	5.61696	2.3016145	5.5435	1.495141084
6.07692	3.485507756	6.1266954	3.364252803	6.07778	2.912041276	6.07778	2.599029077	6.07692	2.877269293	6.07778	2.569803253

**Table C.14 Regression data of 50% slurry with different particle size (with and without 0.5% CPC)**

## ANNEXTURE D

## SETTLING BEHAVIOUR OF 30% FLY ASH SLURRY WITH ADDITIVES

REGRESSION LINE									
Without additive		0.01% of SDS		0.02% of SDS		0.04% of SDS		0.06% of SDS	
time	settling rate	time	settling rate	time	settling rate	time	settling rate	time	settling rate
9.46743741	0.853870586	6.93774225	1.078474849	7.359012	1.033928833	7.359012	0.935016576	8.202041	0.856859486
21	0.455	15	0.607142857	16	0.573333333	16	0.54	18	0.488235294
32.5325626	0.056129414	23.0622577	0.135810866	24.64099	0.112737834	24.64099	0.144983424	27.79796	0.119611102

**Table D.1 Regression data for settling process of 30% fly ash with 4 different concentrations of SDS**

REGRESSION LINE									
without CPC		0.01% CPC		0.02% CPC		0.04% CPC		0.06% CPC	
time	settling rate	time	settling rate	time	settling rate	time	settling rate	time	settling rate
9.46744	0.853870586	6.09589	1.134755587	5.67544	1.217854428	5.25544	1.26195385	5.25544	1.2646218
21	0.455	13	0.683333333	12	0.763636364	11	0.805	11	0.745
32.5326	0.056129414	19.9041	0.231911079	18.3246	0.3094183	16.7446	0.34804615	16.7446	0.2253782

**Table D.2 Regression data for settling process of 30% fly ash with 4 different concentrations of CPC**

REGRESSION LINE									
without Triton x-100		0.01% Triton		0.02% Triton		0.04% Triton		0.06% Triton	
time	settling rate	time	settling rate	time	settling rate	time	settling rate	time	settling rate
9.46743741	0.85387059	8.202041	0.915749791	8.62375	0.889007491	8.62375	0.854839259	7.78046	0.809811979
21	0.455	18	0.514705882	19	0.486111111	19	0.466666667	17	0.471875
32.5325626	0.05612941	27.797959	0.113661973	29.3763	0.083214731	29.3763	0.078494075	26.2195	0.133938021

**Table D.3 Regression data for settling process of 30% fly ash with 4 different concentrations of Triton**

SNO.	TIME (MIN)	WITHOUT ADDITIVE	Height of the fly ash settled (cm)											
			SDS						WITH ADDITIVE					
			Triton X-100						CPC					
1)	0	15.20	0.05gm	0.10gm	0.20gm	0.30gm	0.05gm	0.10gm	0.20gm	0.30gm	0.05gm	0.10gm	0.20gm	0.30gm
2)	2	13.80	14.60	14.60	14.30	14.60	15	14.95	14.5	13.55	15.00	15.30	15.30	15.20
3)	4	12.70	13.15	13.20	13.00	13.55	13.8	13.8	13.3	12.85	13.50	13.80	13.90	13.70
4)	6	11.65	11.80	11.90	12.00	12.50	12.8	12.8	12.3	11.85	12.35	12.65	12.70	12.60
5)	8	10.75	10.60	10.70	10.90	11.60	11.75	11.7	11.3	10.85	11.25	11.50	11.45	11.50
6)	10	9.70	9.50	9.50	10.00	10.65	10.7	10.65	10.35	9.9	10.20	10.40	10.35	10.20
7)	12	8.90	8.50	8.50	9.10	9.75	9.7	9.65	9.4	8.9	9.30	9.30	9.30	8.60
8)	14	8.30	7.85	7.90	8.30	8.90	8.8	8.75	8.55	8.1	8.50	8.50	8.40	8.15
9)	16	7.80	7.35	7.40	7.80	8.20	8.1	8.05	7.9	7.55	7.80	7.70	7.60	7.95
10)	18	7.60	7.00	7.00	7.30	7.75	7.65	7.55	7.45	7.1	7.40	7.20	7.35	7.85
11)	20	7.10	6.75	6.80	7.00	7.35	7.3	7.15	7.05	6.8	7.10	7.10	7.30	7.80
12)	22	6.90	6.55	6.55	6.80	7.00	7	6.9	6.8	6.6	6.95	7.15	7.25	7.75
13)	24	6.75	6.40	6.40	6.60	6.80	6.8	6.75	6.65	6.45	6.85	7.00	7.25	7.75
14)	26	6.60	6.30	6.25	6.45	6.70	6.65	6.6	6.5	6.3	6.80	7.00	7.25	7.70
15)	28	6.50	6.20	6.15	6.35	6.55	6.5	6.5	6.4	6.2	6.80	7.00	7.20	7.70
16)	30	6.40	6.10	6.10	6.30	6.45	6.4	6.4	6.3	6.15	6.75	7.00	7.20	7.65
17)	32	6.30	6.00	6.00	6.20	6.40	6.35	6.35	6.25	6.1	6.70	7.00	7.20	7.60
18)	34	6.25	6.00	6.00	6.20	6.35	6.3	6.3	6.2	6	6.70	7.00	7.20	7.50
19)	36	6.20	6.05	5.95	6.15	6.30	6.25	6.25	6.15	6	6.70	7.00	7.20	7.50
20)	38	6.15	6.05	5.95	6.15	6.30	6.25	6.2	6.1	6	6.70	7.00	7.20	7.45
21)	40	6.10	6.05	5.95	6.10	6.25	6.2	6.2	6.1	6	6.70	7.00	7.20	7.40
22)	42	6.10	6.05	5.90	6.10	6.25	6.2	6.2	6.1	6	6.70	7.00	7.20	7.35
23)	44	6.10	6.05	5.90	6.10	6.20	6.2	6.2	6.1	6	6.70	7.00	7.20	7.30
24)	46	6.05	6.05	5.90	6.10	6.20	6.2	6.2	6.1	6	6.70	7.00	7.20	7.20
25)	48	6.05	6.05	5.90	6.10	6.20	6.2	6.2	6.1	6	6.70	7.00	7.20	7.20
26)	50	6.05	6.05	5.90	6.10	6.20	6.2	6.2	6.1	6	6.70	7.00	7.20	7.15
27)	60	6.05	6.05	5.85	6.05	6.20	6.2	6.2	6.1	6	6.70	7.00	7.15	6.95

Table D.4 Height of fly ash settled in slurry at 30% fly ash concentration with and without additives

Rate of setting of Fly ash (cm/min)																	
SNO.	TIME (min)	WITHOUT ADDITIVE	SDS					WITH ADDITIVE Triton X-100					CPC				
			0.05gm	0.10gm	0.20gm	0.30gm	0.05gm	0.10gm	0.20gm	0.30gm	0.05gm	0.10gm	0.20gm	0.30gm			
			0.73	0.70	0.65	0.52	0.6	0.575	0.6	0.35	0.75	0.75	0.70	0.75			
1)	2	0.70	0.73	0.70	0.65	0.52	0.6	0.575	0.6	0.35	0.75	0.75	0.70	0.75			
2)	4	0.55	0.68	0.65	0.50	0.5	0.5	0.5	0.5	0.58	0.58	0.60	0.55				
3)	6	0.52	0.60	0.60	0.55	0.45	0.525	0.55	0.5	0.55	0.58	0.63	0.55				
4)	8	0.45	0.55	0.60	0.45	0.48	0.525	0.525	0.475	0.53	0.55	0.55	0.65				
5)	10	0.53	0.50	0.50	0.45	0.45	0.5	0.5	0.475	0.45	0.55	0.52	0.80				
6)	12	0.40	0.33	0.30	0.40	0.43	0.45	0.45	0.425	0.40	0.40	0.45	0.23				
7)	14	0.30	0.25	0.25	0.25	0.35	0.35	0.35	0.325	0.275	0.35	0.40	0.10				
8)	16	0.25	0.18	0.20	0.25	0.23	0.225	0.25	0.225	0.20	0.25	0.13	0.05				
9)	18	0.10	0.13	0.10	0.15	0.20	0.175	0.2	0.15	0.15	0.05	0.02	0.02				
10)	20	0.25	0.10	0.13	0.10	0.18	0.15	0.125	0.125	0.07	-0.03	0.02	0.02				
11)	22	0.10	0.07	0.07	0.10	0.10	0.1	0.075	0.075	0.05	0.08	0.00	0.00				
12)	24	0.08	0.05	0.08	0.07	0.05	0.075	0.075	0.075	0.02	0.00	0.00	0.02				
13)	26	0.08	0.05	0.05	0.05	0.08	0.075	0.05	0.05	0.00	0.00	0.02	0.00				
14)	28	0.05	0.05	0.03	0.02	0.05	0.05	0.05	0.025	0.02	0.00	0.00	0.02				
15)	30	0.05	0.00	0.05	0.05	0.02	0.025	0.025	0.025	0.02	0.00	0.00	0.03				
16)	32	0.05	0.02	0.00	0.00	0.03	0.025	0.025	0.025	0.00	0.00	0.00	0.05				
17)	34	0.02	0.00	0.02	0.02	0.02	0.025	0.025	0.025	0.00	0.00	0.00	0.00				
18)	36	0.02	0.00	0.00	0.00	0.00	0.025	0.025	0.025	0.00	0.00	0.00	0.02				
19)	38	0.02	0.00	0.00	0.03	0.02	0	0	0	0.00	0.00	0.00	0.02				
20)	40	0.03	0.00	0.00	0.00	0.00	0	0	0	0.00	0.00	0.00	0.03				
21)	42	0.00	0.00	0.02	0.00	0.00	0	0	0	0.00	0.00	0.00	0.02				
22)	44	0.00	0.00	0.00	0.00	0.02	0	0	0	0.00	0.00	0.00	0.05				
23)	46	0.02	0.00	0.00	0.00	0.00	0	0	0	0.00	0.00	0.00	0.00				
24)	48	0.00	0.00	0.00	0.00	0.00	0	0	0	0.00	0.00	0.00	0.02				
25)	50	0.00	0.00	0.00	0.00	0.00	0	0	0	0.00	0.00	0.00	0.03				
26)	60	0.00	0.00	0.03	0.02	0.00	0	0	0	0.00	0.00	0.02	0.07				
AVG		0.23	0.30	0.29	0.27	0.24	0.25735	0.24306	0.23333	0.23594	0.28	0.38	0.40	0.41			

Table D.5 Setting rate of fly ash slurry at 30% fly ash concentration with and without additives

## ANNEXURE E

## PARTICLE SIZE DISTRIBUTION

## Mechanical Sieving of Fly ash

weight of pan	138.45 grams
weight of fly ash	100 grams
Time of sieving	10 minutes

Sieve size (British standard )	Sieve size	Particle size ( $\mu\text{m}$ )	Fly ash with pan (grams)	weight %	cumulative retained %
bottom pan	<53 $\mu\text{m}$	0 to 53	162.83	24.38	24.38
300	53 $\mu\text{m}$	53 to 75	178.1	39.65	64.03
200	75 $\mu\text{m}$	75 to 106	161.18	22.73	86.76
150	106 $\mu\text{m}$	106 to 150	146.13	7.68	94.44
100	150 $\mu\text{m}$	150 to 250	141.64	3.19	97.63
60	250 $\mu\text{m}$	250 to 355	139.13	0.68	98.31
44	355 $\mu\text{m}$	355 to 500			
30	500 $\mu\text{m}$	500 to 710			
22	710 $\mu\text{m}$	710 to 1180			
16	1180 $\mu\text{m}$	1180 to 2000			
10	2000 $\mu\text{m}$	2000 to 2360			
8	2360 $\mu\text{m}$				

Table E.1 Data obtained during calculation of particle size distribution (PSD) of Fly ash.

CONVERSION TABLE FOR STANDARD TESTSIEVES-			
Indian Standard Sieve Designation	Sieve Series Width of Aperture mm	British Standard Sieve Series Mesh No.	ASTM. No.
5.60 mm	5.60	-	3.5
4.75 mm	4.75	4	4
4.00 mm	4.00	-	5
3.35 mm	3.35	5	6
2.80 mm	2.80	6	7
2.36 mm	2.36	7	8
2.00 mm	2.00	8	10
1.70 mm	1.70	10	12
1.40 mm	1.40	12	14
1.18 mm	1.18	14	16
1.00 mm	1.00	16	18
850 micron	0.850	18	20
710 micron	0.710	22	25
600 micron	0.600	25	30
500 micron	0.500	30	35
425 micron	0.425	36	40
355 micron	0.355	44	45
300 micron	0.300	52	50
250 micron	0.250	60	60
212 micron	0.212	72	70
180 micron	0.180	85	80
150 micron	0.150	100	100
125 micron	0.125	120	120
106 micron	0.106	150	140
90.9 micron	0.090	170	170
75.0 micron	0.075	200	200
63.0 micron	0.063	240	230
53.0 micron	0.053	300	270
45.0 micron	0.045	350	325

**Table E.2 Conversion table showing relation between size in microns, British standard sieve no. system and ASTM standard.**

## ANNEXURE F

**pH OF 40% SLURRY WITH ADDITIVES**

pH results				
Sno.	% Conc.	pH (SDS)	pH (Triton)	pH (CPC)
1.)	0	7.54	7.54	7.54
2.)	0.5	8.24	7.93	7.78
3.)	1	8.58	8.2	7.94
4.)	1.5	8.68	8.31	8.04

**Table F.1 pH data for 40% fly ash concentration slurry with different dosages of SDS, Triton and CPC**

	Sample %	
	Weight (gm)	Percent%
Total Weight	66.66	100%
Fly ash	26.66	40%
water	40	60%
additive	0.33	0.50%
additive	0.66	1%
additive	0.99	1.50%

**Table F.2 Sample concentrations involved in preparation of slurry for pH test**